Volume: 4: 2021 ISSN: 2220 - 7643

Ethiopian Journal of Water Science and Technology (EJWST)

Ethiopian Journal of Water Science and Technology (EJWST)

Volume: 4

: 2021

ISSN: 2220-7643



Ethiopian Journal of Water Science and Technology (EJWST)

Volume: 4 : 2021 ISSN: 2220-7643

Authors	Pages	Title
Gezimu Gelu, Markos Habtewold and Abebaw Bergene	01	The Effect of deficit irrigation on Onion yield and water use efficiency: Concerning moisture stress areas of Arba Minch, Southern Ethiopia
Matusal Lamaro and Abdella Kemal	15	Feasibility of hydropower generation on existing legedadi water supply scheme, addis ababa-ethiopia.
Johannes Dirk	33	Evaluation of Three Low-Cost Particulate Matter (PM2.5) Sensors for Ambient and High Exposure Conditions in Arba Minch, Ethiopia
Demamu Tagele and Tamru Tesseme	62	Shallow Groundwater Quality and Human Health Risk Assessment in Holte, a Town in Southern Ethiopia
Bereket Dora and Samuel Dagalo	90	Comparative Performance Evaluation of HEC-HMS and SWAT Models in Stream Flow Simulation: the Case of Bilate and Gidabo Watersheds, Ethiopia
	123	Guidelines to Authors

Ethiopian Journal of Water Science and Technology (EJWST)

AIM & SCOPE: The Ethiopian Journal of Water Science and Technology (EJWST) is an open-access journal hosted by Arba Minch University, Water Technology Institute. EJWST is a multidisciplinary double-blind peer-reviewed journal that publishes original research papers, critical reviews, and technical notes which are of regional and international significance on all aspects of the water science, technology, policy, regulation, social, economic aspects, management and applications of sustainable use of water resources to cope-up with water scarcity. The journal includes, but is not limited to, the following topics:

Hydrology & integrated water resources management

- ❖ Water resources Potential Assessment; Integrated Watershed Management; Optimal Allocation of Water Resources;
- ❖ Hydraulic modeling; Eco-hydrology and River Basin Governance and water Institutions

Irrigation and Drainage

- Irrigation Potential Assessment;
- Irrigation Scheme Performance Improvements;
- ❖ Agriculture Water Management;
- ❖ Conjunctive Use of Surface and Groundwater Irrigation;
- * Rain water Harvesting and spate Irrigation.

Water Supply and Sanitation

- * Rural and Rural Water Supply and Sanitation;
- ❖ Water Quality Modeling;
- ❖ Wastewater Treatment and Re-use; Solid Waste Management;
- **Services** Ecological Sanitation and Sustainability of Water supply Services.

Renewable Energy

- ❖ Assessment of hydropower Potential and development;
- ❖ Small scale Hydropower and alternative energy sources;
- ❖ Dam and Reservoirs; Wind Energy for Water Pumping and;

Solar Energy for Water pumping

Climate Variability, change, and impacts

- ❖ Impacts of climate change on water resources
- Climate Changes Impacts, Vulnerability,
- ❖ Adaptation options; Climate Forcing & Dynamics and Predictability of weather and climate extremes.

Emerging Challenges

❖ Hydro politics and conflict Resolution; Equitable Resources and Benefit-sharing; Gender and Water Resources Management and Cross-cutting Issues

Editorial Board:

The journal editorial board is comprised of multiple disciplines in the areas of Water Resources Engineering, development, and management. The editorial board welcomes all interested authors to join the review and advisory board of EJWST.

Editor-in-Chief:

Dr.-Ing. Kinfe Kassa (Associate Professor: Water Supply and Environmental Eng'g)

Co-Editor-in-chief:

Dr. Samuel Dagalo (Associate Professor: Water Resources and Irrigation Eng'g)

Editorial Manager:

Dr.-Ing. Abdella Kemal (Associate Professor: Hydraulic and Water Resources Eng'g)

Language Editor:

Dr. Wondifraw Wanna (Assistant Professor: English Language and Literature)

Layout and Graphic Designer:

Chirotaw Kentib (BSc: Computer Science)

Advisory Board:

Prof. Miegel Konrad, Rostock University, Germany

Prof K.S. Hari Prasad, Indian Institute of Technology, Roorkee, India

Prof. Tenalem Ayenew, Addis Ababa University, Ethiopia

Prof. Muluneh Yitayew, Arizona State University, USA

Prof. Dr.-Eng. Markus Disse, Technical University of Munich, Germany

Dr.-Ing. Seleshi Bekele, Ambassador in USA for Ethiopia

Dr. Mekonnen Ayana, Adama Science and Technology University, Ethiopia

Dr. Ababu Teklemariam, Department of Environmental Health Science. University of Swaziland

Dr. Semu Moges, Addis Ababa Institute of Technology, Addis Ababa University, Ethiopia

Dr. Alemseged Tamiru, International Water Management Institute (IWMI)

Dr. Negash Wagesho, President of South Western Ethiopia Region, Ethiopia

Dr. Negede Abate, former Ethiopian Construction Design and Supervision Works Corporation

Dr. Asfaw Kebede, Haremaya University, Ethiopia

Dr. Michael Mehari, Ministry, Water Irrigation and Electricity, Ethiopia

Dr. Beshah Mogesse, UNICEF, Ethiopia

The Effect of deficit irrigation on Onion yield and water use efficiency: Concerning moisture stress areas of Arba Minch, Southern Ethiopia

Gezimu Gelu¹, Markos Habtewold² and Abebaw Bergene²

^{1,2}South Agricultural Research Institute, Arba Minch Agricultural Research Center, Department of Natural Resources Management, Irrigation and Drainage Program. P.O.Box:2228, Arba Minch, Ethiopia.

*Corresponding author email: gezimugelu64@gmail.com Mobile +251964407037

ABSTRACT

To cope with scarce water supply, deficit irrigation is an important tool to achieve the goal of reducing irrigation water use and increasing water use efficiency (WUE) under scarce water resources. This experiment was conducted for the last three years (2018-2020)in Chano Mille Kebelle near Arba Minch to examine the level of deficit irrigation which allows the maximum yield of onion, WUE and economic return without significantly reducing the yield of onion. Randomized Complete Block Design was used to run the experiment with four Replications. The experiment comprised different levels of deficit irrigation treatment: 100% of ETc, 85% of ETc, 75% of ETc and 50% of ETc. Analysis of variance showed that there was a significant difference among treatments in terms of marketable yield, total yield, and WUE in three consecutive years. 100% of ETc gave the maximum marketable and total yield and WUE which was followed by 85% of ETc. Additionally, the combined analysis of the mean showed that the highest marketable yield 24.97ton ha⁻¹and a total yield of 28.63 ton ha⁻¹was observed from 100% of ETc and followed by 22.13 ton ha⁻¹of marketable yield and 26.86 ton ha⁻¹of total yield from 85% of Etc without significant variation. The highest combined WUE of 4.445kg m⁻³ resulted from 50% of ETc compared to the other levels of deficit irrigation (3.12 kg m⁻³, 3.02 kg m⁻³, 4.27 kg m⁻³) from 100%, 85% and 70%, respectively. Given economic return, 100% of ETc yielded the highest net benefit of 208008 Birr/ha and followed by 198558 Birr/ha observed from 85% of ETc without significant economic return. The minimum (123858 Birr/ha gained from 50% of ETc. Based on these findings, 85% of ETc of deficit irrigation under moisture stress areas of Arba Minch should be applied to save water, and increase economic return and command area.

Keywords: Deficit irrigation, Evapotranspiration, Water use efficiency, Moisture stress.

1st received: 29 Apr 2020; received in revised form 15 May 2021; accepted 20 May 2021

1. INTRODUCTION

In the semi-arid areas of Ethiopia, water is the most limiting factor for crop production. In these areas where the number and distribution of rainfall are not sufficient to sustain crop growth and development, another approach is to form use the rivers and underground water for irrigation. Satisfying crop water requirements, although it maximizes production from the land unit, does not necessarily maximize the return per unit volume of water (Oweis et al., 2000).

To quantify the level of deficit irrigation, it is necessary to define the full crop water requirements. Fortunately, Penmann (1948) developed the combination approach to calculate evapotranspiration. Research on crop water requirements has produced several reliable methods for computing them. At present, the Penman-Monteith equation (Monteith and Unsworth, 1990; Allen et al., 1998) is the established method for determining the evapotranspiration of the major herbaceous crops with sufficient precision for management purposes.

Under conditions of scarce water supply, the application of deficit irrigation could provide greater economic returns than maximizing yields per unit of water. Deficit irrigation has been considered worldwide as a way of maximizing water use efficiency (WUE) by eliminating irrigation that has little impact on yield (English, 1990). With deficit irrigation, the crop is exposed to a certain level of water stress either during a particular period or throughout the whole growing season (Kirda, 2000). Deficit irrigation scheduling practice is the technique of withholding, or reducing the amount of water applied per irrigation at some stages of the crop growth to save water, labour, and in some cases energy. This practice does lead to some degree of moisture stress on the crop and a reduction in crop yield (Smith and Munoz, 2002).

In the study area, the water scarcity is alarming from time to time but the food demand is increasing. Especially the vegetable crops need of people in the study area is highly increasing. Particularly onion crops. The studies on water stress levels for onion in Ethiopia and particularly in the study area are limited. In addition, studies on the economic return of applying deficit irrigation to onion crops and other vegetables are rather scarce. Hence, policymakers lack relevant research outputs to disseminate and publicize to the community. Besides, growers, researchers, and decision-makers don't have much knowledge about the water use efficiency of the onion crop in the study area. Consequently, this study was intended to identify the level of deficit irrigation

which allows for achieving optimum onion yield, WUE, and economic analysis of deficit irrigation.

2. MATERIALS AND METHOD

2.1. Experimental site description

This experiment was conducted in Chano Mille situated at a longitude of $37^{\circ}34'59"N$ and latitude of $6^{\circ}75'25"$ E within an elevation of 1192 meters above sea level.

2.2. Experimental design and treatments

The experiment was laid out in a randomized complete block design (RCBD) with four replications and levels of treatment. The treatment was conducted under the furrow irrigation method. All cultural practices were applied following the recommendation made for the study area. The amount of irrigation water applied at each irrigation event was measured using a three-inch Par shall flume. The treatments comprised 100% ETc, 85% ETc, 70% ETc, and 50%ETc. The experimental field was divided into 16 plots with a plot size of 4mX4m. Spacing between plot and replication was 1m. Spacing between row and plant was 40cmX10cm. The experimental plot was pre-irrigated one day before the transplanting of the onion seedling. Before the commencement of deficit irrigation, two to three common light irrigations were supplied to all plots to ensure better plant establishment.

2.3. Climate data

The climatic data of temperature (minimum and maximum), rainfall, relative humidity, and wind speed were used for crop reference and evapotranspiration determination. The climatic data were collected from the nearby meteorological station situated at Arba Minch. During the experiment the mean monthly minimum and maximum temperature ranged from 16.5 to 31.7 °C; relative humidity from 55 to 72 %; wind speed from 95 to 130 km/day, rainfall from 31 to 131 mm, and reference evapotranspiration (ET_o) from 4.2 to 5.22 mm/day.

2.4. Crop data

The maximum effective root zone depth of onion used was 0.6 m while the soil water depletion fraction (P) allowed for this experimental study was 0.25. (Andreas et al., 2002). The crop

coefficient used for initial crop development, mid, and late-stage was 0.7, 1.05, and 0.95, respectively.

2.5. Soil data

The soil data of the experimental site was sampled by the zigzag method across the experimental land. To characterize soils of the study site, soil physical and chemical parameters were determined in the field and laboratory. The laboratory analysis of soil showed that the average composition of sand, silt, and clay was 13%, 21%, and 66%, respectively. Thus, the particle size determination for the experimental site revealed that the soil texture could be classified as clay soil according to the USDA soil textural classification. The topsoil surface had a bulk density of 1.32 g/cm³). When the average soil bulk density (1.32g/cm³) is below the critical threshold level (1.4 g/cm³), it is thought to be suitable for crop root growth.

The average moisture content of the experimental site soil at field capacity was 27% and the permanent wilting point was 15% through one-meter soil depth. Soil p^H was found to be at the optimum value (6.4) for onion and other crops. The value of EC (1.12ds) was lower according to the standard rates specified by Landon (1991). Generally, soil with electrical conductivity of less than 2.0 dS/m at 25°C and p^H less than 8.5 is considered a normal soil according to USDA soil classification. Therefore, the soil of the study area was normal. The weighted average organic matter content of the soil was about 7.085%. The infiltration capacity of the soil was measured by using a double ring inflitrometer and the infiltration rate was 6mm/hour.

2.6. Determination of reference crop evapotranspiration (ET₀)

The reference evapotranspiration (ETo) was determined by CROPWAT -8 model based on the Penman-Monteith model. ETo will be determined by using daily climatic data like relative humidity, temperature: maximum and minimum), wind speed and sunshine hours). The ET_o was calculated using equation (1) FAO (1998).

ETo =
$$\frac{0.408\Delta(Rn-G) + \gamma \frac{900}{T+273}u^{2}(es-ea)}{\Delta + \gamma (1+0.34u^{2})}$$
(1)

Where, ET_o is reference evapotranspiration [mm hour⁻¹]; Rn is net radiation at the grass surface [MJ m-2 hour⁻¹]; G is soil heat flux density [MJ m⁻² hour⁻¹]; T is mean hourly air temperature [°C];

 Δ is saturation slope vapour pressure curve at Thr [kPa °C⁻¹]; γ is psychometric constant [kPa °C⁻¹]; *es* is saturation vapour pressure [kPa]; *ea* is average hourly actual vapour pressure [kPa] and u2 is average hourly wind speed [m s⁻¹].

2.7. Crop water determination

Crop water requirement refers to the amount of water that needs to be supplied, while crop evapotranspiration refers to the amount of water that is lost through evapotranspiration (Allen *et al.*, 1998). To determine crop water requirement, it is important to consider the effect of crop coefficient (Kc) and the effect of climate on crop water requirement, which is the reference crop evapotranspiration (ETo) (Doorenbos and Pruitt, 1977). The daily climate data like maximum and minimum air temperature, relative humidity, wind speed, sunshine hour and rainfall data of the study area were collected to determine reference evapotranspiration. Crop data like crop coefficient, growing season and development stage, effective root depth, and critical depletion factor of onion were also used as input data. Maximum infiltration rate and total available water of the soil were determined to calculate crop water requirement.

Crop water requirement was determined by using the equation (2)

$$ETc = ETo x Kc (2)$$

Where ETc is evapotranspiration; Kc is crop coefficient, and ETo is reference evapotranspiration. The mean monthly ETo for three consecutive years is shown in Table 1.

Table 1: Mean Monthly ETo of the study site

Month	ETo (mm/day)	
January	4.38	
February	4.75	
March	5.22	
April	4.7	
May	4.2	
June	3.89	
July	3.55	
August	3.9	
September	4.07	
October	4.25	
November	4.1	
December	4.11	
Average	4.26	

2.8. Irrigation water management

The total available water (TAW), stored in a unit volume of soil was determined by applying equation (3)

$$TAW = \frac{(FC - PWP)}{100} * BD * D \tag{3}$$

Where FC is the field capacity; PW is the permanent wilting point; BD is bulk density; D is the root depth. For onion production, the irrigation schedule was fixed based on readily available soil water (RAW). The RAW could be computed by using the equation (4).

$$RAW = PX TAW$$
 (4)

Where RAW(mm) is readily available water, P(%) is permissible soil moisture depletion for no stress and TAW(mm) is total available water. The depth of irrigation supplied at any time can be obtained by using the equation (5).

Net irrigation(mm) =
$$ETc(mm)$$
-Peff(mm) (5)

Gross irrigation requirement(GIR) was obtained by using equation (6) as:

$$GIR = \frac{\text{Net irrigation}}{\text{Ea}} \tag{6}$$

The time required to deliver the desired depth of water into each furrow was calculated by using equation (7):

$$t = \frac{d * l * w}{6 * 0} \tag{7}$$

Where:d is the gross depth of water applied (cm;t is application time (min); l is furrow length in (m); w is furrow spacing in (m), and Q is the flow rate (discharge) (l/s). The amount of irrigation water to be applied at each irrigation application was measured by using Par shall flume.

2.9. Measurement of agronomic data

The amount of water applied per each irrigation event was measured by using a three-inch par shall flume. During harvesting time, the yield of onion was measured by using spring balance on a plot basis and the total yield of onion was measured by summing both marketable and unmarketable yields of onion. Un-marketable yield is onion bulb yield which is attacked by worms

and other vectors and whose diameter is below 5mm.

Water use efficiency(WUE, kg m⁻³) was determined by using equation 8:

$$WUE = \frac{Onion \ yield}{evapotranspiration \ of \ onion}$$
 (8)

3. ECONOMIC ANALYSIS

It was carried out to compare the effects of water application and other inputs costs and return to the producers among different treatments. Economic analysis was employed as suggested by CIMMTY (1988) to determine water application levels based on cost and benefits and recommend feasible treatments. The following economic analysis indices were used to examine the feasibility of applying deficit irrigation treatment.

Gross average yield (kg ha-1) (AvY): is the average yield of each treatment.

Adjusted yield (AjY): is the average yield adjusted downward by 10% to reflect the difference between the experimental yield and the yield of farmers.

$$AjY = AvY - (AvY*0.1)$$

Gross field benefit (GFB): was computed by multiplying the farm gate price that farmers receive for the yield when they sell it as adjusted yield GFB = AjY*farm gate price for haricot bean yield.

Total cost (TC) includes the costs of all inputs, such as haricot bean seed, fertilizer, insecticides, and labour. For economic analysis, the total cost can be put into two groups: fixed costs (FC) and variable costs (VC). The total cost is the summation of the fixed (FC) and variable (VC) costs (equation 9).

$$TC = FC + VC \tag{9}$$

The fixed costs (FC) do not vary among the technologies; it includes the cost of land, water tax and fertilizer whereas the variable costs (VC) do vary among the treatments. The variable costs (VC) include labourer wages.

Net benefit (NB): is the amount of money which is left when the total costs (TC) are subtracted from the Gross Field Benefit (GFB). It may be given as:

$$NB = GFB-TC$$
 (10)

3.1. Statistical Analysis

Data analysis was carried out to compare the treatment effect on yield and water use efficiency of onion. The data collected for all relevant variables were subject to analysis of variance (ANOVA) which is appropriate for Randomized complete Block Design (RCBD) (Gomez and Gomez, 1984). The combined analysis of variance across years was conducted by using the analysis for statistics (SAS) software version 9.1 to determine the differences among treatments.. A comparison of means was carried out by employing the least significant differences (LSDs) (Gomez and Gomez, 1984) at 5% levels of significance.

4. RESULTS AND DISCUSSION

4.1. Marketable and Total Yield Response to Deficit Irrigation

Analysis of variance (ANOVA) showed that the application of deficit irrigation has significantly affected the marketable and total yield of onion over three consecutive years as shown in Table 2 at (p=0.05)

Mean values of three consecutive years applying 100% of Etc resulted in maximum yield and total yield of onion without significant variation with 85% of ETc whereas the minimum means were observed in onions with 50% of Etc. . The maximum marketable yield over three years obtained from 100% was 23.93ton ha⁻¹, 26.70 ton ha⁻¹ and 27.13 ton ha⁻¹ in the first, second, and the third year, respectively. The minimum marketable yield observed over three years from 50% was 15.17ton ha⁻¹, 14.34ton ha⁻¹ and 13. 77 ton ha⁻¹ in, the second, and third year, respectively. The maximum total yield observed over three years from 100% was 28.852 ton ha⁻¹, 26.70 ton ha⁻¹ and 27.93 ton ha⁻¹ in the first, second, and third years, respectively. The minimum total yield observed over three years from 50% was 20.981ton ha⁻¹, 18.175ton ha⁻¹ and 14.4 ton ha⁻¹ for the first, second and third years, respectively.

Combined means of marketable yield and total yield using ANOVA showed a significant variation among treatments of deficit irrigation at p=0.05. The maximum combined marketable yield (24.97 ton ha⁻¹) was observed from 100% Etc without significant variation with a mean yield of 22.13 ton ha⁻¹ from 85% of ETc whereas the minimum yield of 20.39 ton ha⁻¹. The maximum combined total yield of 28.63 ton ha⁻¹was observed from 100% ETc without significant variation with 26.86 tons

ha⁻¹ from 85% of Etc whereas the minimum total yield, of 3.015 ton ha⁻¹ was observed from 50% ETc.

Generally, the reason behind the high performance of marketable yield, total yield, and combined mean under 100% of Etc might be due to the sufficiency of soil moisture in the active root zone. At the same time, lower performance under 50% of ETc was due to insufficiency of moisture in the root zone to satisfy the onion water demand during the growth stages of onion. Applying a high level of deficit irrigation significantly affected the metabolic reaction of onion which, in turn, affected the onion yield.

Table 2: Mean average yield and combine mean over three years

Treatment	Y	Year 1		Year 2		Year 3		Combined mean	
	Y	TY	Y	Ту	Y	Ту	Y	Ту	
100 % ETc	23.93 ^a	28.852ª	26.70 ^a	28.70 ^a	27.13 ^a	27.93 ^a	24.97 ^{ab}	28.63 ^a	
85% ETc	22.09 ^a	28.6319 ^a	25.65 ^{ab}	26.325 ^{ab}	25.49 ^a	25.97 ^a	22.13 ^{ab}	26.86 ^{ab}	
70 % ETc	18.78 ^{ab}	24.6986 ^{ab}	19.85 ^{bc}	21.025 ^b	21.14 ^b	22.15 ^b	21.34 ^b	25.3b ^c	
50%ETc	15.17 ^b	20.981 ^b	14.34 ^b	18.175 ^c	13.77 ^c	14.395 ^c	20.39 ^c	23.015 ^c	
CV	22.9	24.4	13.4	12.4	7	5	14.1	22.1	
LSD(p=0.05)	3.779	4.132	4.81	10.525	1.764	1.764	3.7	4.7	

Y= *Marketable yield and Ty*= *total yield of onion*

4.2. Water Use Efficiency of Onion

Analysis of variance (ANOVA) showed that the application of deficit irrigation has significantly affected the water use efficiency of onions as shown in Table 3 at p=0.05. From mean values of three consecutive years, applying 50% of Etc gave maximum mean water use efficiency (WUE) whereas the minimum mean of WUE was observed from 100% of ETc. Without significant variation with applying 85% of Etc, the maximum mean WUE observed from 50% of Etc was 6.7

kg m⁻³, 7.939 kg m⁻³ and 6.149 kg m⁻³ in the first, second, and third years, respectively. Without significant of applying 85% of ETc, the minimum mean WUE observed from 100% of Etc was 5.098 kg m⁻³, 6.108 kg m⁻³ and 6.056 kg m⁻³ in the first, second, and third years, respectively. The maximum combined mean of WUE of (4.445 kg m⁻³) was observed from 50% of ETc whereas the minimum (3.12 kg m⁻³) WUE was observed from 100% of ETc without significantly varying 85% of ETc. The growers should select optimum WUE with optimum marketable yield and total marketable yield. From the statistical analysis, 85% of ETc gave optimum yield without significantly varying 100% of Etc. Applying 85% of Etc saved about 15% of the water that might increase the command area in a water-scarce area.

Table 3: Average and combined mean of water use efficiency (WUE, kg m⁻³)

Treatment	Year-1	Year-2	Year-3	Combined mean
100 Etc	5.098 ^b	6.108 ^b	6.056 ^b	3.12^{8c}
85% Etc	6.021 ^{ab}	6.904 ^{ab}	6.694 ^a	3. 02 ^b
70 % Etc	5.684 ^{ab}	6.488 ^{ab}	6.293 ^{ab}	4.272ª
50% ETC	6.700 ^a	7.939 ^a	6.149 ^{ab}	4.445 ^{ab}
CV	24.3	12.2	5	19.4
LSD	1.177	1.342	0.503	1.385

4.3. Onion water requirement determination

The water requirement of the onion crop for the specific site was calculated by using input data on climate and crop characteristics. Thus, based on the treatment set-up and crop water requirement, the amount of net irrigation was estimated and applied for each treatment. The amount of net irrigation requirement applied for 100% of ETc, 85% of ETc, 70% of Etc, and 50% of Etc was presented in Table 4. Table 4 also shows the application time for each treatment in different stages. It also shows the irrigation interval at which irrigation is applied and the average amount of net irrigation applied to the onion root zone.

Table 4: Irrigation scheduling for the response of onion to deficit irrigation

Days	ays 100% of ETC T-1		rs 100% of ETC T-1 T-2			T-3		T -4		
	NIR	GIR	T1 (100% (ETc) NIR	Time (t1)	T2(85% (ETc)	Time (t2)	T3 (70% ETc)	Time (t3)	T4 (50% ETC) GIR	Time (t4)
10-Dec	21.1	35.2	21.1	15	17.9	12	14.77	7.3	17.6	7
16-Dec	12.9	21.5	12.9	9	11.0	8	9.03	4.4	10.75	4
22-Dec	13.9	23.1	13.9	10	11.8	8	9.73	4.8	11.55	5
26-Dec	17.8	29.7	17.8	12	15.1	11	12.46	6.1	14.85	6
2-Nov	12.2	20.4	12.2	9	10.4	7	8.54	4.2	10.2	4
6-Nov	13.6	22.6	13.6	9	11.6	8	9.52	4.7	11.3	5
10-Nov	14.9	24.9	14.9	10	12.7	9	10.43	5.1	12.45	5
14-Nov	14.9	24.9	14.9	10	12.7	9	10.43	5.1	12.45	5
18-Nov	10	16.7	10	7	8.5	6	7	3.4	8.35	3
22-Nov	10	16.7	10	7	8.5	6	7	3.4	8.35	3
26-Nov	19	31.6	19	13	16.2	11	13.3	6.5	15.8	7
30-Nov	19.9	33.2	19.9	14	16.9	12	13.93	6.9	16.6	7
3-Jan	19.9	33.2	19.9	14	16.9	12	13.93	6.9	16.6	7
7-Jan	12.7	21.2	12.7	9	10.8	8	8.89	4.4	10.6	4
11-Jan	13	21.6	13	9	11.1	8	9.1	4.5	10.8	5
15-Jan	20.8	34.7	20.8	14	17.7	12	14.56	7.2	17.35	7
19-Jan	15.3	25.4	15.3	11	13.0	9	10.71	5.3	12.7	5
23-Jan	15.3	25.4	15.3	11	13.0	9	10.71	5.3	12.7	5
27-Jan	11.8	19.7	11.8	8	10.0	7	8.26	4.1	9.85	4
1-Feb	11.6	19.4	11.6	8	9.9	7	8.12	4.0	9.7	4
5-Feb	19.4	32.4	19.4	14	16.5	11	13.58	6.7	16.2	7
9-Feb	14.2	23.6	14.2	10	12.1	8	9.94	4.9	11.8	5
13-Feb	14.2	23.6	14.2	10	12.1	8	9.94	4.9	11.8	5
19-Feb	10.1	16.9	10.1	7	8.6	6	7.07	3.5	8.45	4
25-Feb	18.8	31.3	18.8	13	16.0	11	13.16	6.5	15.65	7
31-feb	16.4	27.3	16.4	11	13.9	10	11.48	5.7	13.65	6
6-Feb	19.9	33.2	19.9	14	13.9	28.2	13.93	6.9	10	6
12-Mar	14	23.3	14	10	16.9	19.8	9.8	4.8	7	6
18-Mar	20.4	33.9	20.4	14	11.9	28.82	14.28	7.0	10	6

GIR, Gross irrigation requirement, NIR, net irrigation requirement T1, T2, T3, T4, time required to irrigate each treatment, T-1, T-2 T-3 etc., and Treatment.

4.4. Economic analysis

For treatments, the economic return was calculated using CIMMYT (1988) standards and was summarized in Table 4 below. In Table 4, the highest net benefit of 208008 Birr/ha was recorded from 100% ETc which was followed by 19855 Birr/ha) recorded from 85% of ETc through the growing season. The lowest value of economic return or gross income of 23858 Birr/ha was obtained from 50% of ETc. Regarding economic return, 100% of ETc is better than other levels of deficit irrigation. However, there is no significant difference in economic benefit, water use efficiency, and yield with 85% of ETc. Based on the findings of the current study, it is better to apply 85% of ETc because it saves about 15% of water when compared to 100% ETc.

Table 4: Economic analysis of deficit irrigation

SN	Treatment	MY(kg/ ha)	AY(kg/ ha	GFB (birr/ha)	FC(Bir r/ha)	VC(Birr/ ha)	TC(Birr/ ha)	NB(Birr/ha
1	100% ETc	26700	24030	240300	15292	17000	32292	208008
2	85% ETc	25650	23085	230850	15292	17000	32292	198558
3	70% ETc	19850	17865	178650	15292	17000	32292	146358
4	50% ETc	17350	15615	156150	15292	17000	32292	123858

MY- marketable yield, AY, adjusted yield (-10% of MY), GFB-gross field benefit, FC- fixed cost, VC-variable cost TC-total cost NB – net income and ET Birr, Ethiopian Birr.(1 USD dollar=45 Ethiopian birr)

5. CONCLUSION AND RECOMMENDATION

The onion yield decreases with increasing deficit level of irrigation. The maximum marketable onion yield was obtained from 100% of Etc without significant difference with 85% of ETc. Based on the current study, applying 85% of ETc saves water that can increase command area, WUE, and economic benefit. Economic analysis also showed that applying 100% of ETc would give maximum net benefit without significantly varying from applying 85% ETc. Based on economic analysis, applying 85% ETc is economically viable for smallholder farmers in a moisture stress area. So, it is recommended to produce onion at a deficit level of 85 % of ETc in the case of Arba Minch and similar agro-ecologies to produce optimum onion yield and increase command area. As a future

research direction, it is recommended to experiment on different levels of deficit irrigation with appropriate irrigation scheduling techniques and soil moisture monitoring to improve WUE and land productivity.

Acknowledgements

The authors thank Arbaminch Agricultural Research Center and Southern Agricultural Research Institute for allocating the budget for researchers, drivers, and wages for daily workers; facilitating the use of natural resources and logistic provision.

REFERENCES

- Allen, R. Pereira, L.A. Raes, .D Simth, M.,(1998): Crop Evapotranspiration Guidelines for Computing Crop Water Requirement. FAO Irrigation and Drainage Paper Number 56, FAO, Rome.
- Andreas, P. and F. Karen., (2002): Crop Water Requirements and Irrigation scheduling. Irrigation Manual Module 4.Harare.P.86.
- Brady, N.C., and R.R. Weil,(2002): The nature and Properties of Soils.13th ed. Perso education Ltd., USA.
- CSA (Central Statistical Authority (2007): Area and Production of Major Crops. Sample Enumeration Survey. Addis Ababa, Ethiopia.
- Doorenbos, J. and Kassam, A. H. (1979): Yield Response to Water. Irrigation and Drain. Paper No. 33, FAO, Rome, Italy. 193 p.
- Doorenbos, J. and W.O. Pruitt.,(1977): Guidelines for predicting crop water requirements. FAO Irrig. Drain. Paper No. 24.FAO, Rome, Italy. 179 p.
- English MJ,(1990): Deficit irrigation. Analytical framework. *Journal of American Society of Civil Engl16*: 399-412.
- Fereres, E., and Soriano, M.A.(2007): Deficit irrigation for reducing agricultural water use. *Journal Experimental Botany* 58 (2):147–159.
- Kirda C. (2000): Deficit irrigation scheduling based on plant growth stages showing water stress tolerance. Deficit Irrigation Practices.

- Littell, R.C., G.A. Milliken, W.W. Stroup, R.D. Wolfinger, and O Schabenberberet. (2006): SAS for Mixed Models, 2nd Ed. SAS Publishing, Cary, NC.
- Mahbub.H, Tamara.C, Mebougna.D, A.K,C. G,(2015): Modeling of Infiltration Characteristics by Modified Kostiakov Method. http://dx.doi.org/1 .4 236/jwarp.2015.716106
- Oweis, T. Zhang, H and Pala, M. (2000). Water use efficiency of rainfed and irrigated bread wheat in a Mediterranean environment. *Agronomy Journal* 92: 231-238
- Peirce, L.C.,(1987): Vegetables characteristics, production and marketing. John Wiley and Sons. Inc.

 Toronto. Canada
- Purseglove, R..(1988): Tropical Crops Dicotyledons. Fifth edition. Longman Publisher Singapore
- Shankara.N.,J.Lidetde, M.Goffau, M.Hilmi and B.VanDam(2005):Cultivation of Tomato Production, Processing and Marketing.
- Smith M, Munoz G (2002): Irrigation Advisory Services for EffectiveWater Use: A Review of Experience. Irrigation Advisory Services and Participatory Extension in Irrigation Management Workshop Organized by FAO-ICID. Montreal, Canada.
- Staney, W.C. and Yerima, B.(1992): Improvement of soil services for agricultural development: guidelines for soil sampling and fertility evaluation, Ministry of Natural Resources Development and Environmental Protection, Addis Ababa, Ethiopia.
- Walker, W. R.,(2003): Guidlines for Designing and Evaluating Surface Irrigation Systems. FAO Irrigation and Drainage Paper 45 FAO, Rome.

Feasibility of hydropower generation on existing Legedadi water supply scheme, Addis Ababa-Ethiopia

Matusal Lamaro Lagebo^{1*}, Abdella Kemal Mohammed¹

¹ Water Technology Institute, Arba Minch University

ABSTRACT

Hydropower can be harnessed by installing in-pipe turbines with the reduced cost compared with hydropower dam construction. Legedadi Water Supply Scheme is found in Addis Ababa and is fed by gravity. This research assesses the hydropower potential of the existing large water transmission pipelines in line with their financial viability. The research required the collection of data from pipe flow (for 29 years from the system record) and pipe layout drawings believed to be useful for estimating the power. The available pipe layout drawing was processed to prepare a profile view with the help of AutoCAD CIVIL 3D. From the profile view, the gross heads and length of the pipelines were obtained. The exploitable power and financial viability of the projects were estimated by RET Screen software. The raw water main (DN1200) was discovered to have a head of 12.46 m and to convey up to 1.47 m³/s at 90% exceedance over a length of 550 m. The two treated water mains have a head of 19.15 m with a flow of 1.14 m³/s at 90 % exceedance via DN1200 and 0.29 m³/s at 90% exceedance via DN900 over a length of 18.4 km. The most suitable sites for the installation of turbines were at the inlet of the treatment plant and the Kotebe Terminal Reservoir. The Toshiba Hydro-eKIDS turbine was selected since it might work efficiently with large flow variation. The annual energy output from the raw water main to be obtained was 1,208 Mwh, with an estimated cost of \$461,000 and an annual savings or revenue of \$75,946. For the treated water mains, 1,193 Mwh (DN1200) and 344 Mwh (DN900) could be extracted with an estimated cost of 414,500\$ (DN1200) and 135,900\$ (DN900). The annual revenue for treated water mains is 75,068\$ (DN1200) and that for DN900 is 18,842\$.

Keywords: Addis Ababa; Hydropower Potential; Legedadi; AutoCAD CIVIL 3D; RETScreen

Received: 11 May 2021; accepted 15 May 2021.

1. INTRODUCTION

Energy and water appear to be complicated and strongly interrelated (Muhammad et al., 2016; Muhsen et al., 2019). All sources of energy require water in their fabrication processes; at the same time, energy helps to become water resources available for human use. A water supply scheme comprises civil infrastructures (i.e. reservoirs, pipes), hydro-mechanical and electrical equipment, and services that extract, convey, and distribute water to users (Samora et al., 2016). The clear water delivery from the surface or ground its transport and distributions all need energy which incurs significant operational costs for water providers. The water sector consumes approximately 120 million tons of energy globally each year (Capuano, WEO2018). More than half (850 TWh—around 4% of global energy) is in the form of electricity. There is a lack of a report on energy consumption of water sectors specifically in Africa or Ethiopia. However, the investigation by the author in the study area shows there is an increment in energy consumption even from month to month. Additionally, frequent power cuts are common problems in the study area.

There is an indication in the literature that the energy use in water sectors may constantly grow especially in urban areas because of population growth. Although the energy cost for operating these facilities might be quite high, water companies can significantly benefit from harnessing energy in the system so as to compensate for part or all of that cost. Studies reveal that there exists hydropower potential in the gravity-fed water supply pipelines within closed conduits (Kumar and Shahid, 2017).

Addis Ababa gets its drinking water from surface treatment plants (Gefersa and Legedadi) and subsurface (well fields) found in different areas of the city. The Legedadi Water Supply Subsystem, whose flow system is via gravity, is one of the principal sources of drinking water in Addis Ababa City Administration. According to the water balance study by the production case team of Addis Ababa Water and Sewerage Authority (AAWSA) in the year 2018, the scheme had an annual production of 60.27 Mm³. This flow system could provide a hydropower potential benefit using the in-pipe installation.

2. DESCRIPTION OF THE STUDY AREA

The Legedadi Water Supply Scheme is 24 km away from Addis Ababa located in the eastern direction. It is one of the surface sources of drinking water for the city of Addis Ababa and its vicinities. The raw water reservoir catchment area and the treatment plant are situated in Oromia Regional State under the administration of North Shoa Zone in Aleltu Bereh district, Sendafa Town Administration. The scheme consists of two dams: Legedadi (45.9 MCM) and Dire (21.5 MCM) with a modern treatment plant having a capacity of 192,000 m³/d near the Legedadi dam. The raw water from two retention dams is mixed at a junction and fed into the Legedadi Treatment Works through a single pipe of DN1200 over a distance of 550m. Then, the treated water is carried through two main steel pipes. The first pipe has a diameter of DN900 and discharges water for the whole length of 18.4 km to Kotebe Terminal Reservoirs. The second main pipe has a diameter of DN1400 for the first 6.76 km, and it is reduced to DN1200 because of major off take near the Ayat area. Eventually, it discharges treated water over a length of 11.27 km to the Kotebe Terminal Reservoir. To control high pressure created by gravity flow system, four pressure reducing stations are provided for both pipes on the way to Kotebe Terminal reservoir. Figure 1 shows the general layout of the Legedadi water supply system.

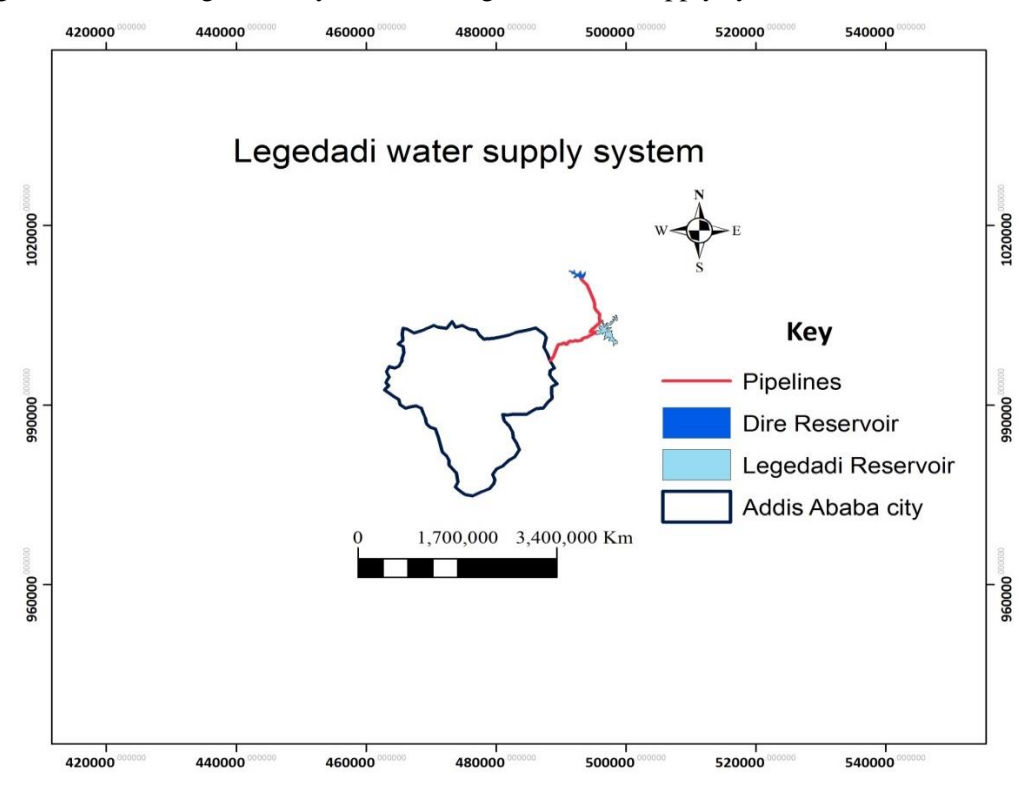


Figure 1 Legedadi Water Supply System

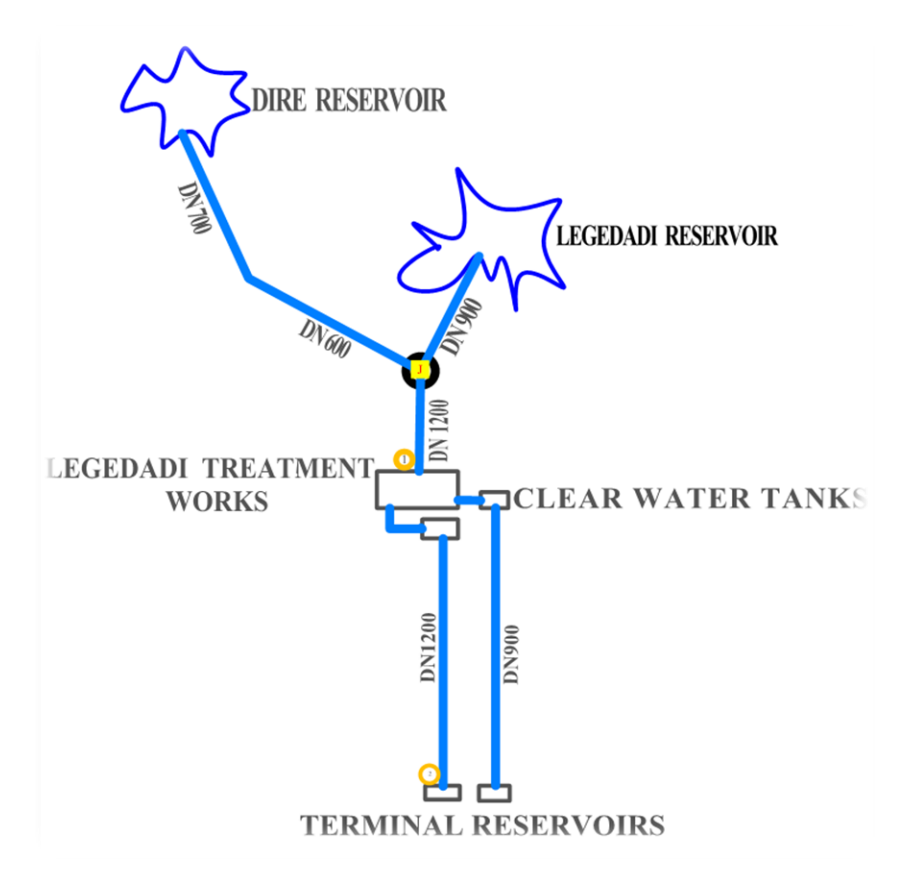


Figure 2. General layout of Legedadi Water Supply System

3. DATA SETS USED IN THE STUDY

In this study, the hydropower potential of the existing water transmission line of the Legedadi Water Supply Scheme was investigated. The necessary data groups to accomplish and achieve the objectives of the study were: pipe flow rate of raw and treated water; construction drawing of pipe layout; locations of intake, treatment plant, and service reservoirs. All the data were secondary and collected from the Addis Ababa Water and Sewerage Authority main office and the project offices. The adequate length of pipe flow (1990–2018) data from system records at the inlet of the treatment plant and service reservoir was obtained. The drawing of the pipe layout in the form of AutoCAD was obtained to process and determine the head.

3.1. Head

Bruno et al. (2010) defined multipurpose systems as those in which electricity generation was not their primary priority. This might suggest the integration of the power plant into the existing infrastructure

while ensuring its primary (water supply) and secondary (hydroelectric power generation) functions. An assessment of the site was believed to be a precondition for any hydropower development (Kusre et al., 2010). The head, flow rate, and overall system efficiency were the main factors taken into account during the assessment. These parameters could be worked out through measurement and manufacturer specifications. Head and discharge could be increased or decreased for the same power output. However, the head could not be varied as it was site-dependent. For the initial location evaluation, different scale topographic maps of the study area and additional field investigation would be sufficient to identify the head for a conventional hydropower project.

To select suitable site and head, the drawing of the pipe layout of the water supply scheme was obtained. The analysis initially involved acquiring pipeline designs to prepare the pipe profile view. This was done with the help of AutoCAD Civil 3D. From the design profile, the elevation of the pipeline at regular intervals, length (chainage or stations), and the corresponding gross head along the transmission mains were obtained. If the flow was transported through a long, pressurized conduit, head loss could reduce the power produced and needed to be calculated. The total head loss could be the sum of major and minor head losses. For this study, the frictional head losses in the pipe material were calculated. To estimate the frictional head losses, the material type, length, diameter, flow rate, and average velocity through the pipe were the necessary data required.

This information was obtained based on the site visit during the data collection stage and the pipeline layout data collected from the office. The friction factor was calculated by applying the Excel software and using the Colebrook-White Equation which required relative roughness of the pipe material and Reynolds number. The relative roughness of the pipe material was the ratio of the absolute roughness coefficient to the diameter of the given pipe. Absolute surface roughness coefficient values for the existing pipe material were taken from the Engineering Toolbox. To calculate Reynolds' Number, average velocity in the pipe was calculated by using flow rate (Q_{50}) from FDC and the kinematic viscosity of water was assumed at 20 0c (1*10⁻⁶). After determining the pipe friction factor, the Darcy-Weisbach Equation (equation 3.3) was applied to determine the total head loss in the pipes.

$$h_{l} = \frac{f*L*V^{2}}{2g*D}$$
 while,
$$\frac{1}{\sqrt{f}} = -2\log\left[\frac{\varepsilon}{3.7D} + \frac{2.51}{Re\sqrt{f}}\right]$$

3.2. Discharge

The next question was how much of the flow could be used for hydropower generation, and how to determine the turbine flow from the previously existing flow of water. Given that the intention was to estimate the maximum potential of the water supply scheme, in this study it was assumed that all of the flow could be passed through the turbine. Hydrological data had to be specified as an FDC in RET Screen, which represented the flow conditions in the site being studied over time. Flow rate values for the raw water transmission pipeline measured at the inlet of the treatment plant and the treated water transmission pipelines at inlet of Terminal for twenty-nine years were obtained from the production department of the authority. The Flow duration curve was plotted for the transmission mains of raw and treated water using flow rate data taken from the production department of the AAWSA. The flow rate variations between supply point and delivery point were determined using the flow rate values upstream and downstream. Microsoft Excel 2016 was used to plot a cluster graph used to determine the transmission mains with the least flow variations. The pipeline with the least flow variation was expected to deliver consistent flow thus giving slight power variations.

Flow rate values falling at 50 and 90 percent exceedance probability on the duration curve were used to determine the power output. The total period method yielded more correct results than the calendar year method which averaged out extreme values. Therefore, for this study total ordered (year) method was adopted since it would give more accurate results.

$$P = (\frac{m}{N+1}) * 100 \tag{2.2}$$

3.3. Financial Viability

Before deciding to invest in a hydropower plant, it is necessary to conduct a financial analysis of the project. The economic analysis is a cost-benefit comparison that allows the investor(s) to make an informed decision about the project. The small hydro cost can be split into three segments: machinery, civil work, and external costs.

As a result, the payback method was used to validate the viability of the project. The payback method might determine the number of years required for the invested capital to be offset by resulting benefits. RET Screen software was used to decide the feasibility of developing the hydropower project on

existing pipelines of the Legedadi Water Supply Scheme. The RET Screen software had a cost analysis worksheet that would enable the user to estimate the cost and credits associated with the project. RET Screen provided a tool called the "Hydro formula costing method" to help estimate the project costs. The formula method used Canadian projects as a baseline and then allowed the user to adjust the results for local conditions. The cost of projects outside Canada compared to the cost of projects in Canada might depend to a great extent on the relative cost of equipment, fuel, labor, equipment manufacturing, and the currency of the country. In general, the cost analysis data particularly cost ratios for equipment, fuel, labor, equipment manufacturing, and, exchange with respect to Ethiopia and Canada were provided for the year 2020.

4. RESULTS AND DISCUSSION

4.1. Site Selection and Head Determination (Raw and Treated)

A gross head of 12.46 m was found in the raw water transmission line from the intake to the Treatment Plant (TP). Typically, a hydropower plant with a head of less than 30 meters is regarded as a low head, though there is no definite line of separation for low, medium, and high heads. The profile view of the raw water line from the intake to the treatment plant's inlet is illustrated in Figure 2. The construction material of the pipe was ductile iron (DCI), and its 550-meter length had a head loss of 0.018 m.



Figure 3. Longitudinal profile of raw water pipe from intake to TP

The 18.4-kilometer pipeline profile shown in Figure 3 transports treated water from the Legedadi clear water tank to the Kotebe Terminal Reservoir in the city, close to the Lamberet Bus Station. The gross head from the off-take point at the Legedadi clear water tank to the Terminal reservoirs was 19.15 m. The Terminal and Legedadi Reservoirs were both built at ground level. The pipeline profile was used to determine the head of in-pipe hydropower installation for the treated water transmission line. The treated water main had eight potential locations as shown in Figure 4 shows the details of the sites described on Table 1). Steel pipe with a tough exterior was recognized as the pipe material type.

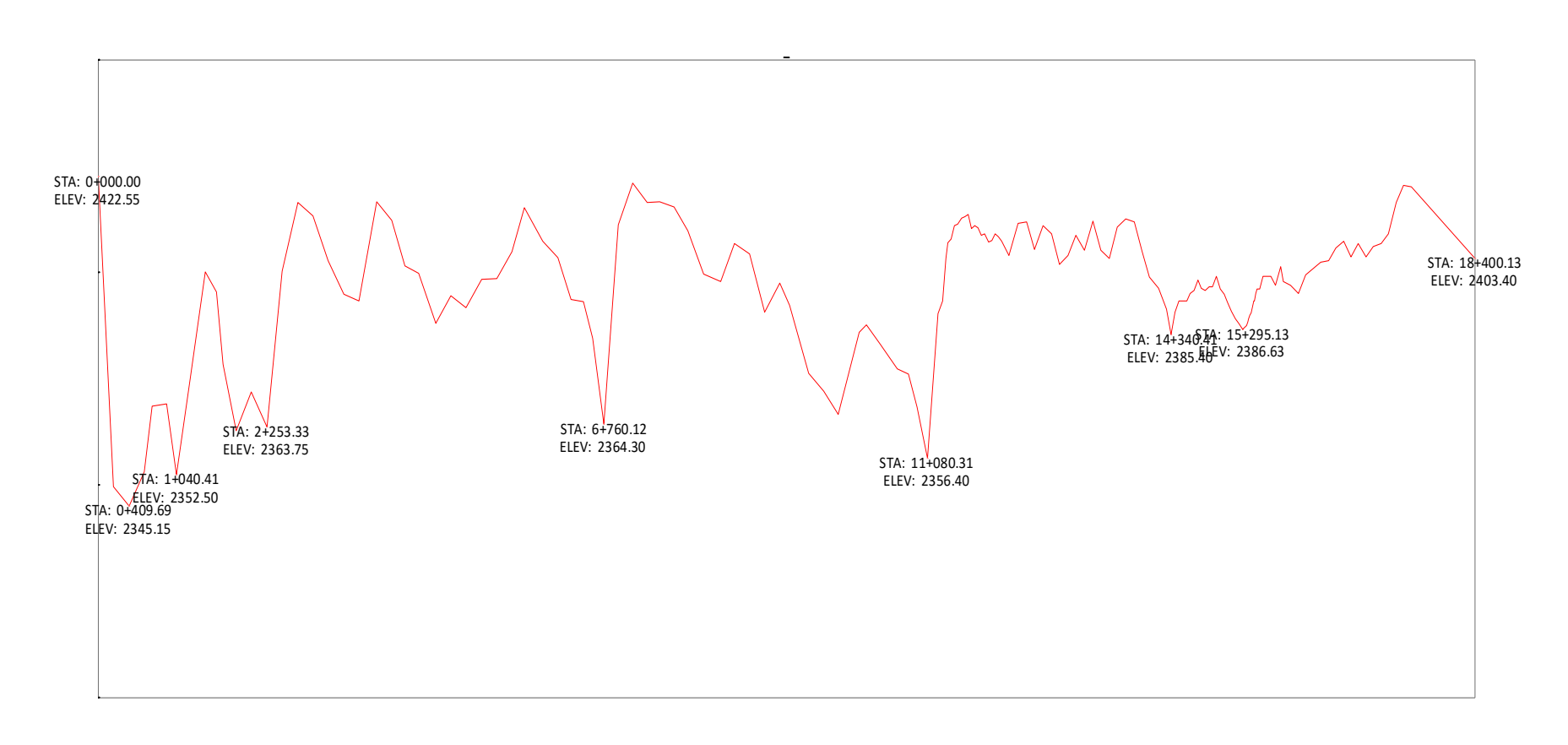


Figure 4. Longitudinal profiles of the LWTP-Terminal Reservoir pipeline

4.2. Discharge Determination (Raw and Treated)

A single value of the flow has no significance in designing a hydroelectric power plant because the flow rate fluctuates considerably in a year, even in a single hour, especially in water supply pipelines. If these fluctuations are not considered in the design stage, the plant may only work efficiently for a short period, resulting in a wasteful investment. The raw water is conveyed from Dire Retention Dam through DN700 and then DN600 and from the Legedadi retention Dam via DN900 pipe. Then after, the raw water from two retention dams are combined at a junction and fed into the treatment plant via a single pipe of DN1200. The flow rates are measured at the inlet of the treatment plant with the help of an electromagnetic flow meter connected to a pipe. The hourly flow duration curve yields average flow rates of 1.82 m³/s and 1.47 m³/s at 50% and 90% probability of exceedance (Figure 5). The flow variation in the raw water main is small because there are no off-takes along the line. The only variations that may exist are due to leakages and transmission losses along the line. The raw water flow can also be theoretically estimated if the head between inlet and outlet is known, as well as the pipe size, type, and total length.

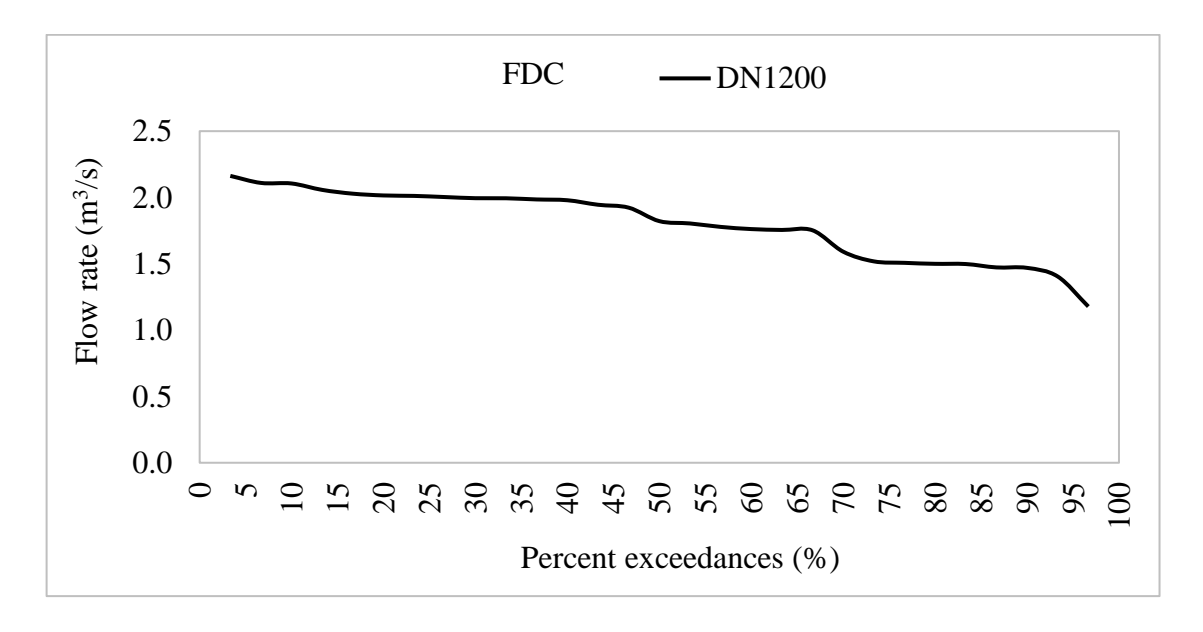


Figure 5. Flow duration curve for raw water main (DN1200).

Using flow information from system records, the flow variations of the treated water mains were determined statistically by calculating the mean (average) and standard deviation. The variations between the outflows (i.e., Legedadi clear water tanks) and inflows (i.e., Terminal service reservoir)

points were compared. As illustrated in Figure 6, the flow variations for DN900 were quite larger than DN1200 owing to several off-takes tapped along the transmission mains. For instance, there are four off-take points for the DN900 pipeline near Civil Service University, Saint Michael Church, CMC roundabout, and Ayat roundabout, whereas for the DN1200 pipeline, there are only two pipelines near CMC roundabout and Saint Michael Church. Off-takes create pressure drop along the pipeline thus reducing the flow rates downstream. Because of leakage at fittings along the transmission mains, the flow rate may be reduced. This makes the DN1200 transmission line the most preferable site for integrating an in-pipe turbine system for hydropower generation.

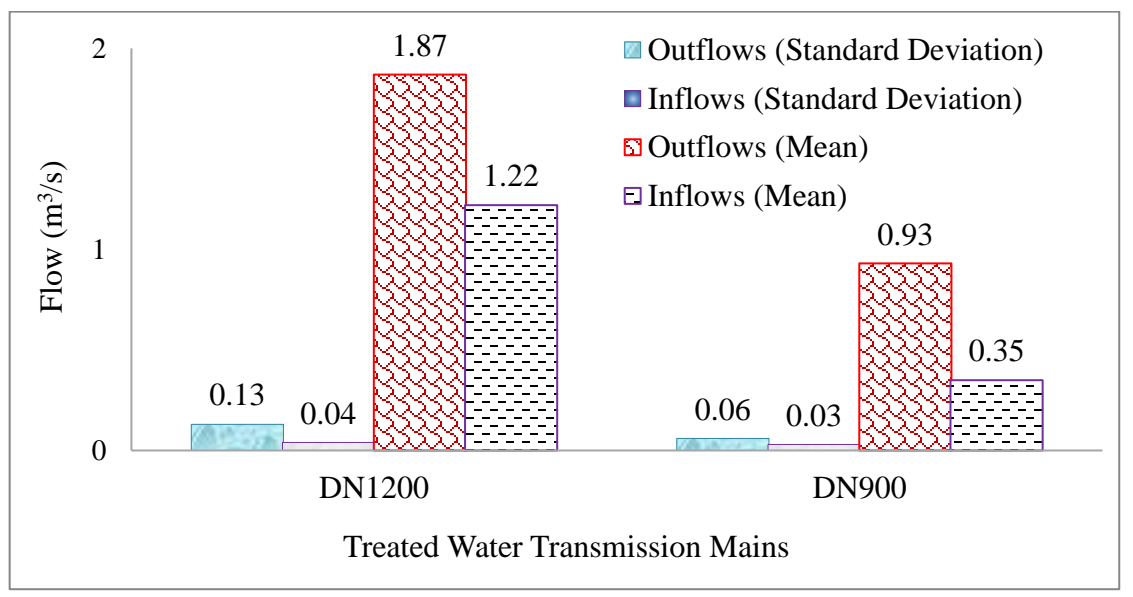


Figure 6. Inflows and Outflows for DN900 and DN1200

Flow duration curves for the inlet point at terminal reservoirs for both DN900 and DN1200 transmission mains are shown in Figure 7. The discharge values for DN1200 treated water main at 50 and 90 percent of exceedience were (1.24m³/s and 1.14m³/s, respectively). According to the FDC analysis, the values for DN900 at the same levels of exceedence were 0.34 and 0.29 m³/s. Because of high flow variations in a pipe, the FDC for treated water mains was nearly horizontal, as shown in the figure. The variations in flow could be ascribed to leakage along the transmission mains and off-take points, as indicated previously. The duration curves showed the expected flow profiles.

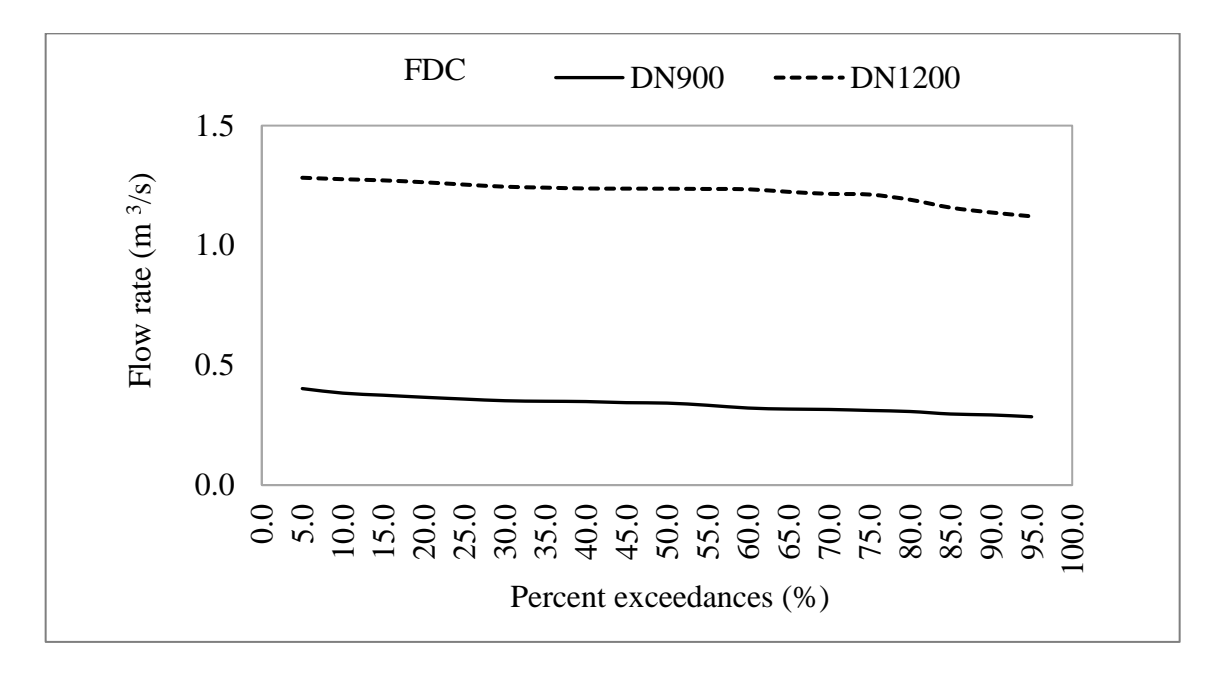


Figure 7. Flow duration curve for treated water mains (DN900 and DN1200)

4.3. Summary of Potential Sites

The identification of potential sites enables the determination of the potential power. This section summarizes the potential sites depending on both discharge and head. There are two main potential areas in the Legedadi Water Supply Scheme: Legedadi Water Treatment Plant and Kotebe Terminal Reservoirs. The location of the site for hydropower generation should be preferably before water treatment works (Kucukali, 2011) because it would be easier to extract more raw water to compensate for the losses. However, in the case of treated water, compensation might be restricted by the capacity of the treatment plant. Another reason was that when the external system was to be installed on treated water mains, they would likely compromise the quality of water. Due to this reason, it is recommendable to locate hydropower sites before the water treatment works or the distribution network (Loots et al., 2015). In this study, potential sites were identified for both raw and treated water mains. For the raw water main, there was only one potential site owing to the short distance between the intake and the treatment plant. This site was identified by its head and discharge. For treated water mains, eight sites were identified using the same criteria at the raw water pipe. Table 1 shows all the potential sites for both raw and treated water mains. Tables 2 and 3 show the RET raw and treated screen output parametres.

Table 1. Potential site for Raw and Treated water mains

Raw Water Main									
Site	Elevation (m)	Distance to intake (m)	Gross head (m)	Diameter (mm)	50% Primary flow (m ³ /s)	90% Secondary flow (m ³ /s)			
TP	2447.54	550	12.46	DN1200	1.82	1.47			
	Treated Water Mains								
					50% Primary flow (m³/s)	90% Secondary flow (m ³ /s)			
Sites	Elevation (m)	Distance to TP (m)	Gross head (m)	Diameter (mm)	DN 1400 and 1200	DN 1400 and 1200			
1	2345.2	0+409.69	77.35	1400	1.72	1.42			
2	2352.5	1+040.41	70.05	1400	1.72	1.42			
3	2363.8	2+253.33	58.75	1400	1.72	1.42			
4	2364.3	6+760.12	58.25	1400	1.72	1.42			
5	2356.4	11+080.31	66.15	1200	1.24	1.14			
6	2385.4	14+340.41	37.15	1200	1.24	1.14			
7	2392.1	15+295.13	30.45	1200	1.24	1.14			
TR	2403.4	18+400.13	19.15	1200	1.24	1.14			

Power and Energy estimation using RET Screen

Table 2. RET Screen output parameters for raw water main

Parameters						
Gross head (m)	12.46					
P50 (Kw)	186					
P90 (Kw)	150					
E50 (Mwh)	1,397					
E90 (Mwh)	1,208					

Table 3. RET Screen output parameters for treated water mains

DN1200								
Gross heads (m) P50 (kw)	77.35 639	70.05 579	58.75 487	58.25 483	66.15 548	37.15 310	30.45 254	19.15 159
P90 (kw)	587	532	448	444	503	284	233	146
E50 (MWh)	5,066	4,594	3,862	3,830	4,342	2,454	2,013	1,264
E90 (MWh)	4,790	4,344	3,652	3,621	4,105	2,319	1,903	1,193
			DN900					
Gross heads(m)	77.35	70.05	58.75	58.25	66.15	37.15	30.45	19.15
P50 (kw)	189	171	144	143	162	91.5	75.1	47.2
P90 (kw)	168	152	128	127	144	81.6	67	42.2
E50 (MWh)	1463	1327	1116	1106	1254	710	583	366
E90 (MWh)	1371	1244	1046	1038	1176	666	547	344

From power potential considerations for treated water mains, all the sites were most favorable except the inlet of the Terminal Reservoir (site having a head of 19.15 m). However, extracting power at these sites will result in a significant reduction in the flow downstream. These sites are also far from the centers that give power service, so there will be transmission losses along the power lines. Therefore, for the above-mentioned reasons, the inlet of the Terminal Reservoir for the treated water mains was selected as the most suitable site.

Impact Characterization of Generating Power on Exixting System

The impact of generating power from an existing system can be characterized by comparing flow, head, and power produced. Figure 8 shows the relationship between the power output and the percentage reduction in flow for the selected site at a head of 12.46 m. For instance, at 158 kw power output, the percentage flow reduction was 2.04% (0.03 m³/s), while at 167 kw power output the percentage flow reduction was 6.8% (0.1 m³/s) for the DN1200 (raw water main).

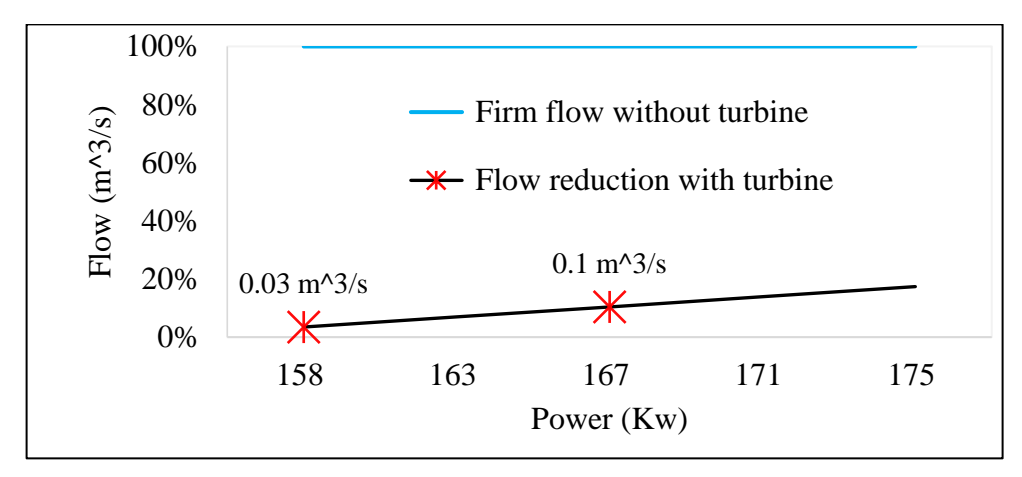


Figure 8. Percentage flow reduction against power at the raw water pipe

The relationship between the power output and the flow reduction for the treated water mains at a selected site of head of 19.5 m is shown in Figure 8. Compared to the raw water mains, the reduction in flow of the treated water mains was two times less per unit power output. In the case of raw water, the reduction was 0.6 liters per kW, while for treated water mains it was 0.3 liters per kW. The reduction of treated water, on the other hand, would be more sensitive than the raw water mains because it could affect the service reservoir level.

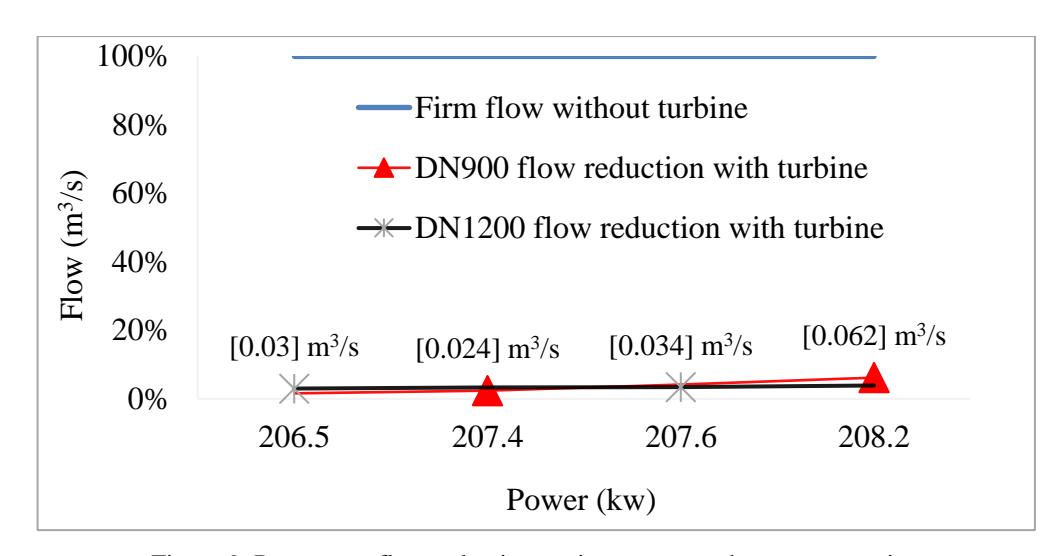


Figure 9. Percentage flow reduction against power at the raw water pipe

Financial viability

The selection of project classification is an important parameter for the correct evaluation of project costing. This is due to larger projects requiring more traditional designs with higher associated risks. The other parameters that affect the financial evaluation were the type of hydro systems selected and

the grid type either isolated or connected with central. It is assumed that like other micro projects, the inflation rate of Ethiopia for the year 2020 was considered at 19.5%. The life of the project was 20 years, with a 70% loan of the initial cost, with an interest rate of 7% and a debt term of 15 years. So, 322,700\$ was obtained from a loan, and 138,300\$ came from the investors, or the equity portion. The total initial cost of the project was 461,000\$. The annual cost and debit payment for the 15-year time period was 40,978\$ which included the operation and maintenance costs. The annual electricity export revenue was estimated to be 75,946\$. Similarly, the hydropower project for the treated water lines (DN1200 and DN900) provided power for 20 years. According to cost analysis, the total initial cost of the project was 414,500\$ (for DN1200) and 135,900\$ (for DN900). So, 290,150\$ (for DN1200) and 95,130\$ (for DN900) were obtained from a loan, and 124,350\$ (for DN1200) and 40,770\$ (for DN900) came from the investors or the equity portion. The annual cost and debit payment for the 15-year time period were 38,074\$ (for DN1200) and 11,669\$ (for DN900), which included the operation and maintenance costs. The annual electricity export revenue was estimated to be 75,068\$ (for DN1200) and 18,842\$ (for DN900) (Table 4).

Table 4. Financial Viability

Cases	DN1200	DN1200	DN900
Cases	(Raw)	(Treated)	(Treated)
Generated energy (Mwh)	1,208	1,193	344
Estimated total cost (\$)	461,000	414,500	135,900
Annual saving (\$)	75,946	75,068	18,842
Pre-tax IRR-equity (%)	2.4	1.9	4.9
Pre-tax IRR-assets (%)	positive	positive	Positive
Simple payback (yrs.)	6.5	6	7.7
Equity payback (yrs.)	3.9	3.3	5.5
Benefit-cost (B-C) ratio	1.4	1.4	1.1

The hydropower project in the Legedadi Water Transmission Line was feasible according to RET Screen-small Hydro Model as the Net Present Value (NPV) and Internal Rate of Return (IRR) for both raw and treated water sites were positive and the benefit-cost ratio (B/C) was above one which is shown in (Table 4). The simple payback was 6.5 years and 6 years for raw and treated water sites, respectively (Table 4). According to the analysis, the raw water main and treated water main (DN1200) had the best benefit-cost ratio; hence it can be concluded that it was better to generate power from it.

5. CONCLUSIONS AND RECOMMENDATIONS

Adequate head and flow are requirements for hydropower generation. The Legedadi Water Supply Scheme has the potential to produce electricity. The raw water pipe had a gross head of 12.46m, an average flow of 1.47 m3/s (available 90% of the time), and provided 150 kW for a 1200 mm diameter pipe with a total length of 550 m from the intake. The treated water pipes had a gross head of 19.5m, average flows of 1.14 m3/s (available 90% of the time), and produced 146 kw and 42.2 kW for 1200 mm and 900 mm diameters, respectively, with a total length of 18.4 kilometers. As to the analysis, the hydropower size from the pipes of Legedadi water supply transmission falls in the range of Pico-to Small-scale Projects in general and can be taken as a mini hydropower project in particular. According to economic analysis the project is feasible.

Certainly, more precise results would be realized in the case of considering detailed data considering the quality of pipe flow data and actual survey data of the pipeline that determine the power potential of the water supply scheme, which were not considered in this study. Hence, the results of this study should be taken as an initial basis for further studies of power assessment.

REFERENCES

- Bruno, S. G., Chou lot, A., & Denis, V. (2010). Energy recovery in existing infrastructures with small hydropower plants.
- Capuano, L. (2018). International energy outlook 2018 (IEO 2018).US Energy Information Administration (EIA): Washington, DC, USA, 2018, 21.
- Capuano, L. (2018). International energy outlook 2018 (IEO 2018).US Energy Information Administration (EIA): Washington, DC, USA, 2018, 21.

- Kucukali, S. (2011). Water supply lines as a source of small hydropower in Turkey: A Case in Edremit. Paper presented at the World Renewable Energy Congress 2011, Linkoping, Sweden.
- Kumar, P., & Shahid, M. (2017). Harvesting Electricity from Water MainsHydropower System Generates Power from WaterPipelines International Journal of Advance Research in Science and Engineering, 6(8), 732-739.
- Kusre, B., Baruah, D., Bordoloi, P., & Patra, S. (2010). Assessment of hydropower potential using GIS and hydrological modeling technique in the Kopili River basin in Assam (India). Applied Energy, 87(1), 298-309.
- Loots, I., van Dijk, M. Barta, B. van Vuuren, & S. J. Bhagwan, J. N. (2015). A review of low head hydropower technologies and applications in a South African context. Renewable and Sustainable Energy Reviews, 50, 1254-1268. DOI:10.1016/j.rser.2015.05.064
- Muhammad W., Bin C., Tasawar H., Ahmed A., & Bashir A. (2016). Energy consumption for water use cycles in different countries: A review. Applied Energy, 868–885.

 DOI:10.1016/j.enconman.2014.04.057
- Muhsen, H., Ibrahim, M., Alsheikh, A., Qanadilo, M., & Karadsheh, A. (2019). Turbine Design and Its Impact on Energy Harvesting from In-Pipe Hydro Systems. International Journal of Mechanical Engineering and Robotics Research, 8(5).
- Samora, Manso, Mário, Anton, & Helena. (2016). Energy Recovery Using Micro-Hydropower Technology in Water Supply Systems: The Case Study of the City of Fribourg Water, 8(344), 1-16. DOI:10.3390/w8080344

Evaluation of Three Low-Cost Particulate Matter (PM2.5) Sensors for Ambient and High Exposure Conditions in Arba Minch, Ethiopia

Johannes Dirk Dingemanse

Faculty of Water Supply and Environmental Engineering, Water Technology Institute, Arba Minch University, Ethiopia. Email: johannesdirk.dingemanse@amu.edu.et

ABSTRACT

The burden of disease from ambient and indoor air pollution is highest in low-income countries, while their resources for monitoring air pollutants are the lowest. PM2.5 is the primary indicator of air pollution. Reference monitors of PM2.5 are expensive, but there is an increased use of low-cost sensors (LCS). Three LCS, the UCB-PATS+ (PATS), Airvisual Pro (IQAV) and Sensirion SPS30 (SPSA) are being used in Arba Minch, Ethiopia, but their quality has not yet been evaluated under circumstances common to low-income countries, and the variety of metrics used in evaluation studies make comparisons difficult. This study aims to evaluate the three LCS under circumstances encountered in Arba Minch, with metrics commonly used and officially prescribed. Measurements were conducted with the LCS at 2 ambient and 4 high exposure (kitchen) concentrations, and at four of those locations with the gravimetric reference method as well. The quality of the three LCS was evaluated within identical, with reference, and between different types, with commonly reported (regression slope and R²) and officially prescribed (Pearson correlation, bias, accuracy, expanded uncertainty) metrics. The SPSA has low within variation in both ambient and high-exposure situations, meets official requirements compared to the reference, and shows a stable bias across different time and concentration levels. The IQAV and PATS within variations are not up to official standards but show strong linear associations. The IQAVs as a group, and PATSs individually, meet official reference requirements at daily level. Between comparison reveals that all LCS show strong linear associations even at 10-minute average level. For SPSA the association is similar across all ranges, and for the others the association is strong when different ranges are taken into account. Generally, all LCS are a good alternative for expensive reference methods. The strong linear associations suggest the possibility of correcting LCS measurement data based on other studies' results and based on other LCS, across different concentration ranges. Projects with a budget of \$600 can already supply 10 measurement locations. Higher-budget projects can contribute to the quality of low-budget projects when they do not only use expensive monitors, but also LCS at the same location.

Keywords: Airvisual Pro, ambient air pollution, indoor air pollution, low-cost sensors, low- income countries, PM2.5, quality evaluation, UCB-PATS+, SPS30

Received: 08 Sept 2022; accepted 06 Oct.2022

1. INTRODUCTION

Air pollution is one of the top of factors that adversely affects people's health (Babatola, 2018; Gakidou et al., 2017; Shaddick et al., 2018). An estimated 4.2 and 3.2 million premature deaths per year are attributed to ambient (outdoor) and indoor air pollution, respectively (World Health Organization, 2021b, 2022). A common proxy for air pollution, and the pollutant with most health effects, is particulate matter, specifically particles with a diameter of less than 2.5 μm (PM2.5) (World Health Organization, 2021b). The reference method for monitoring PM2.5 is filter-based gravimetry. This method typically assesses concentrations on a 24-hour average level (EPA, 2006; European Commission, 2010), and is associated with high operating costs (Sousan et al., 2021). There are various continuous monitors (monitoring concentrations at hour- or even second level) that are recognized as equivalent to the reference method. These are also expensive, as they cost \$11,500-30,000 per monitor (Mooney et al., 2006). In recent years, there has been an increase in the use of low-cost sensors (LCS) (Sousan et al., 2021). This trend is of utmost importance for low-income countries, where both the burden of disease is high (World Health Organization, 2021b, 2022), and the resources for PM2.5 monitoring instruments are low.

Three PM2.5 LCS (IQAir Airvisual Pro (IQAV), UCB-PATS+ (PATS) and Sensirion SPS30 (SPSA)) have been used for published (Dingemanse et al., 2022; Dingemanse & Dingemanse-de Wit, 2022) and ongoing research projects in Arba Minch. The quality of these LCS have been the subject of different studies. For PATS, Pillarisetti et al. (2017) reported an ordinary regression result of R² of 0.90 (slope 1.5) in comparison with the reference method. Also, they reported an R² of 0.90 (slopes 1.7 – 4.8) in comparison with a continuous monitor, and an R² of 0.96 (slope 0.92) between two identical PATSs., At a non-smoking residence in the United States, Zamora et al. (2020) found an R² of 0.90 in comparison with a gravimetrically corrected continuous monitor, and an R² of 0.99 between two IQAV units. Under ambient conditions, Feenstra et al. (2019) reported an R² of 0.7 with slopes of 0.76-0.87 for the IQAV in comparison with a continuous monitor. Under laboratory conditions, Sousan et al (2021) found Pearson correlations of 0.99 between SPSA and a gravimetrically corrected continuous monitor, with slopes of 0.7 to 2 depending on the particle type, and a variation between identical sensors of 5-20%. Also under laboratory conditions, Nguyen et al. (2021) found an error of 2.7% for the SPSA in comparison

with a continuous monitor at a range of 0-25 μ g/m³, and an error of 16-26% between 50-1,000 μ g/m³. Based on ambient field measurements, Falzone et al. (2020) reported expanded uncertainties lower than European requirements of 25% for the SPSA.

Quality evaluations usually include a comparison of identical LCS and/or a comparison with the reference method or a continuous monitor. The quality of LCS is evaluated with a variety of metrics. Most reported is the R², with corresponding slope and/or intercept from a regression (Karagulian et al., 2019). From a combination of several studies, Karagulian et al. (2019) use an R² of at least 0.75 together with a slope close to 1 to select the best performing LCS. While this metric indicates the strength of association between two variables, it is not necessarily the best indicator of data quality (Karagulian et al., 2019). Official guidelines for testing the equivalence of PM2.5 measurement methods have been made by the Environmental Protection Agency of the United States of America (EPA) (EPA, 2006), the National Institute for Occupational Safety and health (NIOSH) (NIOSH, 2012), and by the European Commission in the Guide to the Demonstration of Equivalence of Ambient Air Monitoring Methods (DEM) (European Commission, 2010). For identical instruments, EPA and NIOSH require a Coefficient of Variation (CV) of +- 10%, while the DEM requires an in-between sampler uncertainty of maximum 2.5 $\mu g/m^3$. For comparison with the reference method, EPA uses the Pearson correlation (r, >=0.97), a slope of 1 ± 0.1 and an intercept of $\pm5~\mu\text{g/m}^3$. The NIOSH requires an accuracy of 25% at 95% confidence level in comparison with the reference method and prescribes correction of the data if the absolute bias is >10%. Like NIOSH, the DEM has set the required uncertainty at 25%, but prescribes detailed formulas for calculating this uncertainty based on orthogonal regression and requires an evaluation of this uncertainty at a concentration level of 30 µg/m³. Data correction is prescribed for slope and/or intercept if those are significantly different from 1 or 0, respectively.

The LCS quality evaluation can be done under various concentration levels. Typical PM2.5 concentration ranges used for ambient testing are 0-40 μ g/m³ (Falzone et al., 2020; Sousan et al., 2021). Indoor or occupational concentrations can be over 2,000 μ g/m³ (Sousan et al., 2021). EPA guidelines and the DEM are for ambient monitoring, which can be seen from the slope +- 5 μ g/m³, in-between uncertainty of 2.5 μ g/m³ and evaluation of uncertainty at concentration level of 30 μ g/m³. The requirements of NIOSH are not specific to a concentration level (both in-between

sampler comparison and accuracy versus the reference method is set at a relative percentage). While a sensor preferably reacts the same under different circumstances, in reality studies find different slopes or correction factors for different concentration levels (Falzone et al., 2020; Nguyen et al., 2021) and particle types (Sousan et al., 2021).

Quality evaluation can also be done on different time periods. Both EPA and the DEM require an evaluation at 24-hour average level. This corresponds with the short-term 24-hour average air quality standard (World Health Organization, 2021a) and matches with the usual time needed to get sufficient filter load for the reference method. Continuous monitors, and LCS alike, can report concentrations at time periods of 1 second. Studies that evaluate LCS at time levels lower than 24-hour use continuous monitors calibrated by the gravimetric reference method as 'reference' (Karagulian et al., 2019), or simply use a continuous monitor as it is (Pillarisetti et al., 2017).

The circumstances and metrics used in LCS quality evaluations do not yet cover the situation encountered in low-income countries. The PATS shows different slopes for different situations (Pillarisetti et al., 2017), warranting its own quality evaluation. The IQAV has been validated only in high-income countries, where 'common residential sources' do not include cooking on biomass or coffee ceremony, old cars, or open waste burning. For high concentrations, the SPSA is evaluated up to 1,200 µg/m³ PM2.5 under laboratory circumstances (Nguyen et al., 2021; Sousan et al., 2021). However, concentration levels in indoor air pollution field circumstances in low-income countries can be much higher than 1,200 µg/m³ (Dingemanse et al., 2022). For the SPSA, under ambient concentrations, different results for two different locations in Belgium are reached (Falzone et al., 2020), and again those are not the ambient circumstances encountered in Ethiopia. Finally, the evaluations of LCS are conducted with a variety of metrics, time averaging periods and concentration ranges, which makes comparison hard. In this study, I present an evaluation of those LCS, based on data gathered in different ongoing research projects in Arba Minch, Ethiopia, with an extensive use of available metrics, time periods and concentration ranges.

The main objective of this study is to evaluate the quality of the IQAir Airvisual Pro, UCB-PATS+, and Sensirion SPS30 under field circumstances common to low-income countries, based on data

gathered in ongoing research projects in Arba Minch, Ethiopia. The evaluation consists of three parts:

- A comparison of identical LCS (within comparison);
- A comparison of LCS with the gravimetric reference method (reference comparison);
- A comparison amongst different LCS (between comparison).

2. MATERIALS AND METHODS

2.1 Study area

Arba Minch town is the administrative center of Gamo Zone, which is one of 14 Zones in the Southern Nations, Nationalities and People's Regional State (SNNPR) of Ethiopia. Three LCS are used in (ongoing) research projects in Arba Minch, Ethiopia. Students have conducted measurements in indoor and ambient situations (Dingemanse et al., 2022; Dingemanse & Dingemanse-de Wit, 2022). At different locations, parallel measurements with multiple instruments have been conducted for quality evaluations. For this study, data from six locations was used: two ambient locations and four restaurant / kitchen locations. The two ambient locations represented low and medium ambient concentrations (in front of a residence in a low-traffic area, and at a hotel compound close to the road in the city center). The four kitchen locations represented high concentrations encountered owing to cooking or coffee preparation with biomass fuel. One location was in a small local restaurant, in a room with coffee preparation and next to a kitchen with biomass fuel cooking. Another location was in the kitchen of a small restaurant with biomass fuel cooking. The two final locations were both in a big kitchen with multiple (>5) cooking fires. While in the same kitchen, the two locations considered different. This is because the instruments were placed at separate locations in the kitchen, and cooking fires closest to those locations were used at different moments, resulting in different concentration patterns. Table 1 gives an overview of the six locations and the instruments used at those locations.

Table 1. Measurement locations, with their LCS and number of reference measurements (n_{ref}). IQAV, PATS and SPSA LCS are identified as respectively Iq_X , Pa_X and Sp_X , in which x denotes the instrument's number.

Location	ID	Air pollution sources	LCS	n_{ref}
Residence	A 1	Neighborhood	Sp1, Sp2, Sp4, Iq1	
Hotel	A2	Traffic, neighborhood	Sp3, Sp5, Iq2	3
Local	K1	Cooking fires, coffee	Sp2, Iq5	
restaurant		preparation		
Kitchen 1	K2	Cooking fires	Sp4, Iq3	3
Kitchen 2a	K3	Cooking fires	Sp6-7, Iq3-5, Pa1, Pa3-4	8
Kitchen 2b	K4	Cooking fires	Sp8-9, Iq6-8, Pa2, Pa5-6	4

2.2 Materials

2.2.1 LCS

This study evaluated three LCS: the UCB-PATS+ (PATS), the Airvisual Pro (IQAV) and the Sensirion SPS30 (SPSA). Individual LCS are coded as Pa1-Pa6, Iq1-Iq8 and Sp1-Sp5, for 6 PATSs, 8 IQAVs and 5 SPSAs, respectively. All three LCS types estimate the PM2.5 concentration based on scattering of IR light (Pillarisetti et al., 2017; Sousan et al., 2021; Zamora et al., 2020). The PATS and IQAV are commercially available 'plug-and-play'-instruments, meaning that the particle sensor is built into a case with other components for data storage and usability. The SPSA is only a particle sensor that needs to be connected to either a computer or a microprocessor together with other components for data storage and access. For this study, data collection with the SPSA was done by connecting it to an Arduino Mega microprocessor, together with a micro-SD module, a DS3231 real-time clock and a power bank. The PATS is designed for personal sampling and (high) indoor concentrations, but not for low ambient concentrations (lower detection limit is 10 µg/m³). In this study, the PATS was not used at ambient locations A1 and A2. The IQAV is used both in ambient and indoor situations but is not meant for very high concentrations ($>5,000 \,\mu g/m^3$), since the highest reported value of the IQAV is set to 4,488 $\mu g/m^3$. On the SPS30, no such minimum or maximum values are set (the sensor needs to be programmed by the user), but the manufacturer specifies a range up to 1,000 µg/m³. Table 2 gives an overview of the most important characteristics of the three LCS.

Table 2. Specifications for the LCS evaluated in this study

Parameter	PATS	IQAV	SPSA
Name	UCB-PATS+	AirVisual Pro	Sensirion SPS30
Range	10-50,0000	0-4,488	0-1,000
Logging interval	>2s	>10s	>1s
Cost (\$)	500	269	30^{a}
Internal storage	Yes	Yes	No ^a
Internal battery	+36 hours	2-4 hours	No ^a

a. The SPSA needs additional costs for battery and data storage. The total set-up as used in this study has a cost of approximately \$60.

2.2.2 Reference instrument

Reference measurement methods for PM2.5 are based on gravimetry. As reference instrument, the Ultrasonic Personal Aerosol Sampler (UPAS) was used, as this instrument was the only available gravimetric instrument in Arba Minch, Ethiopia. The UPAS is a gravimetric instrument designed for measuring medium to high concentrations. . A filter is loaded with particles with a flowrate of 1 l/min. A cyclone ensures that only particles with a diameter smaller than 2.5 μ m enter the inlet. Over ranges of 20-1,000 μ g/m³, Volckens et al. (2017) found strong correlations with the EPA federal reference method. Afshar-Mohajer et al. (2021, p. 131) found that "the UPAS may be a suitable alternative for [Respiratory Dust] mass sampling" for ranges of 100-500 μ g/m³ in occupational settings. For gravimetric analysis of the filters, a Mettler AE240 Dual Range balance was used, having a readability of 10 μ g and a reproducibility of \pm 20 μ g (IET, n.d.).

2.3 Methods

2.3.1 LCS measurements

All instruments were fixed at 1.5- 2 meters high and connected to a power source. The measurement frequency of the LCS ranged from 10 seconds to 3 minutes. For this study, all data was averaged to 10-minute time periods. Figures A1 and A2 in the Annex show the data availability for all LCS at all locations, as well as the concentration ranges encountered at those locations. At location A2, power was switched off during nighttime. As a result, there was approximately 50% data loss for Iq2 at location A2. At locations A1 and A2 (as reported by the

SPSA), daily averages ranged between 3-30 and 10-50 $\mu g/m^3$. 99%-percentile of 10-minute averages were 70 and 107 $\mu g/m^3$, respectively. At locations K1 through K4, hourly averages ranged from 2 to higher than 10,000 $\mu g/m^3$ for the SPSA. 99% percentile 10-minute averages were 30,000, 13,000, 3,000 and 1,300 $\mu g/m^3$, respectively.

2.3.2 Reference measurements

Measurements with the reference instrument were conducted 3 times 48 hours at location A2, and 24-hours (or up to a full filter) 3 times at locations K2, 4 times at K3 (2 instrument) and 4 times at K4. Table 3 shows an overview of the reference measurements.

Table 3. Details of reference measurements conducted at locations A2, K2, K3 and K4, and the LCS at those locations.

No.	Loc.	Start	Duration	Filter load	Parallel LCS
			(hour)	(µg)	
1	A2 ^a	'21-10-01 12:19	48	90	Iq1, Sp3, Sp5
2		'21-10-03 12:35	48.3	110	
3		' 21-10-06 17:54	47.4	130	
4	K2	. 21-10-01 11:38	20	1,460	Iq3, Sp4
5		'21-10-03 12:55	16.4	970	
6		' 21-10-04 09:56	20.6	1,390	
7	К3	. 22-06-08 15:15	21.3	340	Sp6, Sp7,
8		. 22-06-09 13:02	22.1	210	Iq3, Iq4, Iq5,
9		' 22-06-13 10:40	23.7	1,130	Pa1, Pa3, Pa4
10		. 22-06-14 11:13	23.6	430	
11		' 22-06-08 15:12	21.2	350	
12		. 22-06-09 13:03	22.1	240	
13		'22-06-13 10:46	23.6	1,130	
14		²²⁻⁰⁶⁻¹⁴ 11:14	23.6	430	
15	K4	'22-06-08 15:10	21.4	500	Sp8, Sp9,
16		'22-06-09 13:22	21.9	320	Iq6, Iq7, Iq8,
17		²²⁻⁰⁶⁻¹³ 10:59	23.5	610	Pa2, Pa5, Pa6
18		²²⁻⁰⁶⁻¹⁴ 11:05	24.0	560	

a. Only three filter comparisons are available at A2, and these should be seen as indicative, as the instrument in combination with the available analytical scale is not designed for such low concentrations. Even with 48-hour use, the filter load is only 90-130 µg, which with a repeatability of 20 µg gives an uncertainty of 15-22% for only the gravimetric analysis.

2.4 Data corrections

Between '21-10-05 and '22-03-05 Sp1 at location A reported the time with a 1-to-5-hour delay. This data was shifted based on visual inspection of the daily morning and afternoon concentration peaks.

The DEM allows for removal of up to 2.5% percent of outliers based on Grubb's outlier test at 99% level (European Commission, 2010). This outlier removal was done for Sp3 and Sp5 at location A2.

Only for purpose of the comparison with the reference method at location A2, the missing data of Iq1 was filled by data from Sp3. The slope resulting from orthogonal regression techniques as prescribed in the DEM, based on available data pairs between Sp3 and Iq1, was used to predict the missing data of Iq1 missing data based on data of Sp3.

At locations K3 and K4, there was data loss during the reference measurements. LCS results with more than 15% data loss during measurements with the reference method are not used in the reference comparison.

2.5 Quality evaluation

2.5.1 Within comparison

To compare identical samplers, the linear association was quantified with the slope (S) resulting from Ordinary Least Squares (OLS) regression without intercept, and the corresponding coefficient of determination (R^2). Furthermore, the coefficient of variation (CV) and in-between sampler uncertainty (u_{bs}) were calculated.

The **Coefficient of Variation** (CV) was calculated with equation 1 (Sousan et al., 2016):

$$CV = \frac{1}{n} \sum_{\mu_i} \frac{\sigma_i}{\mu_i} \tag{1}$$

Where, σ_i is the standard deviation and μ_i is the mean of measurements of identical LCS during time period i, and n is the number of time periods.

The **in-between sampler uncertainty** (u_{bs}) was calculated with equation 2 (European Commission, 2010):

$$u_{bs} = \sqrt{\frac{\sum (y_{i,1} - y_{i,2})^2}{2n}} \tag{2}$$

Where, $y_{i,1}$ and $y_{i,2}$ are the results of parallel measurements for time period i, and n is the number of time periods.

2.5.2 Reference comparison

Pearson correlation coefficient (r), slope (S) and corresponding R^2 based on OLS regression without intercept, accuracy, bias and expanded uncertainty were computed to for the comparison with the reference instrument.

EPA has requirements concerning slope and intercept. In all situations, the regression of slope without intercept yielded either a higher R^2 than the R^2 for regression with intercept, or a very high R^2 (>=0.97). Therefore, for this study only results for regressions without intercept were included. The **bias** (B) was calculated with equation 3 (NIOSH, 2012):

$$B = \frac{1}{n} \sum \left(\frac{x_i}{y_i} - 1 \right) \tag{3}$$

Where, x_i is the concentration of the LCS and y_i the concentration of the reference instrument for time period i, and n is the number of time periods.

The **accuracy** (Ac) is "the theoretical maximum error of the measurement, expressed as the proportion or percentage of the amount being measured, without regard for the direction of the error, which is achieved with 0.95 probability" (NIOSH, 2012, p. 3). The accuracy should be lower than 25%. The accuracy was calculated as the upper value of the confidence interval at 90% of the relative difference between the LCS measurement reference measurement. For this, all $\frac{x_i}{y_i}$ values were calculated, and the confidence interval at 90% was calculated based on these values.

If |B| is higher than 10%, NIOSH prescribes to correct the bias in the data. Equation 4 was used for calculating corrected data x_{new} based on the old data x_{old} .

$$x_{new} = \frac{x_{old}}{B+1} \tag{4}$$

The names Ac_BC and Ac_AC were used to distinguish between accuracy before and after correction, respectively.

The expanded uncertainty (W_{CM}) of the LCS versus the reference instrument is calculated at a level of 30 μ g/m³, and should be maximum 25% (European Commission, 2010). A linear relationship between the LCS and reference data is assumed. For establishing this linear relationship, algorithms of orthogonal regression should be used. If slopes are significantly different from 1, and/or the intercept is significantly different from 0, the DEM prescribes to correct the data for this slope and/or intercept. Formulas are extensively shown in the DEM (DEM section 9.5 and DEM Appendix B). To distinguish between W_{CM} before and after correction, the names W_{CM_BC} and W_{CM_AC} were used, respectively. In all data comparisons conducted in this study, the slope without intercept was significant. For that reason, all reported W_{CM_AC} were based on correction for slope only.

2.5.3 Between comparison

For comparison of different LCS, accuracy and expanded uncertainty were used to quantify the degree of equivalence. W_{CM} is used at a level of 30 μ g/m³ with averages of 24-hour time-periods (European Commission, 2010). Therefore, this metric was used for comparing 24-hour averaged data of LCS at ambient locations (A1 and A2). The accuracy was used as metric for all comparisons at the high-exposure locations (K1-K4) and for all comparisons of averages over time periods smaller than 24 hours. Additionally, for comparability with other studies, R^2 for OLS regression without intercept has been calculated.

2.5.4 Quality evaluation summary

Table 4 gives a summary of the quality evaluation metrics used in this study.

Table 4 Summary	z of anali	ty metrics	used for	evaluating	LCS	measurement results.
Table T. Sullilliai	or quan	ty mounts	uscu ioi	Cvanuaning	$L \cup D$	incasurement results.

Evaluation	Metric	Locations	Reference	Score / requirement
Within LCS	S & R ²	All	Often used	$R^2 > 0.75$ at least; $R^2 > 0.9$ 'very
				good'
	CV	All	EPA, NIOSH	<10%
	u_{bs}	A1, A2	DEM	$<2.5 \mu g/m^3$
Reference	R	All	EPA	>0.97
	S	All	EPA	1 ± 0.1
	\mathbb{R}^2	All	Often used	$R^2 > 0.75$ at least; $R^2 > 0.9$ 'very
				good'
	B & Ac	All	NIOSH	Correction if $ B > 10\%$,
				Ac<25%
	\mathbf{W}_{CM}	A2	DEM	Correction for slope,
				W_{CM} <25%
Between LCS	S & R ²			$R^2 > 0.75$ at least; $R^2 > 0.9$ 'very
		All	Often used	good'
	W_{CM}	A1, A2	a	Correction for slope,
				W _{CM} <25%
	B & Ac	All	a	Correction for B, Ac<25%

a. There is no official reference for quality metrics of LCS inter-comparison, because technically even if there is big difference, it is not known which of the LCS is right. Nevertheless, the W_{CM} and accuracy metrics of EGDE and NIOSH are used to express the agreement between two different LCS.

2.6 Data processing software

All data processing and visualization was done with Python 3.8 (Python Core Team, 2020), with the packages Numpy (Harris et al., 2020), Pandas (The pandas development team, 2020), Matplotlib (Hunter, 2007) and Scipy (Virtanen et al., 2020). All data used and code created in this study is made available on the OSF repository, *https://doi.org/10.17605/OSF.IO/YTV79*.

3. RESULTS

3.1 Within comparison

Figure 1 shows the slopes of regressions without intercept and corresponding R^2 values for one LCS versus one or more identical LCS.

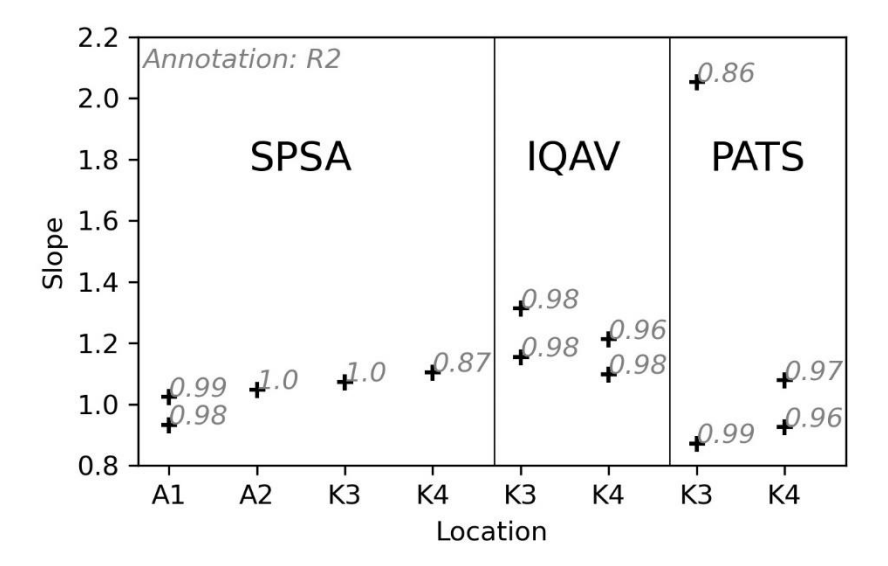


Figure 1. Slopes, annotated with corresponding R2s, between identical LCS at all measurement locations. For locations with three identical LCS, two slopes are shown (instrument 1 vs 2 and instrument 1 vs 3).

Slopes of the SPSA were close to 1, ranging from 0.93 to 1.10. This implies that the different SPSAs showed a similar signal. Identical IQAVs showed higher variation (slopes 1.10-1.31). The PATS at location K4 showed also relatively small slopes (0.93-1.08), but at K3 variation between identical PATSs was high (slopes 0.87-2.05). R²s were generally very good, except for the SPSA at location K4 (0.87) and one PATS at K3 (0.86).

Similar results can be seen from the CV and u_{bs} . Figure 2 shows the CV for all locations, and the u_{bs} for only ambient locations.

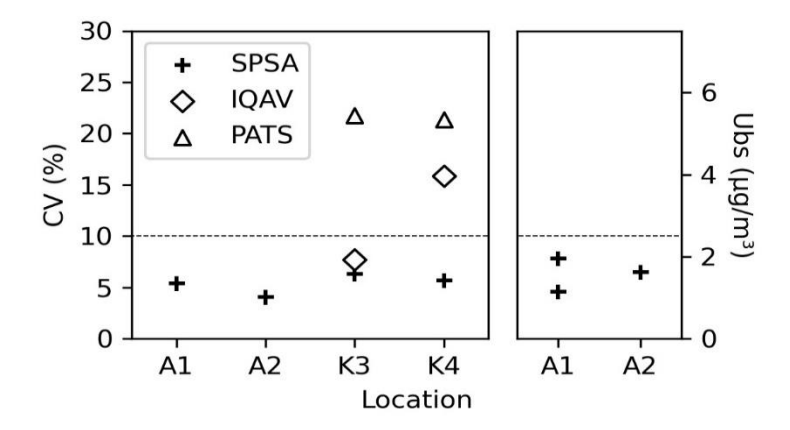


Figure 2. Coefficient of variation (CV) and in-between sampler uncertainty (ubs) for the LCS at different locations.

At all locations, the CV of the SPSA was lower than the required 10%. At the ambient locations, the u_{bs} was lower than the required 2.5 μ g/m³. The IQAV at K4 showed higher variation (CV 16%) while the PATS showed high variation at both kitchen locations (22 and 21%). This implies that those individual sensors might require separate calibrations.

3.2 Reference comparison

Figure 3 shows all filter measurement results with averages of parallel LCS measurements during the same time period.

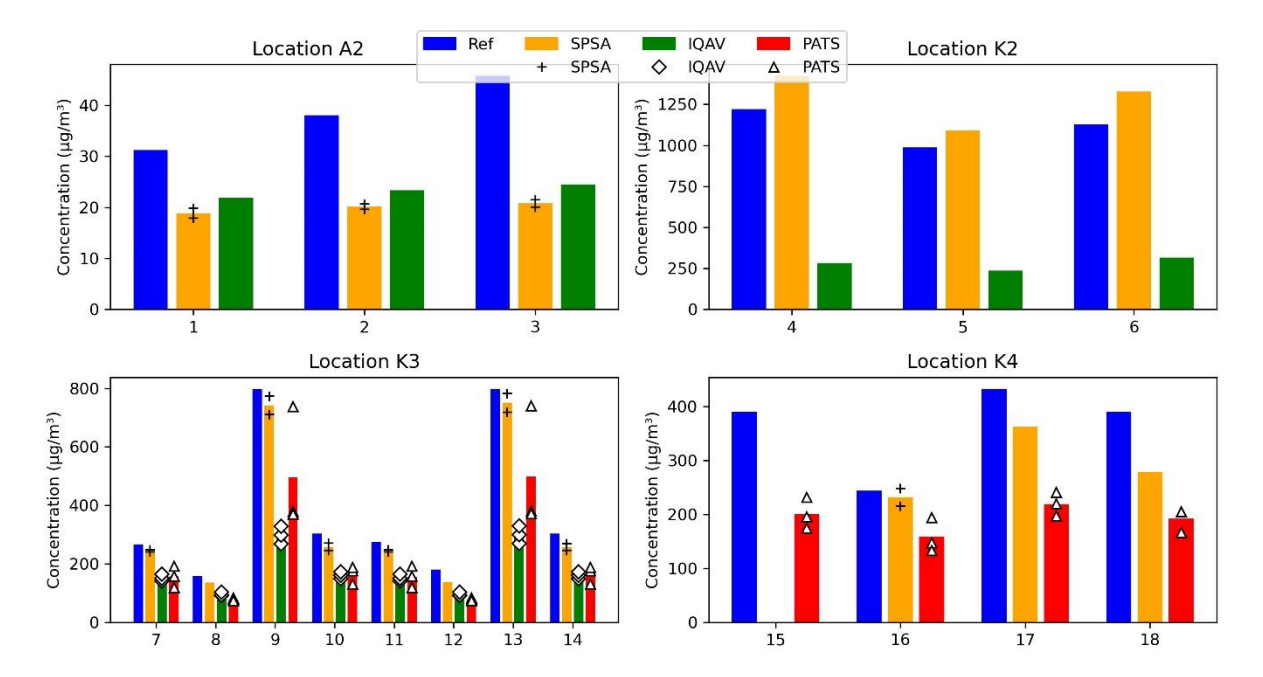


Figure 3. PM2.5 measurement results for all 18 reference measurements and parallel LCS measurements. With multiple identical LCS, results are shown with markers, and average results are shown with bar.

Filter measurement results at location A2 ranged from 31-46 μ g/m³. Filter measurements at the kitchen locations ranged from 158 to 1,220 μ g/m³. Table 5 shows the quality evaluation for individual instruments and groups of identical instruments at location A2.

Table 5. For location A2, the number of data pairs (n), and results for quality metrics in the comparison of LCS with the reference method.

LCS	N	r	S, R^2	Acc_BC	В	Acc_AC	W_{cm_BC}	W_{cm_AC}
Sp3	3	0.93	2, 0.99	60	-	21	542	38
					0.49			
Sp5	3	1.00	1.9,	59	-	24	614	42
			0.98		0.45			
Sp3,5	6	0.70	1.9,	53	-	16	567	27
			0.98		0.47			
Iq1	3	0.99	1.7,	52	-	22	306	37
			0.99		0.38			

Pearson correlations between individual LCS and the reference method were good (>0.93), but were lower when all SPSA measurements were combined (0.7). Interestingly, all R^2 values were very high (>0.98). The slopes and biases showed the need for corrections (LCS results were lower than reference results), but after bias correction, all LCS reached the required 25% accuracy (16-24%). The best accuracy was reached when all data of the SPSA were combined. This combination was also the only dataset that came close to the requirement of W_{CM} (25%).

Table 6 shows the quality evaluation at locations K2-K4. Results are shown for individual LCS, combinations of identical LCS at the same locations, and combinations of identical LCS across all kitchen locations.

Table 6. The number of data pairs (n), and results for quality metrics in the comparison of LCS with the reference method.

Location	LCS	n	r	S, R^2	Ac_{BC}	Bias	Ac_{AC}
K2	Sp4	3	0.99	0.9, 1	22	0.15	5
	Iq3	3	0.69	4, 0.99	79	-0.75	14
K3	Sp6	8	1.00	1.1, 1	18	-0.15	7
	Sp7	6	1.00	1, 1	10	-0.07	
	Sp6,7	14	1.00	1.1, 1	14	-0.12	7
	Iq3	8	0.99	2.6, 0.96	59	-0.53	22
	Iq4	8	0.99	2.4, 0.97	55	-0.50	19
	Iq5	8	0.99	2.1, 0.97	51	-0.45	19
	Iq3-5	24	0.97	2.3, 0.96	52	-0.49	17
	Pa1	8	0.99	2, 0.99	50	-0.47	12

Location	LCS	n	r	S, R^2	Ac_ _{BC}	Bias	Ac_AC
	Pa3	8	1.00	1.1, 0.98	44	-0.32	30
	Pa4	8	1.00	2.2, 1	57	-0.56	6
	Pa1,3,4	24	0.88	1.5, 0.9	50	-0.45	26
K4	Sp8	3	0.93	1.2, 0.99	34	-0.19	15
	Sp9	1					
	Sp8,9	4	0.90	1.2, 0.99	28	-0.14	20
	Pa2	4	0.96	1.8, 1	50	-0.45	11
	Pa5	4	0.96	2.2, 1	59	-0.53	15
	Pa6	4	0.73	1.7, 0.98	55	-0.39	30
	Pa2,5,6	12	0.69	1.9, 0.98	51	-0.46	19
K2-4	Sp6-9	21	0.99	1, 0.98	15	-0.08	
K2,4	Iq3-5	27	0.91	2.7, 0.92	56	-0.52	25
K3,4	Pa1-6	36	0.87	1.6, 0.92	49	-0.45	22

Pearson correlations were good (>0.9) in all cases, except for Iq3 at K2 (0.69), all PATSs combined at K3 (0.88), Pa6 at K4 (0.69) and all PATSs of all locations (0.87). The EPA requirement (>0.97) was met by multiple LCS, and most notably by the combination of all SPSA across all kitchens. This implies that the relationship between the SPSA and the reference was not location dependent. For SPSA, slopes were generally close to 1 (0.9-1.2 for individual, and 1.0 for all combined) with corresponding R²s >0.98. IQAVs showed slopes of 2-4 while the PATSs showed slopes of 1.1-2.2. When corrected for the bias, almost all LCS reached the required accuracy of 25%. The required accuracy was not reached by Pa3 (30%), the combination of PATSs at K3 (26%) and Pa6 (30%). All SPSAs combined did not require bias correction because |B|<10% (-8%).

Generally, all LCS had a good to very good correlation with the gravimetric reference method, and with corrections requirements could be met. The SPSA needed the least correction, while the PATSs needed correction on an individual level. In other words, similar SPSA results under different circumstances can be readily compared, while PATS results need to be handled individually. Interestingly, the quality evaluation showed that the IQAV with a correction factor can give trustworthy results at a daily basis even if the IQAV is not designed for the high circumstances encountered in K2-K4 (concentrations at raw-data level often exceeded the maximum of $4,488 \, \mu g/m^3$).

3.3 Between comparison

3.3.1 Ambient locations

Figure 4 shows the comparison of daily averaged concentrations between different LCS at the ambient locations, expressed in W_{CM_AC} , and R^2 of OLS regression without intercept.



Figure 4. Comparison between individual LCS at locations A1 (left panel) and location A2 (middle panel), and all available data pairs between any IQAV and SPSA at either location (right panel). Wcm_AC and R² are in each panel shown respectively top right and bottom left

With R^2s of 0.96 or higher, the linear association between the SPSAs and IQAVs was strong. The comparison also met the required W_{CM_AC} of 25% both for individual LCS, and all data pairs of all LCS from the two locations combined (W_{CM_AC} =15%).

The association was also strong at lower time-averaging levels. Figure 5 shows the biases and accuracies for individual SPSAs and all SPSAs combined as X versus one IQAV as Y.

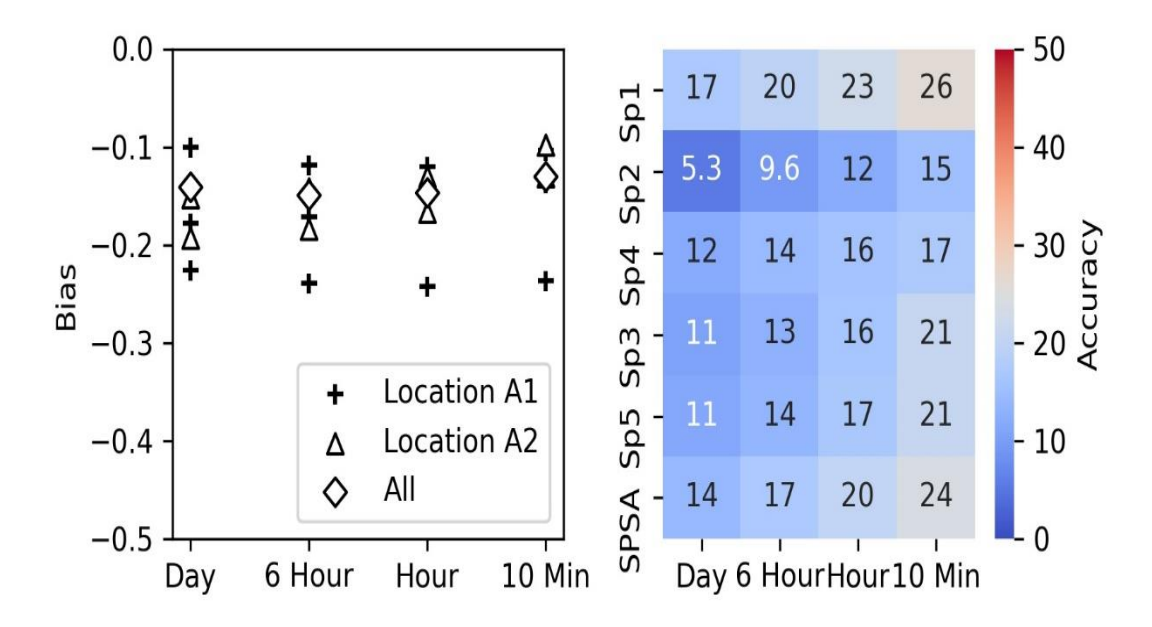


Figure 5. Biases (left panel) and Ac_AC (right panel), for individual SPSA and all SPSA combined compared to an IQAV, at locations A1 and A2. Results are shown for comparisons at four different time averaging periods

The negative bias of SPSA versus IQAV implies that the SPSA was measuring lower than the IQAV (see equation 3). Biases ranged from 10-25%. Corrected for this bias, accuracies ranged from 5.3 to 26%. This is far lower than up to slightly over the required 25%. Furthermore, the bias for all SPSA versus IQAV data pairs remained stable across the different time averages (between 10 and 15%), suggesting a stable relation between the SPSAs and IQAVs. In other words, the SPSA and IQAV units can be used interchangeably, and results can be compared across different ambient concentration ranges and time averaging periods, especially if data is corrected for the bias of 10-15%.

3.3.2 Kitchen locations

Figure 6 shows accuracies and R²s for all individual LCS compared amongst each other, for daily averaged time periods.

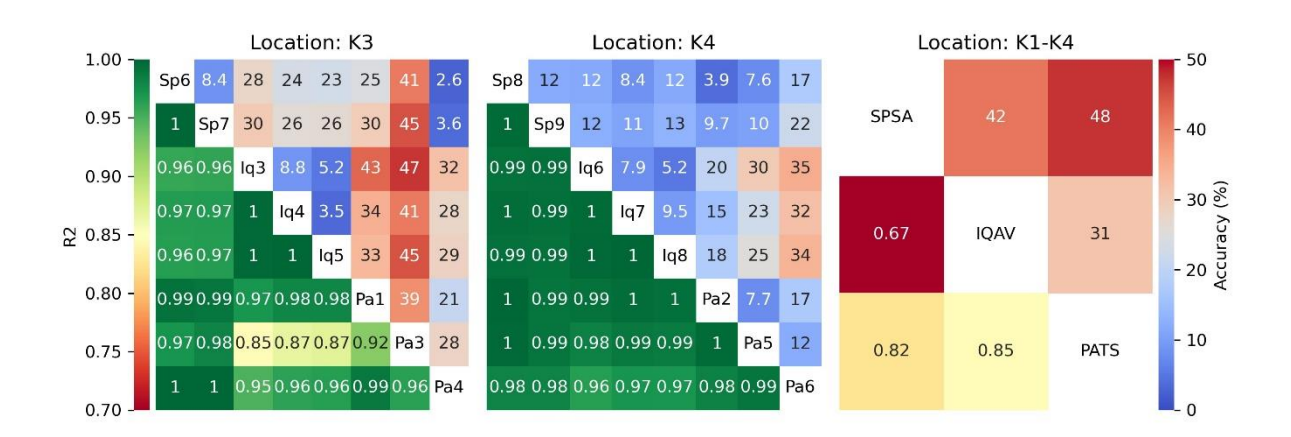


Figure 6. Comparison of daily averaged data of individual LCS at locations K3 (left panel) and location K4 (middle panel), and all available data pairs between any two different LCS at any kitchen location (right panel). Ac_{AC} and R^2 are in each panel shown respectively top right and bottom left

Linear associations between individual LCS were very high. The R²s between PATSs and SPSAs were >0.97, and between IQAVs and SPSAs were >0.96. Only for Pa3 in comparison with IQAVs the R²s were lower than 0.9 (0.85-0.87). The associations were significantly lower when all data from identical LCS, from any of the kitchen locations, were combined (R²s of 0.64-0.85). Similarly, on an individual level some instruments showed Ac_AC<25%, but variation for all paired combinations was higher (32-48%). This indicates that different LCS cannot be interchanged with an identical correction across different locations.

The fact that SPSA and PATS were not interchangeable without individual attention, is most likely related to the fact that the PATS sensors individually fell short as well (accuracies between Pa3 and the other two PATSs >25%). The problems of the IQAV are related to the fact that the maximum reported value is set to 4,488 μ g/m³ (while PATS and the SPSA reported raw values of over 50,000 μ g/m³).

The accuracies were worse for a 10-minute averaging level than for a daily averaging level. The underlying reason for this is that biases can be different at different concentration ranges. Concentration variations are more apparent at small time-averaging levels. Figure 7 shows the Ac_AC for all LCS versus one SPSA at the same location, for different concentration ranges, at a 10-minute averaging level.

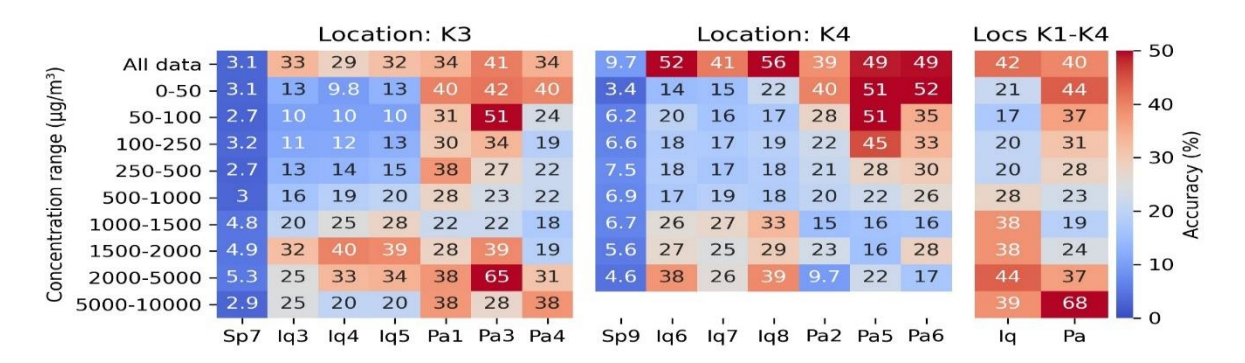


Figure 7. Comparison of daily averaged data of individual LCS versus Sp6 or Sp8 at locations K3 (left panel) and location K4 (middle panel), and all available data pairs between one SPSA and any other LCS type at any kitchen location (right panel). Ac_{AC} is shown for different concentration ranges as measured by the SPSA. If Ac_{AC} for LCS_i vs LCS_i is different from LCS_i vs LCS_i, the lowest of the two is taken

As expected, when taking all 10-minute averaged data, none of the accuracies of individual LCS versus one SPSA were lower than 25% (29-56%) except for the SPSA itself (3.1-9.7%). However, when looking at specific concentration ranges, there were multiple accuracies lower than 25%. Even when combining all data-pairs across all kitchens, accuracies lower than 25% could be reached for some ranges. This was the case between 0 and 500 μ g/m³ for the IQAV, and between 500 and 2,000 μ g/m³ for the PATS.

These accuracies could be low because each individual dataset was corrected for an individual bias. Figure 8 shows all biases of individual LCS versus an SPSA at the same location in locations K3 and K4.

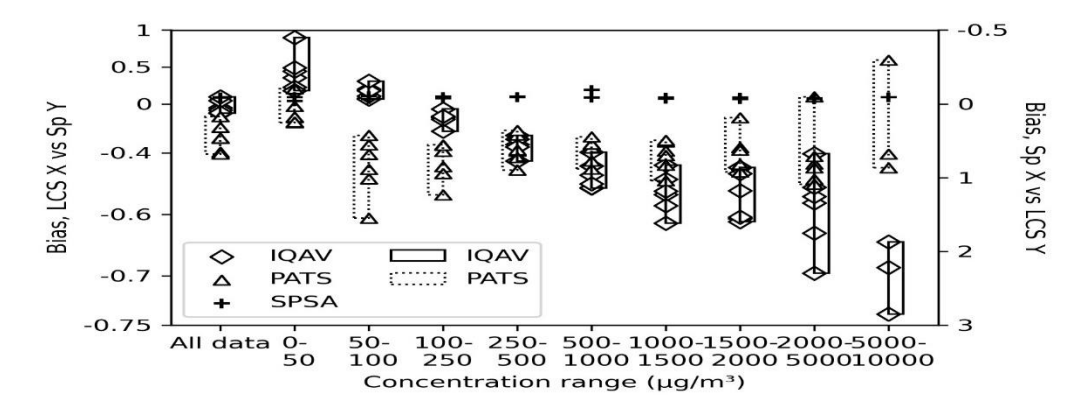


Figure 8. Biases of 10-minute averaged measurement results of individual LCS versus one SPSA, across different concentration ranges. Rectangular bars show the range of the individual biases. From equation 3 it follows that bias B=1 between i and j equals B=-0.5 between j and i. Axes are scaled such that the positive bias of LCS_i vs LCS_j (LCS_i / LCS_j -1) is equally sized to its corresponding negative bias (i.e. the positive bias of LCS_j / LCS_i -1)

The SPSA sensor compared to an identical sensor had a low bias across all concentration ranges. For the IQAV, the bias versus the SPSA sensor differed across ranges. It was close to zero at concentrations of 50-250 μ g/m³, but it increased negatively (measuring increasingly lower than the SPSA) with higher concentrations. The spread in bias for different IQAVs was small for concentration ranges up to 1,000 μ g/m³. That is to say, one correction factor can be used for all identical IQAV. The increasing underestimation with increasing concentrations is because of the IQAV reporting maximum 4,488 μ g/m³. Above the 10-minute averaged 1,000 μ g/m³, at raw-data level there are increasingly concentrations >4,488 μ g/m³, which by the IQAV are simply reported as 4,488 μ g/m³, leading to an increasing underestimation.

For the PATS, the spread of bias was relatively small for concentrations of 50-2,000 μ g/m³. For concentrations of 250-2,500 μ g/m³, the bias was in the same order of magnitude. At concentrations below 50 as well as above 2,000 μ g/m³, the spread in biases was higher. This means that identical PATS require individual attention in those concentration ranges. The overestimation versus the SPSA below 50 μ g/m³ is due to the PATS reporting minimum 10 μ g/m³, resulting in the inverse of what for the IQAV happens for high concentrations.

4. DISCUSSION

4.1 LCS under ambient conditions

The evaluation of LCS compared to the reference method under ambient conditions (n=3) was limited in comparison with other studies (Sousan et al. (2021) n=8, Falzone et al. (2020) n=24, or gravimetrically corrected continuous monitors used by Feenstra et al. (2019) and Zamora et al. (2020)). This study found high R²s versus the reference, but the SPSA and IQAV underreported concentrations with slopes of respectively 2 and 1.6. The underreporting of the SPSA is also found by Sousan et al. (2021) for salt particles (slope 2.0). It is also found by Falzone et al. (2020) in the field (1.35-1.38). For the IQAV, however, Feenstra et al. (2019) found the IQAV measuring higher than a reference concentration, and Zamora et al. (2020) found it measuring close to a reference concentration (bias of 0.04). The difference might be due to circumstances in this study (biomass burning on the streets and in neighborhoods as a prominent source) that are different from field circumstances in studies conducted in high-income countries. The difference might also be due to

the uncertainty of the reference method used in this study for ambient concentrations (see Table 3 note a). Additional comparisons with reference instruments under ambient conditions common to low-income countries are needed to gain more insight in this. This study did however show a very low variation within SPSA (much like Sousan et al. (2021) for salt particles), as well as low difference between SPSA and IQAV across different time averaging levels (Ac_AC<25%). The low within and between variation shown in this and other studies can be combined with other studies' promising findings in comparison with reference instruments. These low variations point to the usability of the LCS interchangeably under ambient circumstances.

4.2 LCS under high-exposure conditions

Perhaps lacking in ambient circumstances, this study on the other hand included concentration levels not encountered in other evaluation studies. 10-minute averaged concentrations in this study as reported by the LCS were >10,000 μ g/m³, while other evaluations of LCS under non-ambient conditions only went up to 1,200 μ g/m³ PM2.5 (Sousan et al., 2021). The quality of the LCS under circumstances in this study was similar to the quality level found in other studies. For SPSAs compared to a reference method, Nguyen et al. (2021) found a standard deviation (SD) of 16.6-26% (here 1-24%) while Sousan et al. (2021) reported r=0.99 (here as well), but diversity in slopes (here: close to 1). Within SPSAs, this study's CV is similar to Sousan et al. (2021) for salt particles, or, translated into absolute SD (up to 22 μ g), similar to Nguyen et al. (2021) (26 μ g). For the PATS, this study's R² >0.92 with a common slope of 1.6 is similar to that reported by Pillarisetti et al. (2017) (R² 0.9, slope 1.5). The variation *within* PATS found in this study is not up to NIOSH standards (CV>10%), but linear association is similar to that reported by Pillarisetti et al. (2017) (R² 0.92).

The IQAV was altogether not evaluated under high circumstances by other studies. Even despite the higher reporting limit, this study revealed a usability on a daily level ($Ac_{AC} < 25\%$).

4.3 LCS between comparison

Quality evaluations *between* LCS are rare. That is understandable from a 'true quality' evaluation point of view: when comparing LCS, it is not known which of the LCS gives the true value. Nonetheless, the comparison of measurement results from different LCS is informative. In the case

of a strong association (preferably the same over different instruments and concentration ranges), findings for one LCS can be extrapolated to the other. The low variance *within*, as well as the low and stable bias compared to the *reference* across different ranges for the SPSA are especially promising results. These results suggest that an instrument that needs to get more individual attention (such as the PATS), in the absence of an (expensive) reference method can be calibrated with an SPSA. Similarly, while the IQAV is not designed for high concentrations as in this study, with correction the IQAV can give trustworthy results on a daily level (in comparison with SPSA R²s>0.96).Below 1,000 µg/m³, the IQAV can even be reliable at a 10-minute averaged level.

6. CONCLUSIONS AND RECOMMENDATIONS

Three low-cost PM2.5 sensors were compared *within* identical sensors, with a *reference* method, and *between* each other in Arba Minch, Ethiopia, under ambient and high-exposure circumstances. Strong linear associations (R² mostly >0.9) were witnessed at both ambient and kitchen locations. This was the case across different time periods and across different concentration ranges. Under ambient situations, *within* SPSAs official standards were met (CV<10%, u_{bs}<2.5 μg). After bias correction, both the IQAV and the SPSA met standards for accuracy (Ac_{AC}<25%). When using these LCS in high-exposure situations, the IQAV at daily level needs a correction for a bias of 50%. It needs a similar correction at 10-minute averaging levels up to concentrations of 200 μg/m³. At higher concentration levels, the required accuracies can be obtained by range-wise correction based on an SPSA that measures at the same location. When using the PATS, individual sensors need individual attention, but in comparison with the reference method or even by correcting with an SPSA from the same location can be upgraded to required accuracy levels. The comparability *within* SPSAs implies that findings under one circumstance, albeit distinguishing between ambient and prominently biomass-burning situations, can be applied in other circumstances.

This study shows that, when distinguishing ambient and predominantly high-exposure biomass fuel situations, LCS can be used interchangeably: either within one project or for the purpose of combining results from multiple studies in which different LCS are used. Of the three evaluated LCS, the SPSA seems to be the most flexible choice in an environment where both ambient and high-exposure situations are researched. If budget is available for quality evaluations with a

reference instrument, more attention to ambient situations in low-income countries is recommended, to include situations such as busy streets and open waste burning in bigger cities. With a limited budget it is recommended to opt for a multitude of LCS rather than one or two expensive monitors.

Acknowledgements

The author thanks Afework Tadema and Meseret Tesfaye for constructing the SPSA set-ups. Thanks also go to Dagmawi Matewos for organizing the K3 and K4 measurement locations. Finally, thanks go to Tourist Hotel Arba Minch and the owners of the different restaurants for allowing measurements at their premises.

REFERENCES

- Afshar-Mohajer, N., Foos, R., Ramachandran, G., & Volckens, J. (2021). Field Evaluation of the Ultrasonic Personal Aerosol Sampler (UPAS) for Respirable Dust Exposure in a Taconite Mine. *Annals of Work Exposures and Health*, 65(1), 127–135. https://doi.org/10.1093/annweh/wxaa094
- Babatola, S. S. (2018). Global burden of diseases attributable to air pollution. *Journal of Public Health in Africa*, 9(3), 813. https://doi.org/10.4081/jphia.2018.813
- Dingemanse, J. D., Abiyu, M. A., Tesfaye, K. G., & Roro, F. F. (2022). Using student science to identify research priority areas for air pollution in a university environment: An Ethiopian case study. *Clean Air Journal*, *32*(2), Article 2. https://doi.org/10.17159/caj/2022/32/2.13470
- Dingemanse, J. D., & Dingemanse-de Wit, G. (2022). An evaluation of best practices in an air quality student science project in Ethiopia. *Aquademia*, 6(1), ep22001. https://doi.org/10.21601/aquademia/11828
- EPA. (2006). General requirements of an equivalent method determination (Subchapter C). (40 CFR Parts 53).
 - https://www.ecfr.gov/current/title-40/chapter-I/subchapter-C/part-53/subpart-C
- European Commission. (2010). Guide to the demonstration of equivalence of ambient air monitoring methods. European Commission.

- https://www.academia.edu/65705447/Guide_to_the_Demonstration_of_Equivalence_of_ Ambient_Air_Monitoring_Methods
- Falzone, C., Romain, A.-C., Broun, V., & Gérard, G. (2020). PM2.5 low-cost sensor perfomance in ambient conditions. EnviroInfo 2020 - Digital edition. https://orbi.uliege.be/handle/2268/256111
- Feenstra, B., Papapostolou, V., Hasheminassab, S., Zhang, H., Der Boghossian, B., Cocker, D., & Polidori, A. (2019). Performance evaluation of twelve low-cost PM2. 5 sensors at an ambient air monitoring site. *Atmospheric Environment*, 216, 116946.
- Gakidou, E., Afshin, A., Abajobir, A. A., Abate, K. H., Abbafati, C., Abbas, K. M., Abd-Allah, F., Abdulle, A. M., Abera, S. F., Aboyans, V., Abu-Raddad, L. J., Abu-Rmeileh, N. M. E., Abyu, G. Y., Adedeji, I. A., Adetokunboh, O., Afarideh, M., Agrawal, A., Agrawal, S., Ahmadieh, H., ... Murray, C. J. L. (2017). Global, regional, and national comparative risk assessment of 84 behavioural, environmental and occupational, and metabolic risks or clusters of risks, 1990–2016: A systematic analysis for the Global Burden of Disease Study 2016. *The Lancet*, 390(10100), 1345–1422. https://doi.org/10.1016/S0140-6736(17)32366-8
- Harris, C. R., Millman, K. J., van der Walt, S. J., Gommers, R., Virtanen, P., Cournapeau, D., Wieser, E., Taylor, J., Berg, S., Smith, N. J., Kern, R., Picus, M., Hoyer, S., van Kerkwijk, M. H., Brett, M., Haldane, A., del Río, J. F., Wiebe, M., Peterson, P., Gérard-Marchant, P., Sheppard, K., Reddy, T., Weckesser, W., Abbasi, H., Gohlke, C., Oliphant, T. E. (2020). Array programming with NumPy. *Nature*, 585(7825), 357–362. https://doi.org/10.1038/s41586-020-2649-2
- Hunter, J. D. (2007). Matplotlib: A 2D graphics environment. *Computing in Science & Engineering*, 9(3), 90–95. https://doi.org/10.1109/MCSE.2007.55
- IET. (n.d.). Mettler Analytical Balance AE240 Dual Range Balance Data Sheet. IET Used Lab Equipment.
 https://www.ietltd.com/pdf datasheets/Mettler%20AE240%20Data%20Sheet.pdf
- Karagulian, F., Barbiere, M., Kotsev, A., Spinelle, L., Gerboles, M., Lagler, F., Redon, N., Crunaire, S., & Borowiak, A. (2019). Review of the Performance of Low-Cost Sensors for

- Air Quality Monitoring. *Atmosphere*, 10(9), Article 9. https://doi.org/10.3390/atmos10090506
- Mooney, D., Willis, P., & Stevenson, K. (2006). *A guide for local authorities purchasing air quality monitoring equipment*. (AEAT/ENV/R/2088 Issue 2). AEA Technology PLC. https://uk-air.defra.gov.uk/library/reports?report_id=386
- Nguyen, N. H., Nguyen, H. X., Le, T. T. B., & Vu, C. D. (2021). Evaluating Low-Cost Commercially Available Sensors for Air Quality Monitoring and Application of Sensor Calibration Methods for Improving Accuracy. *Open Journal of Air Pollution*, *10*(01), Article 01. https://doi.org/10.4236/ojap.2021.101001
- NIOSH. (2012). Components for Evaluatino of Direct-Reading Monitors for Gases and Vapors (No. 2021–162; DHHS Publication). National Institute for Occupational Safety and Health. https://stacks.cdc.gov/view/cdc/11956
- Pillarisetti, A., Allen, T., Ruiz-Mercado, I., Edwards, R., Chowdhury, Z., Garland, C., Hill, L. D., Johnson, M., Litton, C. D., Lam, N. L., Pennise, D., & Smith, K. R. (2017). Small, Smart, Fast, and Cheap: Microchip-Based Sensors to Estimate Air Pollution Exposures in Rural Households. *Sensors*, 17(8), Article 8. https://doi.org/10.3390/s17081879
- Python Core Team. (2020). *Python: A dynamic, open source programming language*. (3.7.9). www.python.org
- Shaddick, G., Thomas, M. L., Amini, H., Broday, D., Cohen, A., Frostad, J., Green, A., Gumy, S., Liu, Y., Martin, R. V., Pruss-Ustun, A., Simpson, D., van Donkelaar, A., & Brauer, M. (2018). Data integration for the assessment of population exposure to ambient air pollution for Global Burden of Disease assessment. *Environmental Science & Technology*, 52(16), 9069–9078. https://doi.org/10.1021/acs.est.8b02864
- Sousan, S., Koehler, K., Thomas, G., Park, J. H., Hillman, M., Halterman, A., & Peters, T. M. (2016). Inter-comparison of Low-cost Sensors for Measuring the Mass Concentration of Occupational Aerosols. *Aerosol Science and Technology: The Journal of the American Association for Aerosol Research*, 50(5), 462–473. https://doi.org/10.1080/02786826.2016.1162901
- Sousan, S., Regmi, S., & Park, Y. M. (2021). Laboratory evaluation of low-cost optical particle counters for environmental and occupational exposures. *Sensors*, 21(12), 4146.

- The pandas development team. (2020). *pandas-dev/pandas: Pandas* [Python]. https://pandas.pydata.org/
- Virtanen, P., Gommers, R., Oliphant, T. E., Haberland, M., Reddy, T., Cournapeau, D., Burovski, E., Peterson, P., Weckesser, W., & Bright, J. (2020). SciPy 1.0: Fundamental algorithms for scientific computing in Python. *Nature Methods*, *17*(3), 261–272.
- Volckens, J., Quinn, C., Leith, D., Mehaffy, J., Henry, C. S., & Miller-Lionberg, D. (2017). Development and evaluation of an ultrasonic personal aerosol sampler. *Indoor Air*, 27(2), 409–416. https://doi.org/10.1111/ina.12318
- World Health Organization. (2021b). *Ambient (outdoor) air pollution*. WHO Newsroom. https://www.who.int/news-room/fact-sheets/detail/ambient-(outdoor)-air-quality-and-health
- World Health Organization. (2021a). WHO global air quality guidelines. Particulate matter (PM2.5 and PM10), ozone, nitrogen dioxide, sulfur dioxide and carbon monoxide. World Health Organization. https://apps.who.int/iris/handle/10665/345329
- World Health Organization. (2022). *Household air pollution and health*. WHO Newsroom. https://www.who.int/news-room/fact-sheets/detail/household-air-pollution-and-health
- Zamora, M. L., Rice, J., & Koehler, K. (2020). One year evaluation of three low-cost PM2.5 monitors. *Atmospheric Environment*, 235, 117615. https://doi.org/10.1016/j.atmosenv.2020.117615

ANNEX

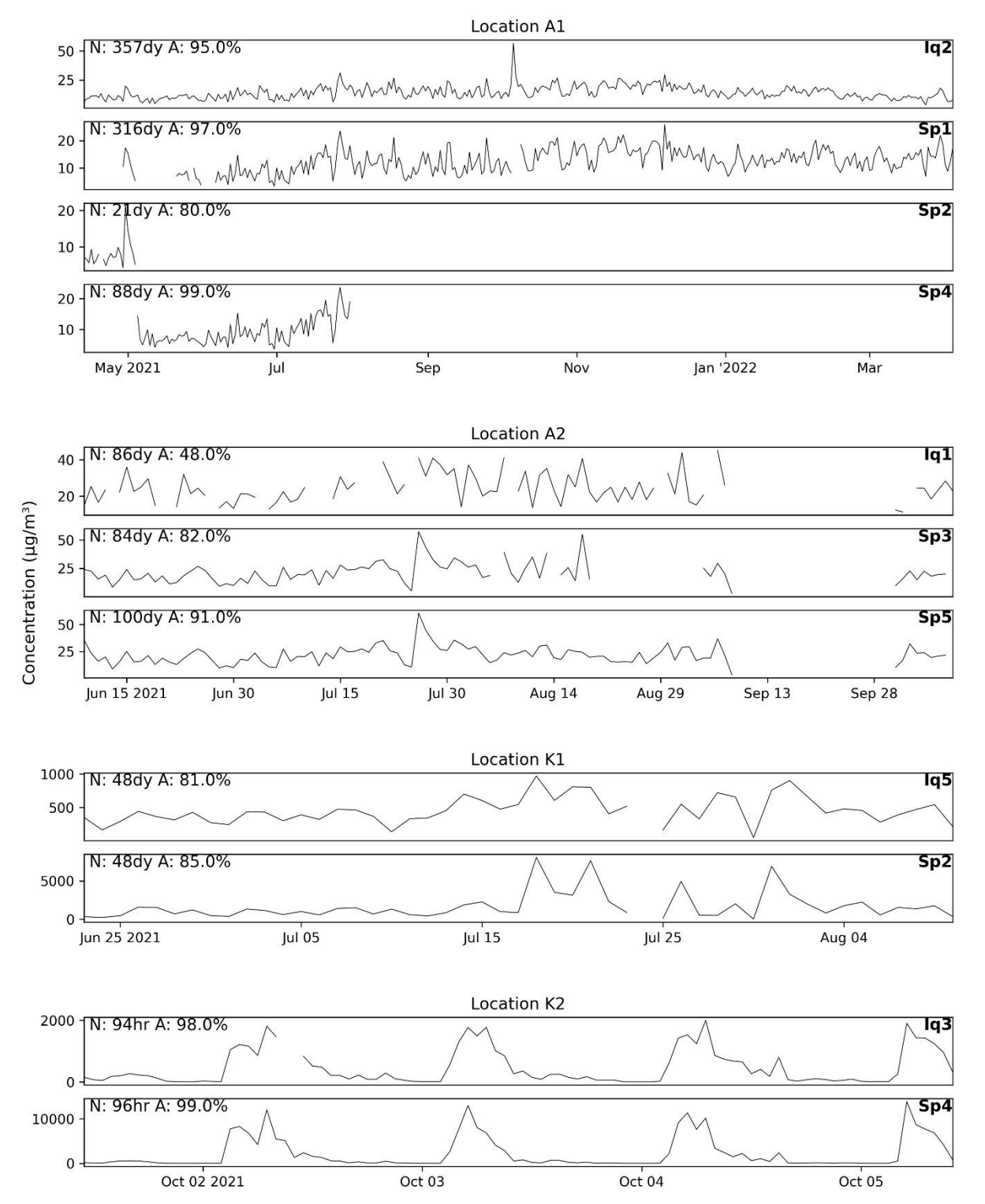


Figure A1. PM2.5 concentrations as reported by all LCS at locations A1, A2, K1 and K2, annotated with the total time period (N, in days (dy) or hours (hr)), and the percentage of available 10-minute averages (A) within that time period.

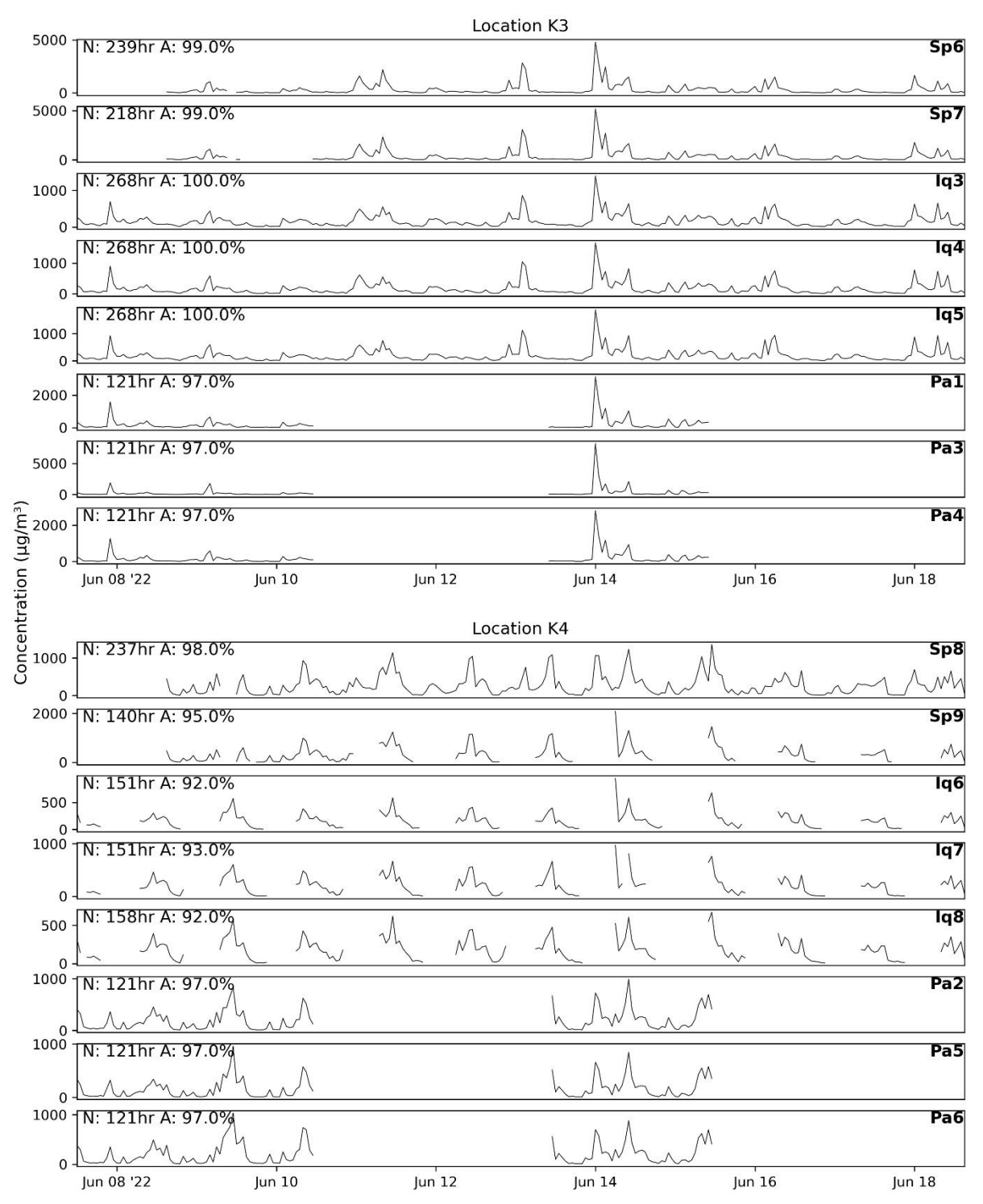


Figure A2. PM2.5 concentrations as reported by all LCS at locations K3 and K4, annotated with the total time period (N, hours (hr)), and the percentage of available 10-minute averages (A) within that time period.

Shallow Groundwater Quality and Human Health Risk Assessment in Holte, a Town in Southern Ethiopia

Demamu Tagele Haligamo¹ and Tamru Tesseme Aragaw¹

¹Faculty of Water Supply and Environmental Engineering, Arba Minch Water Technology Institute, Arba Minch University, Arba Minch City, Ethiopia

Correspondence to tamruiit@gmail.com

ABSTRACT

Groundwater quality and human health risk assessment are critical for the long-term usage of household water supplies. The purpose of this study was to evaluate groundwater quality and human health risk in Holte, a town in the Derashe Special Woreda in southern Ethiopia. Water samples from seven shallow groundwater wells were taken and examined for hydrogeochemical properties. The Water Quality Index (WQI) was developed to assess the suitability of groundwater for drinking. Groundwater hydrochemistry types and evolutionary processes were investigated. The results suggested that the typical pH of groundwater samples had an average pH of 7.99. The values of electrical conductivity (EC), bicarbonate (HCO3) and total dissolved solid (TDS) in all samples were above the recommended upper limit of World Health Organization (WHO) for drinking water. Based on the hydrochemical findings, the orders of cationic abundance and anionic abundance in the groundwater were $Ca^{2^+} < Mg^{2^+} < K^+ < Na^+$ and $F^- < SO_4^{2^-} < Cl^-$ < HCO₃⁻, respectively. According to the Piper Tri-linear Diagram, the majority of groundwater samples were found to have Mixed Ca-Na-HCO3. The Gibbs fields results showed that evaporation dominated groundwater quality, whereas chemical weathering of rock-forming minerals dominated the remaining samples. The calculated WQI result showed that 57.1% (4 handpumps) of groundwater samples from the town had acceptable water quality, but 42.9% (3 handpumps) had poor water quality. The finding of this study suggests that groundwater quality parameters should be tested and monitored on handpumps at sample locations 1, 2, and 3 in the town to minimize human health risks and ensure long-term socioeconomic development.

Keywords: Shallow Groundwater Quality, Water Quality Index, Health Risk Assessment, Hydrochemistry

Received: 17 October 2022 accepted 18 Nov 2022.

1. INTRODUCTION

Groundwater (GW) has an essential role in maintaining social and economic development of humankinds. The needs for two-third of the world's population will be fulfilled by groundwater alone (Adimalla et al. 2020). It is a primary source for domestic use in many rural areas of the world including developing countries (Alam et al. 2020; Lapworth et al. 2017). In India, the annually used groundwater is around 250 billion m³ which is about 38.55% of 1123 billion m³ usable water (Bhat, 2014); while in Saudi Arabia, groundwater constitutes 80% of the total usable water (2259 billion m³) (Aly et al. 2013).

In comparision to surface water, groundwater is a main source of water supply for many communities' in different countries and regions, because of its some advantages like stable spatiotemporal distribution, low or no bacteriological contamination, better water quality, low turbidity, constant water temperature and closeness to the community (Tai et al. 2012). However, it is mostly polluted because of human activities (industrial effluent, wastewater irrigation, land cover change and urbanization), and agriculture activity (excessive use of fertilizer and pesticide) (Qian et al. 2014; Qian et al. 2016; Nigus et al. 2020; Bhalme and Nagarnaik, 2012). There are also natural factors like geologic structures and hydrogeological settings that may also cause variations in hydro-chemical characteristics of groundwater (Nigus et al. 2020; Yahong et al. 2016).

Ions in excess amounts are causes for groundwater pollution. These are nitrogen pollution (Kuhr et al. 2013; Jalali, 2011), fluorine pollution (Daniele et al. 2013; Feifei et al. 2021; Wu and Sun, 2015), arsenic pollution (Nasrabadi and Bidabadi, 2013), organic contamination (Han et al. 2013), hardness pollution (salts of Ca and Mg) (Muhammad et al. 2013; Yahong et al. 2016), and sodium and sulfate pollution (Yahong et al. 2016). Studies also reported contamination of groundwater with pathogens such as escherichia coli, enterobacter, streptococcus, salmonella and shigella spp (Nchofua et al. 2020). Studies conducted in the rural areas of Ethiopia indicated that wells have high level of microbal contamination (E. coli) (Mengesha et al. 2004; Tsega et al. 2014).

Based on a study conducted in Thailand in Ubon Ratchathani province, groundwater samples were identified with higher concentration of lead (maximum of 66.9µg/L) and zinc (maximum of

 $302\mu g/L$) (Wongsasuluk et al. 2014). A study conducted in China revealed a higher concentration of Mg^{2^+} (54.72 mg/L), $SO_4{}^{2^-}$ (355.42 mg/L) and NO^{3^-} (43.60 mg/L) in groundwater samples (Nigus et al. 2020). There were also other studies that groundwaters showed higher concentration of arsenic (maximum of $420\mu g/L$) (Nasrabadi and Bidabadi, 2013), fluoride (4.3 mg/L) (Daniele et al. 2013), and total hardness (785.34 mg/L) (Nigus et al. 2020).

A study conducted in China showed that Water Quality Index (WQI) values for groundwater samples varied between 58.37 and 246.23, with an average value of 103.07. Among 31 samples, 67.74% of groundwater samples were of medium quality and identified as suitable for drinking purposes. The water quality of six groundwater samples (19.35%) and four groundwater samples (12.9%) were poor and extremely poor, respectively, and considered unfit for drinking (Daniele et al. 2013; Feifei et al. 2021; Wu and Sun, 2015). Another study conducted on shallow groundwater identified that out of the 34 sample sites, 10 groundwater sample sites (29.4%) had good quality, 19 sample sites (55.9%) were classified as fair quality, 5 sample sites (2.9% and 11.8%) were identified to have poor and very poor quality, respectively (Nigus et al. 2020).

Groundwater is used for drinking in the Rift Valley part of Ethiopian (Ramya, 2018). Researchers studied the groundwater chemistry in the Ethiopian Rift Valley and ravealed that their chemical compositions were different (Ayenew, 2008; Ayenew et al. 2008; Shankar and Nafyad, 2019; Yitbarek et al. 2012). Volcanic aquifers were identified as sources of fluoride in the great Rift Valley groundwater (Furi et al. 2011). In addition, liquid waste discharges from cities were identified as groundwater pollutants in the Rift Valley (pollution of groundwater in the Dire Dawa groundwater basin) (Taye, 1988). Tamiru, 2004 reported that untreated waste discharge to rivers were causes for pollution of groundwater in Addis Ababa (Tamiru, 2004). Dinka et al. (2015) found that anthropogenic activities caused pollution of groundwater in Matahara region.

A rapid assessment of drinking water quality in Ethiopia reported a high nitrate and fluoride concentration in more than 30% of water sources (Dagnew et al. 2007). Treatment of contaminated groundwater requires adequate knowledge and skill, and it is costly (Hasan, 2014). Regular monitoring and detailed studies of groundwater quality provides an early warning before further contamination and hence expensive cleanup is need. There is not much study conducted around the study area on groundwater quality, but majority of the communities rely on groundwater for

drinking purpose. Hence, variations in groundwater quality were investigated on 7 handpumps selected in the study area. This may serve indicators of groundwater quality of the town and the nearby towns.

2. METHODS AND MATERIALS

2.1. Study area

This study was conducted on seven hand pumps in Holte town, Derashe Special Woreda. However, the lab analysis was done at Arba Minch University in southern Ethiopia on June 7-8, 2022 (Fig. 1). Holte town was established on March 3, 2010 GC. It is bordered with Gato town in the South, Wozeka town in the North, Gomayide town in the East and Gidole town in the West. It is situated at about 547 Km South West of Addis Ababa, 326 Km away from Hawassa city, and 50 km southwest of Arba Minch. The town covers an area of 7.1 km². It is situated on plain landforms within the great Ethiopia Rift Valley and stretches from 1110m up to 1190m above sea level. The town experiences a mean annual temperature with the range of 15°c to 27°c, grouped in the "Kola" climate (weather condition) of the country (Tilahun et al. 2022). In 2013, the town has a total population of 20,416 of which 10,953 were females and 9,463 were males. There are about 2,783 households in the town. The town has 7 villages. The people of the town mainly use groundwater wells installed as hand pumps for different domestic purpose.

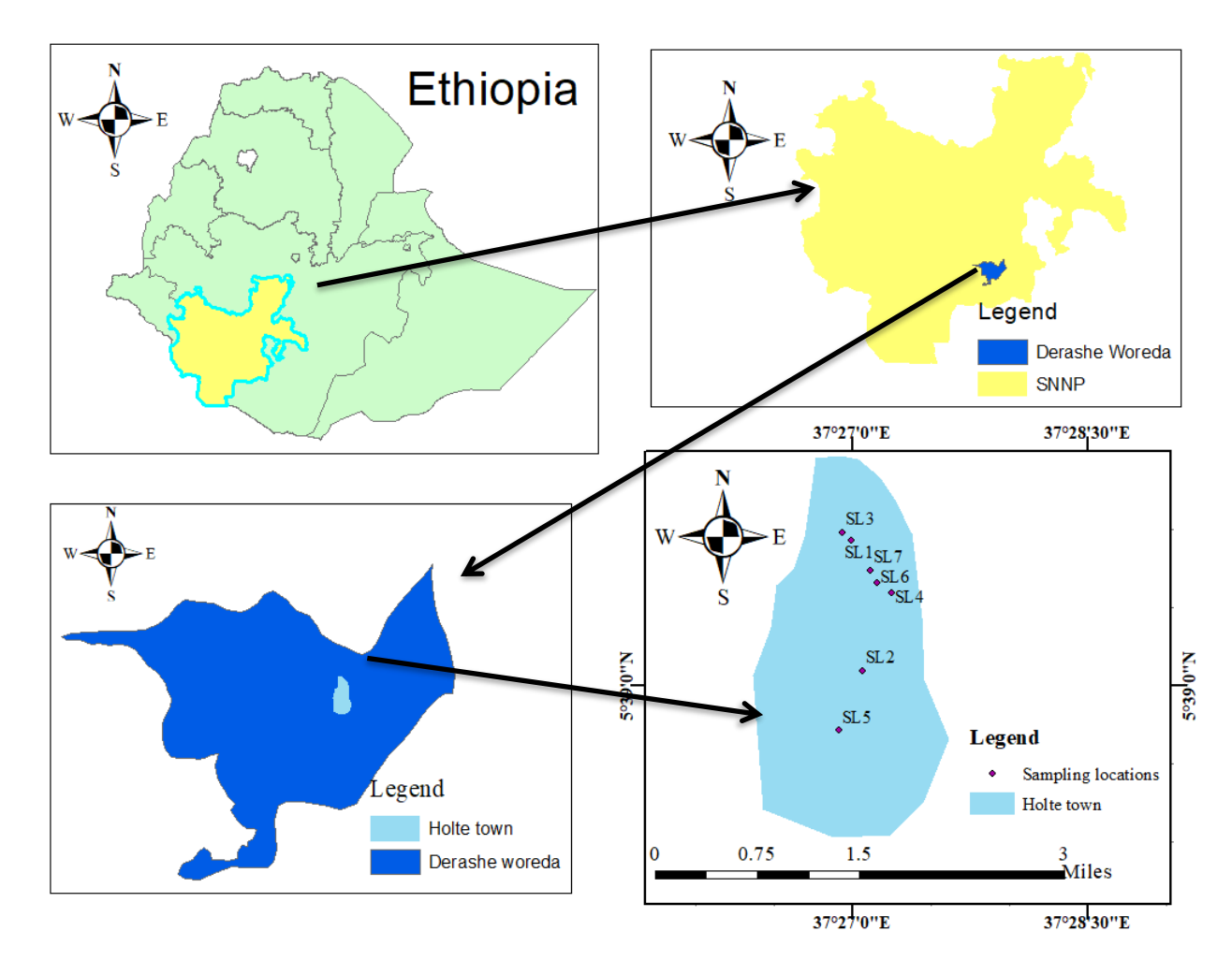


Figure 1: Map of Ethiopia, SNNPR, Derashe special woreda and Holte town, respectively.

2.2. Sample collection and analysis

Groundwater samples were collected from purposively selected 7 hand pumps at different seven sites in the town. The seven hand pumps were selected purposively because of their coverage throughout the town. The samples were collected using a sterilized 1 L sample bottles based on the sampling procedure of the American Public Health Association (APHA, 2005). Each of groundwater sample were analyzed in Arba Minch University Water Quality Lab for various physicochemical parameters, such as pH, EC (electrical conductivity), total dissolved solids (TDS), calcium (Ca²⁺), magnesium (Mg²⁺), sodium (Na⁺), potassium (K⁺), chloride (Cl⁻), sulfates (SO4²⁻), fluoride, bicarbonate (HCO₃⁻), total alkalinity and total hardness. The standard procedures recommended by WHO were used (WHO, 2011). The details were described in Table 2.

Table 1. Method employed to measure parameters in ground water

No.	Parameters to be measured	Measuring method
1	pН	pH meter
2	Total dissolved solids (TDS)	Gravimetric method
3	Electrical Conductivity (EC)	Conductivity meter
4	Potassium (K ⁺)	Flame Photometric Method
5	Sodium (Na ⁺)	Flame Photometric Method
6	Calcium (Ca ²⁺)	Titration method
7	Magnesium (Mg ²⁺)	Titration method
8	Chloride (Cl ⁻)	Titration method
9	Bicarbonate (HCO ₃ ⁻)	Titration method
10	Sulfate $(SO_4^{2^-})$	Spectrophotometric Method
11	Fluoride (F ⁻)	Spectrophotometric Method
12	Total Hardness (TH)	Titration method
13	Total alkalinity (TA)	Titration method

2.3. Quality control

To assure the data quality, the result of physicochemical analysis was checked with the anion-cation balance. The principle of the anion cation balance is that the sum of cations and sum of anions are equal because the solution must be electrically neutral. In an electrically neutral solution, the sum of the cations should be equal to the sum of anions in milli-equivalent per liter (Gebrerufael et al. 2019; Hounslow, 1995). Based on the electro neutrality, analysis of water samples with a percent balance error $< \pm 5\%$ is regarded as acceptable (Fetter, 2001; Gebrerufael et al. 2019). The cations and anions balance results of the water samples analysis from Holte town are reliable as the charge balance error for more than 95% of the groundwater samples fall within the accepted limits of $< \pm 5\%$. Laboratory analysis result of the 7 groundwater samples were used to determine the groundwater chemistry of Holte town.

The analysis per each parameter of a sample was conducted in triplicate (Jagaba et al. 2020) and the average was taken to assure the quality of the data and to check the accuracy of the experimental results.

2.4. Hydro-chemical facies and evolution mechanisms

Water chemistry is influenced by water–rock interaction taking place from the recharge area to sampling location (Purushothaman et al. 2014). Hydro-geochemical types reflect the effects of

chemical reactions occurring between the minerals within the lithological framework and groundwater (Varol, 2015). In this study, the groundwater samples were classified hydrochemically using major cations and anions with conventional Piper tri-linear diagram to determine the similarities between groundwater in the area. In addition, the Gibbs diagram was used to understand the genesis of groundwater. The present study used Piper tri-linear and Gibbs diagram similar to other studies (Şehnaz, 2017).

2.5. Calculation of water quality index (WQI)

In this study, WHO standards of 2011 adopted from previous studies were used to compute the WQI's for different physicochemical parameters by the Weighted Arithmetic Index method (Jagaba et al. 2020; Tiwari, 1985) to assess the suitability of groundwater in the study area for drinking purposes. It requires three important parameters like assigned weight to each parameters, relative weight of each parameter in relation to others and quality rating scale (Brhane, 2018). Different researchers have reported variable weights assigned to a particular water quality parameter. Based on the literature, this study assigned weight values ranging from 1 to 5 (Tables 6), where 5 meant most significant and 1 less significant. The relative weights, quality rating scale and water quality index (WQI) were determined using the following equations (Jagaba et al. 2020; Vasanthavigar et al. 2010; Feifei et al. 2021; Gebrerufael et al. 2019; Tirkey et al. 2017).

$$W_i = \frac{w_i}{\sum w_i}$$
, i start from 1 up to n.....(1)

Where

- ▶ W_i is the relative weight
- \triangleright w_i is the weight of each parameter
- n is the number of parameters.

Tables 6 and 7, also highlights the relative weight for each parameter as computed. For each of the parameters, a quality rating scale (qi) was determined using the relationship in Equation (2) below:

$$q_i = \frac{C_i \times 100}{S_i} \dots (2).$$

Where

- + q_i is the quality rating
- \leftarrow C_i is the concentration of each chemical parameter in (mg/L)
- $lacktriangleq S_i$ is the WHO drinking water standard for each of the parameters

The sub-index and WQI were computed using the relationship in Equations (3) and (4) respectively

$$SI_i = w_i \times q_i \dots (3).$$

$$WQI = \Sigma SI_i \dots (4).$$

Where,

- SI_i is the sub-index of the i^{th} parameter
- q_i is the rating based on the concentration of the i^{th} parameter

After calculating the WQI, the following ranges were used to categorize the water quality type as excellent, good, poor, very poor and unsuitable for drinking (table 3).

Table 2. Water Quality Index use and the status of respective groundwater (Şehnaz, 2017)

Range	Water Type
<50	Excellent water
50–100	Good water
100–200	Poor water
200–300	Very poor water
>300	Water unsuitable for drinking purposes

2.6. Data analysis

Data were analyzed by using statistical package for social science (SPSS.version.23), and Excel 2010. Statistical measures (descriptive statistics) of the groundwater quality parameters were determined by using the SPSS software ver. 23. Cations and anions were also calculated (Table 5). Microsoft Excel was employed for plotting graphs (Piper diagram and Gibbs diagram). The data were displayed using the parameters of the minimum value, maximum value, and mean value. The results/findings of the study were finally displayed using tables and graphs

3. RESULTS AND DISCUSSION

3.1. Descriptive statistical results

Lab result and descriptive statistics of 13 physicochemical parameters of groundwater in the study area were summarized (Table 4 and 5). The analysis result indicated that the pH ranged from 7.8–8.1, which was slightly basic/alkaline. The TDS and EC of the groundwater samples varied from 1790 to 2500 mg/L and 3580 to 4980µs/cm, respectively.

Mean/average of each cation for all samples occured in the order of $Ca^{2^+} < Mg^{2^+} < K^+ < Na^+$ and mean/average of each anion concentrations were in the order of $F^- < SO_4{}^{2^-} < Cl^- < HCO_3{}^-$. Krishna, (2019) that reported anion concentration as $F^- < SO_4{}^{2^-} < Cl^- < HCO_3{}^-$. This was in conformity with the finding of the current study. However, Igibah (2019) reported that groundwater quality showed wide spatial variations owing to human and agricultural effects with an anion order of $SO_4{}^{2^-} > HCO_3{}^- > F^- > Cl{}^-$. This was contrary to the finding of current study. In table 4, SL from 1 to 7 indicates the 7 sample locations

Table 3. Quality of seven groundwater samples analyzed at Arba Minch University, Water Quality Laboratory, southern Ethiopia in June, 2022. All units is mg/L, except pH and conductivity (μ s/cm).

No	Parameter	Unit	The seven ground water sample						
			SL1	SL2	SL3	SL4	SL5	SL6	SL7
1	Total Alkalinity	mg/L	776	780	800	680	600	804	920
2	Bicarbonate alkalinity (HCO ₃ ⁻)	mg/L	776	780	800	680	600	804	920
3	Chloride (Cl ⁻)	mg/L	150.0 2	90.80	465.86	51.32	61.19	73.04	84.88
4	Total hardness	mg/L	180	168	412	172	228	132	112
5	Electrical conductivity (EC)	μs/cm	4220	4030	4980	3700	4450	3800	3580
6	Total dissolved solids (TDS)	mg/L	2112	2019	2500	1800	2234	1900	1790
7	Calcium (Ca ²⁺)	mg/L	16.03	20.84	28.86	28.86	22.44	8.02	4.81
8	Magnesium (Mg ²⁺)	mg/L	34.02	28.19	82.62	24.3	41.8	27.22	24.3
9	Fluoride (F ⁻)	mg/L	0.17	0.03	0.01	0.01	0.01	0.00	0.21
10	Sulfate (SO ₄ ²⁻)	mg/L	21.47	18.82	17.65	17.65	7.06	17.94	15.88
11	рН	pH scale	8.00	8.00	7.80	8.00	7.90	8.10	8.10
12	Sodium (Na ⁺)	mg/L	331.8	289.2	461.2	264.4	184.8	334.8	335.8
13	Potassium (K ⁺)	mg/L	47.2	53.6	134	56.4	10.5	55	53.2

Table 4. Comparison of lab results with WHO and Ethiopian standards of drinking water quaity, Arba Minch City, southern Ethiopia in June, 2022. All units is mg/L, except pH and conductivity (µs/cm).

Parameters	Range	Mean	WHO limit (WH O, 2011)	Ethiopia n limit (ES Agency, 2013)
рН	7.8–8.1	7.99	6.5–8.5	6.5–8.5
Total dissolved solids (TDS)	1790–2500	2051	1000	1000
Electrical conductivity (EC)	3580–4980	4109	1500	
Total Hardness (TH)	112–412	201	300	300
Total Alkalinity (TA)	600–920	766	500	200
Calcium (Ca ²⁺)	4.81-28.86	18.55	300	75
Magnesium (Mg ²⁺)	24.3-82.62	37.49	50	50
Sodium (Na ⁺)	184.8-335.8	314.57	200	200
Potassium (K ⁺)	10.5-134	58.56	12	1.5
Fluoride (F ⁻)	0.00 - 0.21	.06	1.5	1.5
Sulfate (SO ₄ ²⁻)	7.06-21.47	16.64	250	250
Chloride (Cl ⁻)	51.3-465.9	139.59	250	250
Bicarbonate (HCO ₃ ⁻)	600–920	766	500	

Chemical characteristics of ground water

3.2. Chemical characteristics of ground water

3.2.1. Major Cations in the groundwater of the town

a. Calcium (Ca²⁺) concentration

Calcium (Ca²⁺) in the water samples determined groundwater hardness. It also functioned as a pH stabilizer and also gave water a better taste. According to WHO and Ethiopian standards, the maximum permissible limit for Ca²⁺ in drinking water must be 300 mg/L and 75 mg/L, respectively. The result of this study showed that all groundwater samples analyzed were found within the permissible limit of drinking water between 4.81–28.86 mg/L (Table 5). Its spatial distribution in the study area was shown in Fig. 2A.

b. Magnesium (Mg²⁺) concentration

According to WHO and Ethiopian standards, the maximum permissible limit for Mg^{2^+} in drinking water should be 50 mg/L (Table 5). The value of Mg^{2^+} in groundwater was found above 50 mg/L in *sample location (SL) 3* (82.62 mg/L). Concerning Mg^{2^+} content of the groundwater's, almost all the groundwater samples were found to be suitable for drinking except the one found in *sample location (SL) 3*. Basalt that contained ferromagnesian minerals such as olivine, pyroxenes, and amphibole were identified as a source of Mg^{2^+} (Shankar and Nafyad, 2019; Wagh et al. 2019). The higher concentration of Mg^{2^+} in *location (SL) 3* might be due to the presence of the basalt that contained ferromagnesian minerals. Its spatial distribution in the study area was shown in Fig. 2B.

c. Sodium (Na⁺) concentration

According to WHO and Ethiopian standards, the maximum permissible limit for Na⁺ in drinking water ought to be 200 mg/L. Sodium concentration was higher in all sampled sites beyond the limit except *sample location (SL)* 5 (184.8 mg/L). Deep percolation of water from the topsoil layers might be the possible source of sodium owing to its longer residence time and water-rock interactions (Shankar and Nafyad, 2019; Wagh et al. 2019). Its spatial distribution in the study area was shown in Fig. 2D.

d. Potassium (K⁺) concentration

According to WHO standard of 2011 and Ethiopia drinking water quality standard, potassium concentration in drinking water should be below 12 mg/L and 1.5 mg/L to be in a good zone, respectively. Good zone are much more suitable for drinking purposes. The potassium in groundwater of the study area was greater than the standard/beyond the good zone in all sampled areas according to Ethiopia standards except *sample location (SL)* 5 (10.5mg/L) based on WHO limit. Since the areas were previously farmlands, the source of potassium might be the leaching of potassium fertilizer through the soil or due to the dissolution of potassium rich minerals. The spatial distribution in the study area was shown in Fig. 2C.

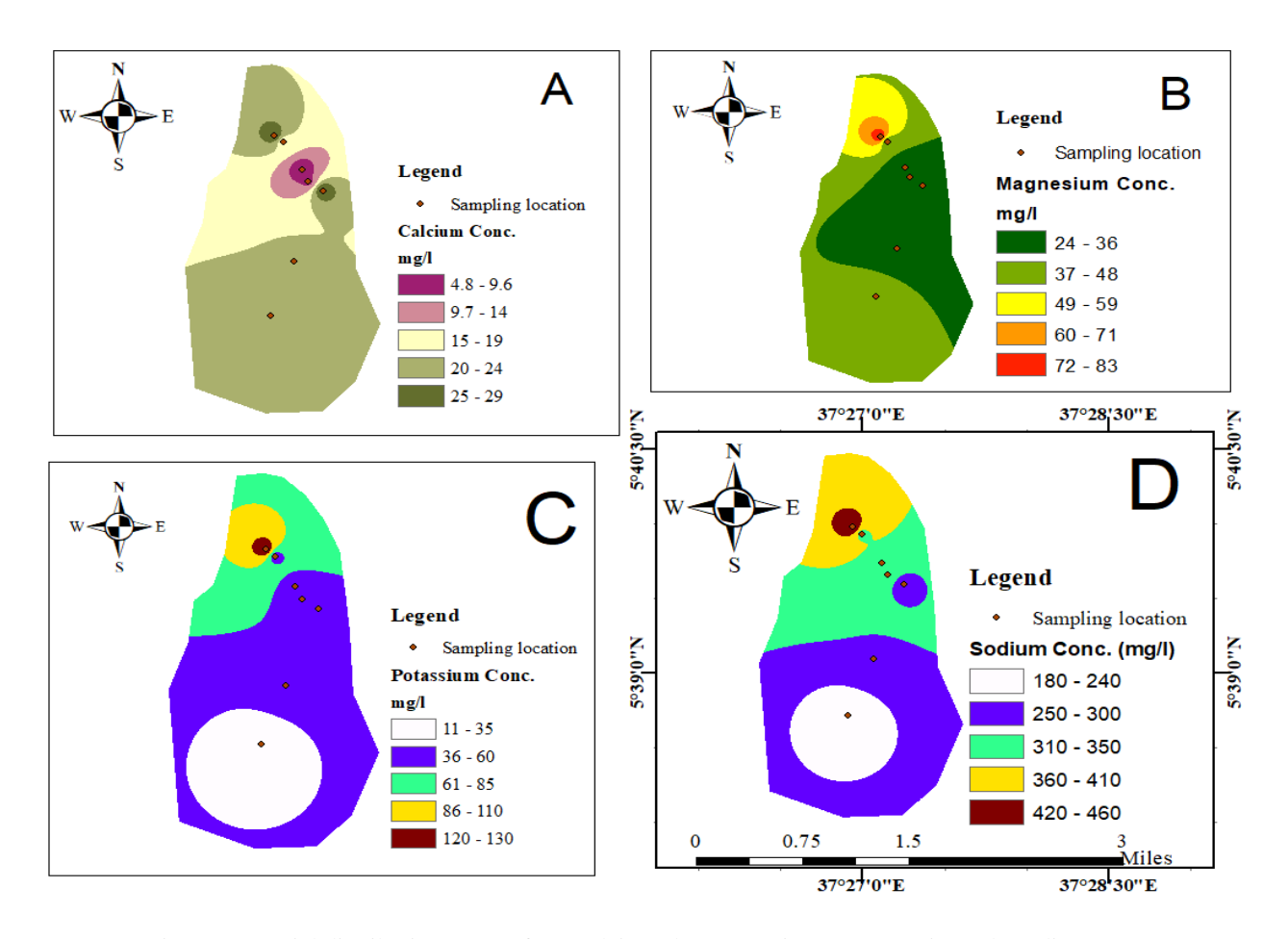


Figure 2. Spatial distribution maps of (a) Calcium (b) Magnesium (c) Potassium (d) Sodium

3.2.2. Major Anions in the groundwater of the town

a. Bicarbonate (HCO₃⁻) concentration

According to WHO standard of 2011, the maximum permissible limit for HCO₃⁻ in drinking water should be 500 mg/L. In the study area, bicarbonate concentration was very high in all sampled areas of the town. Studies indicated that silicate and carbonate weathering processes were sources of bicarbonate (Bala, 2005). All part of the study area had HCO₃⁻ concentration more than 500 mg/L . The possible source of HCO₃⁻ could be the magmatic release of CO₂ by the active fault zones (Shankar and Nafyad, 2019; Mechal et al. 2017). The spatial distribution in the study area was shown in Fig. 5A.

b. Chloride (Cl⁻) concentration

According to WHO standards of 2011 and Ethiopian water quality standards, the maximum permissible limit for Cl⁻ in drinking water ought to be 250 mg/L. All of the chloride concentration in groundwater in the study area was below the recommended WHO standard except sample location (SL) 3 (465.86 mg/L). Chloride originates from water-soluble chloride salts present in minerals. Rainwater, weathering and leaching of domestic effluents are sources of chloride in water. At higher concentration chloride damages metallic pipes and gives water a salty taste. The spatial distribution in the study shown in Fig. area was 3.

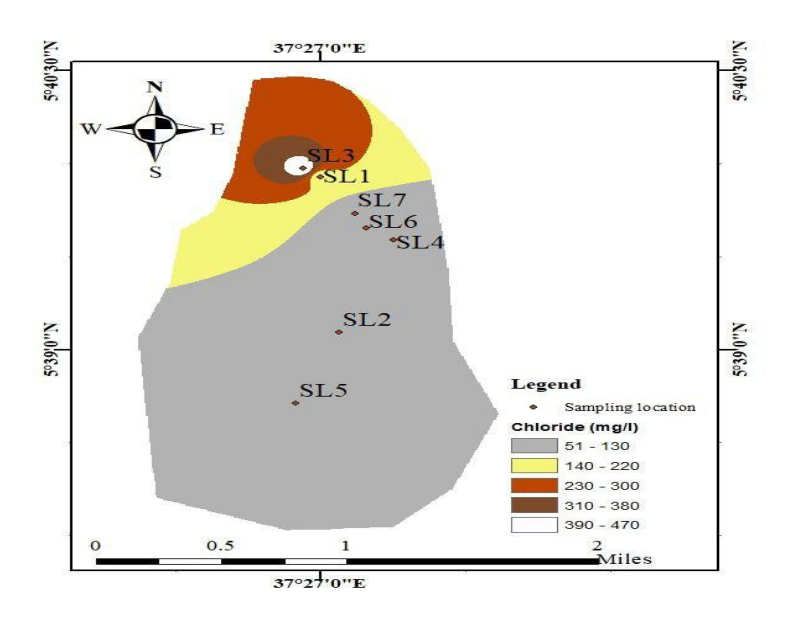


Figure 3. Spatial distribution map of chloride

c. Sulphate (SO₄²⁻) concentration

According to WHO standards of 2011 and Ethiopian water quality standards, the maximum permissible limit for SO₄²⁻ in drinking water should be 250 mg/L. In the study area, all of the

samples had the prescribed limit for drinking purposes. The spatial distribution in the study area was shown in Fig. 4A.

d. Fluoride (F⁻) concentration

According to WHO standards of 2011 and Ethiopian water quality standards, the maximum permissible limit for F⁻ in drinking water ought to be 1.5 mg/L. Fluoride concentration in groundwater was within the desirable limit of WHO standards and Ethiopian standard in the study area. The result of this study was supported by findings of other study conducted on groundwater in Ethiopia (Shankar and Nafyad, 2019). The spatial distribution in the study area was shown in Fig. 4B.

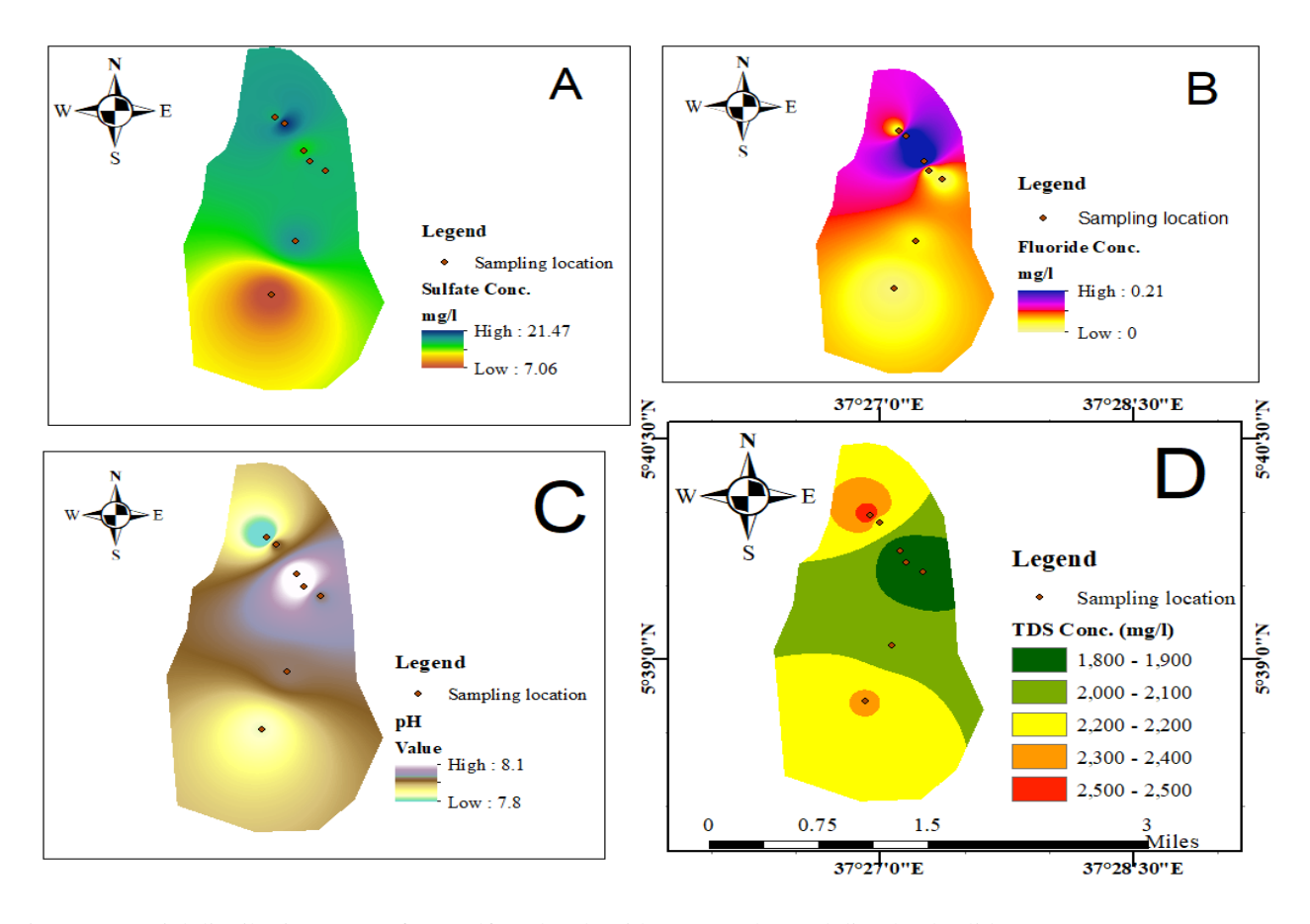


Figure 4. Spatial distribution maps of (a) Sulfate (b) Fluoride (c) pH (d) Total dissolved solid

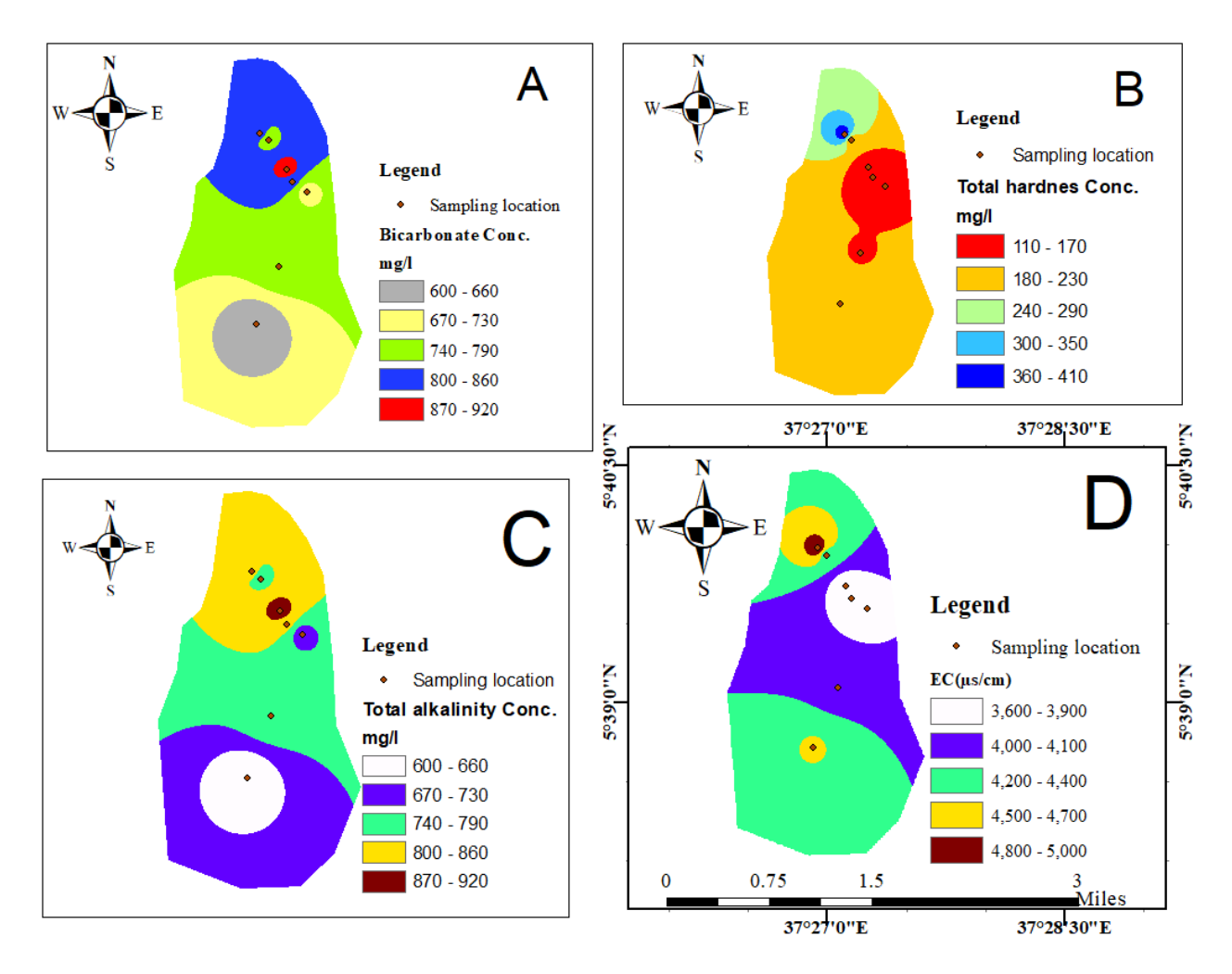


Figure 5. Spatial distribution maps of (a) bicarbonate (b) total hardness (c) total alkalinity (d) electrical conductivity

3.3. Other Chemical Constituents in the Groundwater of the Study Area

A. Total Dissolved Solids Concentration

The suitability of groundwater for drinking should be determined based on the concentration of TDS value of less than 1000 mg/L according to WHO standards of 2011 and Ethiopian water quality standards. The TDS value in all the groundwater samples were higher than the standards. These values indicated that there was a high content of soluble salt in the groundwater samples which can't be used for drinking may be due to its unknown health risk. The spatial distribution in the study area was shown in Fig. 4D.

B. pH of the groundwater in the study area

According to WHO standards of 2011 and Ethiopian water quality standards, the standard pH value in drinking water ought to be between 6.5 and 8.5. All the pH value in groundwater of the study area was below the recommended standard. The spatial distribution in the study area was shown in Fig. 4C.

C. Electrical conductivity (EC) of groundwater samples in the study area

Electrical conductivity is used to measure an ability to conduct electric current through dissolved salts that is found in groundwater which helps to know the enrichment of dissolved salt content in the groundwater. The presence of an excess amount of charged particles would limit the quality of groundwater desirability for drinking purpose. According to WHO standards of 2011, the maximum permissible limit for EC in drinking water should be 1500 mg/L. The value of EC in groundwater in the study area was above the standard in all groundwater samples. The spatial distribution in the study area was shown in Fig. 5D.

D. Total hardness (TH) of groundwater samples in the study area

Water hardness (TH) is caused by the existence of cations in water, specifically calcium and magnesium, and anions like carbonate, bicarbonate, chloride, and sulfate. It is known by precipitation of soap scum and requires additional use of soap to accomplish cleaning purpose. According to WHO standards of 2011, the maximum permissible limit for TH in drinking water should be 300 mg/L. The value of TH in groundwater in the study area was below the standard in all groundwater samples except *sample location (SL) 3* (412 mg/L). The spatial distribution in the study area was shown in Fig. 5B.

E. Total Alkalinity(TA) of groundwater samples in the study area

Alkalinity is important water quality parameters used to measure the capacity of neutralized acids. According to WHO standards of 2011, the maximum permissible limit for TA in drinking water ought to be 500 mg/L and 200 mg/L, respectively. The value of TH in the groundwater of the study area was above the standard in all groundwater samples. The spatial distribution in the study area was shown in Fig. 5C.

3.4. Hydro-geochemical facies

The chemical composition of the analyzed groundwater samples of the study area was represented by plotting them in the Piper tri-linear diagram. These diagrams reveal the distribution of the groundwater samples in different subdivisions of the diamond-shaped field of the piper diagram, the analogies, and dissimilarities. The dominant groundwater type of the study area was the mixed Ca–Na–HCO₃ type and Na–HCO₃ type (Fig. 6). Studies reported that Na/Ca–HCO₃ water is dominant in escarpment and Na–HCO₃ type of water is dominant in the rift floor (Kawo and Shankar, 2018; Shankar and Nafyad, 2019). Hot springs and groundwater in the rift valley has a Na–HCO₃ water type, with high Na⁺ and HCO₃²⁻ concentration (Ayenew, 2005; Shankar and Nafyad, 2019). Haji et al. (2018) reported that high concentration of fluoride is related to Na–HCO₃ type of waters. However, this was not confirmed in the current study since all the fluoride concentration of the groundwater were within the recommended standards (Table 5).

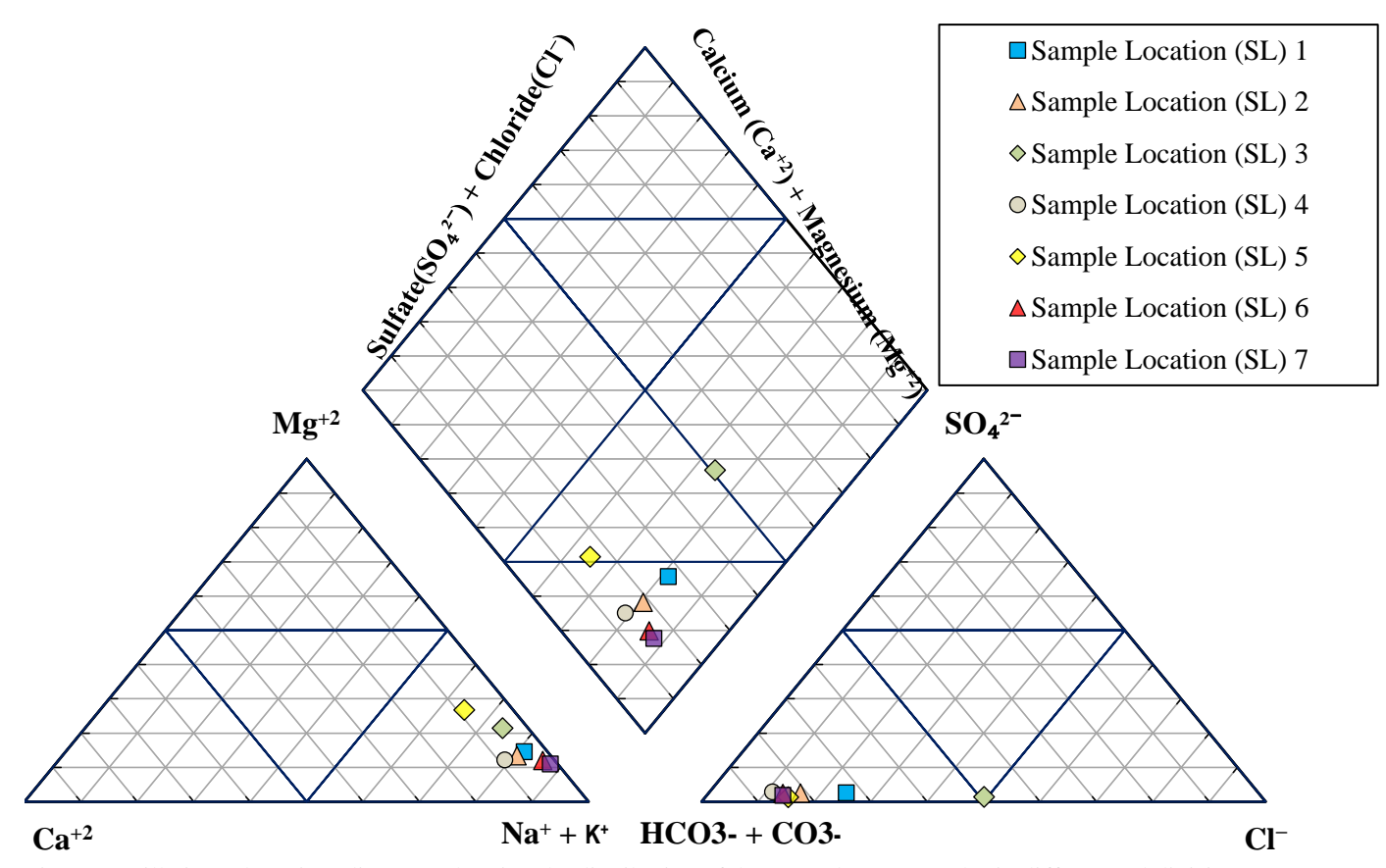


Figure 6. Hill piper plot (piper diagram) showing the distribution of the groundwater samples in different subdivisions of the diamond-shaped field

3.5. Groundwater evolution mechanisms

Previously, Gibbs diagrams are mainly helpful for the rapid identification of the evolution mechanism of surface waters (Gibbs, 1970), but now, they are widely applied in groundwater studies (Amiri, 2020; Feifei et al. 2021; Somvir, 2017). The diagram for this study was developed using prepared Excel. There are natural factors that control the chemical characteristics of groundwater such as rainfall, evaporation, and water and rock interactions. To understand the groundwater chemistry and the relationship of chemical components of groundwater from their respective aquifers such as chemistry of the rock types, chemistry of precipitated water and rate of evaporation a diagram in which ratios of dominant anions and cations are plotted against the values of total dissolved solids (TDS) was suggested. The result on the diagram is representing the ratio-I for cations $[(Na^+)/(Na^+ + Ca^{2^+})]$ and ratio-II for anions $[Cl^-/(Cl^- + HCO_3^-)]$ as a function of TDS. This is used to assess the functional sources of dissolved chemical constituents, such as precipitation-dominance, rock-dominance and evaporation dominance (Somvir, 2017).

The data of groundwater samples in this study were plotted on the Gibbs diagram (Fig. 7). The Na⁺/(Na⁺ + Ca²⁺) of all groundwater samples was greater than or close to 0.8, and the Cl⁻/(Cl⁻ + HCO₃⁻) of all samples was less than 0.5. The TDS values of all groundwater samples varied between 1000 and 10000 mg/L. The result indicated that about 50% of samples indicate chemical weathering of rock-forming minerals which influenced the groundwater by means of dissolution of rocks through which water was circulating. But, 50% of samples represented evaporation dominance. Evaporation increases salinity through high concentration of Na⁺ and Cl⁻ might be owing to anthropogenic activities like using fertilizers and irrigation.

Han et al. (2010) using Gibbs diagram indicated that water—rock interactions and rock weathering were the main factors controlling the chemical characteristics of groundwater in some area of Xinzhou Basin. In addition, Somvir, (2017) identified that chemical weathering of rock-forming minerals influenced groundwater quality by means of dissolution of rocks, and evaporation dominance.

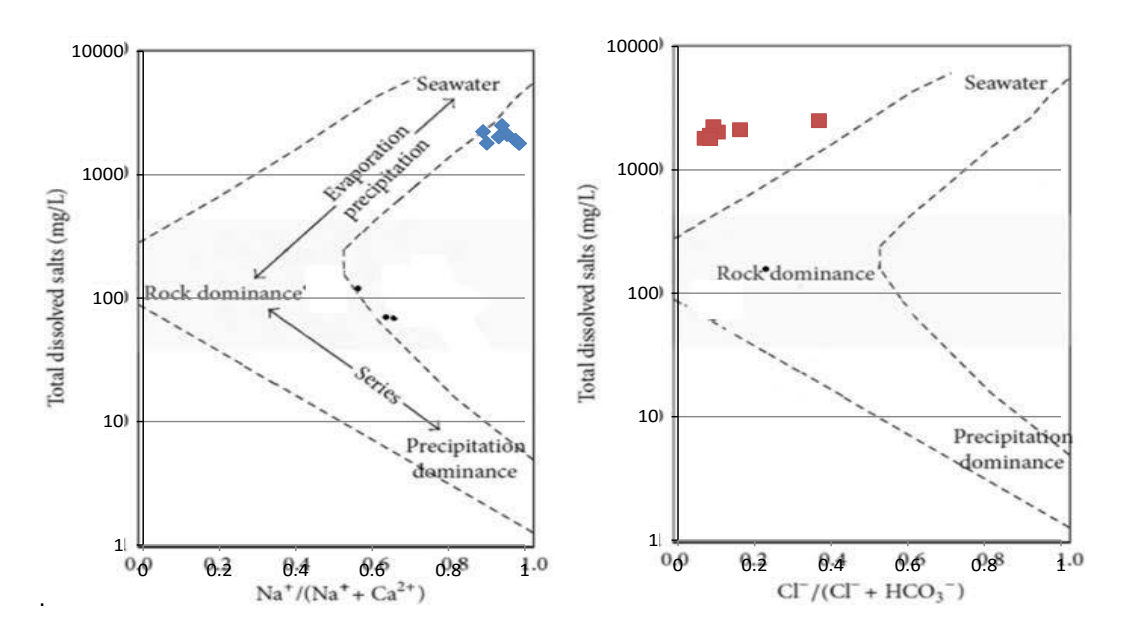


Figure 7. Gibbs diagrams of groundwater samples. $(Na^+/(Na^++Ca^{2^+}))$ and $Cl^-/(Cl^-+HCO_3^-)$

3.6. Water quality index (WQI) result for the groundwater sites

First, 12 important water quality parameters were selected as displayed in Table 6 and a weight was assigned to each parameter depending upon the effect on human health. In addition, the limit values of the World Health Organization's guidelines (WHO) 2011 were utilized in the calculations (Table 6). The highest weight of 5 was assigned to parameters such as Ca^{+2} and F^{-1} which had the major effects on water quality especially during drinking. SO_4^{-2} , TH and TDS were assigned a weight of 4. EC, pH, Mg^{+2} , Cl^{-1} and HCO3- were assigned a weight of 3. Na^{+1} and K^{+1} were assigned a weight of 2 taking their importance into consideration in water quality. The relative weights (W_i) were computed for each parameter and results were given in Table 6. The WQI values were calculated using related equations (Equations (2)–(4)) (displayed in the methodology section), and WQI results and water types for individual samples were presented in Table 3.

The WHO standards of 2011 was used for the WQI calculation, and weight was given to each parameter and relative weight was calculated. WQI of the study area ranged from 84.4 to 174.3. The result of WQI indicated that about 57.1% (4 out of 7) and 42.9% (3 out of 7) of groundwater samples fell in the category of good and poor water quality, respectively (Table 7). The spatial

distribution of WQI indicated that slightly more than half of the town had good quality of groundwater with some sites having poor groundwater quality.

Table 5: Relative weight of chemical parameters

Parameters	WHO limit	Weight (w _i)	Relative weight
EC	1500	3	0.073
рН	6.5-8.5	3	0.073
TDS	1000	4	0.097
TH	300	4	0.097
Ca^{+2}	300	5	0.122
${ m Ca^{+2}} \ { m Mg^{+2}}$	50	3	0.073
Na ⁺	200	2	0.049
\mathbf{K}^{+}	12	2	0.049
$\mathbf{F}^{\text{-}}$	1.5	5	0.122
$SO_4^{2^-}$	250	4	0.097
Cl^{-}	250	3	0.073
HCO3-	500	3	0.073
		$\Sigma w_i = 41$	$\Sigma W_i = 1.000$

Table 7: The Calculated WQI value for individual water samples

Sample No.	Sample Site	WQI	Classification
1	Sample Location (SL) 1	104.6	Poor water
2	Sample Location (SL) 2	100.6	Poor water
3	Sample Location (SL) 3	174.3	Poor water
4	Sample Location (SL) 4	94.7	Good water
5	Sample Location (SL) 5	84.4	Good water
6	Sample Location (SL) 6	97.9	Good water
7	Sample Location (SL) 7	97.5	Good water

4. CONCLUSIONS AND RECOMMENDATIONS

The pH values of groundwater were slightly basic in nature (average = 7.99). The pH of groundwater samples indicated alkaline in nature. The EC, HCO_3^- and TDS values of all the samples exceeded the upper limit of WHO standards for drinking water. The chloride concentration in groundwater for all samples of the study area were within the desirable limit of WHO standards except *sample location (SL)* 3 which exceeded the maximum allowable limit of 250 mg/L.

The order of abundance of cations in the groundwater was $Ca^{2^+} < Mg^{2^+} < K^+ < Na^+$ and the order of anionic abundance was $F^- < SO_4{}^{2^-} < Cl^- < HCO_3{}^-$. Based on the hydro-geochemical facies identified, the majority of the samples were represented by Ca–Na–HCO3 type and Na–HCO3 type of water. The Piper Tri-linear diagram indicated that most of the groundwater samples fell in Mixed Ca–Na–HCO3 types. Quality of groundwater in the samples was mainly dominated by evaporation while remaining samples were dominated by chemical weathering of rock forming minerals.

The result of WQI indicated that 57.1% (4 out of 7) and 42.9% (3 out of 7) of groundwater samples fell in the category of good and poor groundwater quality, respectively.

Overall, groundwater quality parameters should be monitored and regularly inspected in the riskey areas of sample location (*SL*) 1, 2 and 3 in Holte town to avoid human health related problems and ensure sustainable socio-economic development. The local government should ensure that land use plans and regulations should protect the local environment and groundwater sources. The residents should be educated about groundwater and the town facilities should have good pollution prevention practices to avoid further environmental degradations. Also, further geochemical and groundwater quality investigations should be carried out to reduce the possibility of groundwater contamination and thus keep the community safer.

Abbreviations

EC: Electrical Conductivity; GW: Groundwater; TA: Total Alkalinity; TH: Total Hardness; TDS: Total Dissolved Solids; WQI: Water Quality Index; WHO: World Health Organization; SL: Sample Location

Authors' contributions

Mr. Demamu Tagele and Dr. Tamru Tesseme carried out the water quality analysis and statistical portion of the study, data analysis, interpretation of results and manuscript writing, reviewed and finalized the manuscript. The authors read and approved the final manuscript.

Funding

No fund was allocated for this study.

Availability of data and materials

All available data are found in the research article.

DECLARATIONS

Ethics approval and consent to participate

The ethical approval was obtained from Arba Minch University, Water Technology Institute, Department of Water Supply and Environmental Engineering.

Competing interests

The authors declare that they have no competing interests.

REFERENCES

- APHA (2005). Standard methods for the examination of water and wastewater (21st ed.).
- World Health Organization (WHO). (2011). Guidelines for Drinking-water Quality. Fourth edition.
- A. Keshav Krishna, K. R. M. a. B. D. (2019). Assessment of groundwater quality, toxicity and health risk in an industrial area using multivariate statistical methods. 8, 26. doi: https://doi.org/10.1186/s40068-019-0154-0
- A.H. Jagaba, S. R. M. K., G. Hayder, L. Baloo, S. Abubakar, A.A.S. Ghaleb, I.M. Lawal, A. Noor, I. Umaru, N.M.Y. Almahbashi (2020). Water quality hazard assessment for hand dug wells in Rafin Zurfi, Bauchi State, Nigeria. *Ain Shams Engineering Journal*. doi: https://doi.org/10.1016/j.asej.2020.02.004
- Adimalla, N., Dhakate, R., Kasarla, A. & Taloor, A. K. (2020). Appraisal of groundwater quality for drinking and irrigation purposes in Central Telangana, India. Groundwater for Sustainable Development. *10*.

- Agency, Ethiopian Standard. (2013). Ethiopian Standard under the direction of the Technical Committee for Water Quality (TC 78) and Ethiopian Standards Agency (ESA). First Edition 2013.
- Vasanthavigar M., et al. (2010). Vasanthavigar M et al. Application of water quality index for groundwater quality assessment: Thirumanimuttar sub-basin, Tamilnadu, India. *Environmental Monitoring and Assessment 171*, 595–609.
- Alam, R., Ahmed, Z. and Howladar, M.F. (2020). Evaluation of heavy metal contamination in water, soil and plant around the open landfill site Mogla Bazar in Sylhet, Bangladesh. Groundwater for Sustainable Development. *10*, 100311.
- Aly, A., Alomran, A., Alwabel, M., Almahaini, A. & Alamari, M. (2013). Hydrochemical and quality of water resources in Saudi Arabia groundwater: a comparative study of Riyadh and Al-Ahsa Regions. *Proceedings of the International Academy of Ecology and Environmental Sciences*, 3, 42.
- Amiri, V. B., R. (2020). Fluoride occurrence and human health risk from groundwater use at the west coast of Urmia Lake, Iran. *Journal of Geoscience*, *13*, 921.
- Ayenew, T. (2005). Major ions composition of the groundwater and surface water systems and their geological and geochemical controls in the Ethiopian volcanic terrain. *SINET*, *Ethiopian Journal Science*, 28(2), 171-188.
- Ayenew, T. (2008). The distribution and hydrogeological controls of fluoride in the groundwater of central Ethiopian rift and adjacent highlands. *Environmental Geology*, *54*(6), 1313-1324. doi: https://doi.org/10.1007/s00254-007-0914-4
- Ayenew, T., Kebede, S., Alemyahu, T., . (2008). Environmental isotopes and hydrochemical study as applied to surface water and groundwater interaction in the Awash river basin. *Hydrological Processes*, 8. doi: https://doi.org/10.1002/hyp.6716
- Bala Krishna, P. M. a. R., A. L. (2005). Solute Sources and Processes in the Achankovil River Basin, Western Ghats, Southern India. *Hydrological Sciences Journal*, *50*(2), 341-354. doi: https://dx.doi.org/10.1623/hysj.50.2.341.61798
- Bhat, T. A. (2014). An analysis of demand and supply of water in India. *Journal of Environment and Earth Science*, 4, 67-72.

- Dagnew, T., Assefa, D., Woldemariam, G., Solomon, F. and Schmoll, O. . (2007). Rapid Assessment of Drinking-Water Quality in the Federal Republic of Ethiopia. The Federal Democratic Republic of Ethiopia, Ministry of Health, Environmental Health Department, Country Report, Addis Ababa.
- Daniele L, C. M., Vallejos A, Dı'az-Puga M and Pulido-Bosch A. (2013). Geochemical simulations to assess the fluorine origin in Sierra de Gador groundwater (SE Spain). Geofluids. 2(13), 194–203.
- Dinka, M. O., Loiskandl, W. and Ndambuki, J. M. (2015). Hydrochemical characterization of various surface water and groundwater resources available in Matahara areas, Fantalle Woreda of Oromiya region. *Journal of Hydrology: Regional Studies*, *3*, 444-456. doi: https://doi.org/10.1016/j.ejrh.2015.02.007
- Feifei Chen, L. Y., Gang Mei, Yinsheng Shang, Fansheng Xiong and Zhenbin Ding (2021). Groundwater Quality and Potential Human Health Risk Assessment for Drinking and Irrigation Purposes: A Case Study in the Semiarid Region of North China. *Water*, *13*. doi: https://doi.org/10.3390/w13060783
- Fetter, C. W. (2001). Applied hydrogeology + Visual Modflow, Flownet and Aqtesolv student version software on CD ROM. Prentice Hall, Upper Saddle River. 597.
- Furi, W., Razack, M., Abiye, T.A., Ayenew, T. and Legesse. (2011). Fluoride enrichment mechanism and geospatial distribution in the volcanic aquifers of the Middle Awash basin, Northern Main Ethiopian Rift. *Journal of African Earth Sciences*, 60, 315-327. doi: https://doi.org/10.1016/j.jafrearsci.2011.03.004
- Gebrerufael Hailu Kahsay, T. G., Fethanegest Woldemariyam and Tesfa-alem Gebreegziabher Emabye. (2019). Evaluation of Groundwater Quality and Suitability for Drinking and Irrigation Purposes Using Hydrochemical Approach: The Case of Raya Valley, Northern Ethiopia. *Momona Ethiopian Journal of Science (MEJS)*, 1(1), 70-89. doi: http://dx.doi.org/10.4314/mejs.v11i1.5
- Gibbs, R. J. (1970). Mechanisms Controlling World Water Chemistry. Science 1088–1090.
- GK., Brihane. (2018). Characterization of hydro chemistry and groundwater quality evaluation for drinking purpose in Adigrat area, Tigray, northern Ethiopia. *Water Science* 32(2), 213–229.

- Haji, M., Wang, D., Li, L., Qin, D. and Guo, Y. (2018). Geochemical Evolution of Fluoride and Implication for F– Enrichment in Groundwater: Example from the Bilate River Basin of Southern Main Ethiopian Rift. Water. *10*(12), 1799. doi: https://doi.org/10.3390/w10121799
- Han D, T. X., Jin M, Hepburn E, Tong C and Song X. (2013). Evaluation of organic contamination in urban groundwater surrounding a municipal landfill, Zhoukou, China. *185*, 3413–3444. doi: 10.1007/s10661-012-2801-z
- Han, D. M. L., X.; Jin, M.G.; Currell, M.J.; Song, X.F.; Liu, C.M. . (2010). Evaluation of groundwater hydrochemical characteristics and mixing behavior in the Daying and Qicun geothermal systems, Xinzhou Basin. J. Volcanol. Geotherm 189, 92–104.
- Hasan, S. (2014). Effect of Climate Change on Groundwater Quality for Irrigation Purpose in a Limestone Enriched Area. Doctoral Dissertation.
- Hounslow, A. W. (1995). Water quality data: analysis and interpretation. CRC Press, Florida.
- Igibah CE, T. J. (2019). Assessment of urban groundwater quality using Piper trilinear and multivariate techniques: a case study in the Abuja, North-central, Nigeria. *Environ System Research* 8(14).
- Kawo, N. S. and Shankar K. (2018). Groundwater quality assessment using water quality index and GIS technique in Modjo River Basin, central Ethiopia
- Journal of African Earth Sciences, 147, 300-311. doi: https://doi.org/10.1016/j.jafrearsci.2018.06.034
- Shankar Karuppannan and Nafyad Serre Kawo (2019). Groundwater Quality Assessment Using Geospatial Techniques and WQI in North East of Adama Town, Oromia Region, Ethiopia. *Hydrospatial Analysis*, *3*(1), 22-36.
- Kuhr P, H. J., Kreins P, Kunkel R, Tetzlaff B, Vereecken H and Wendland F. (2013). Model based assessment of nitrate pollution of water resources on a federal state level for the dimensioning of agro-environmental reduction strategies: the North Rhine-Westphalia (Germany) case study. *Water Resource Management*, 27, 885–909. doi: 10.1007/s11269-012-0221-z

- Lapworth, D., Nkhuwa, D., Okotto-Okotto, J., Pedley, S., Stuart, M., Tijani, M. & Wright, J. (2017). Urban groundwater quality in sub-Saharan Africa: current status and implications for water security and public health. *Hydrogeology Journal*, 25, 1093-1116.
- Li P, Qian H. and Wu J. (2014). Accelerate research on land creation. Nature. 510, 29–31.
- Li P., Wu J. and Qian. H. (2016). Hydrochemical appraisal of groundwater quality for drinking and irrigation purposes and the major influencing factors: a case study in and around Hua County, China. *Arab J Geosci*, *9*(1), 15. doi: 10.1007/s12517-015-2059-1
- Jalali M. (2011). Nitrate pollution of groundwater in Toyserkan, western Iran. *Environvironmental Earth Science*, 62, 907–913. doi: 10.1007/s12665-010-0576-5
- Mechal, A., Birk, S., Dietzel, M., Leis, A., Winkler, G., Mogessie, A. and Kebede, S. (2017). Groundwater flow dynamics in the complex aquifer system of Gidabo River Basin (Ethiopian Rift): A multi-proxy approach. *Hydrogeology Journal*, 25(2), 519-538. doi: https://doi.org/10.1007/s10040-016-1489-5
- Mengesha, A., Wubshet, M. and Gelaw, B. . (2004). A Survey of Bacteriological Quality of Drinking Water in North Gondar. *The Ethiopian Journal of Health Development*, 18, 112-115.
- Muhammad Mohsin, S. S., Faryal Asghar and Farrukh Jamal. (2013). Assessment of Drinking Water Quality and its Impact on Residents Health in Bahawalpur City. *International Journal of Humanities and Social Science*, 3(15).
- Nasrabadi T. and Bidabadi N. (2013). Evaluating the spatial distribution of quantitative risk and hazard level of arsenic exposure in groundwater, case study of Qorveh County, Kurdistan Iran. *Iran Journal Environvironmental Health Science Engineering*. doi: 10.1186/1735-2746-10-30
- Nchofua Festus Biosengazeh, N. A. M., Njoyim Estella Buleng Tamungang, and Antoine David Mvondo. (2020). Assessment of Ground Water Quality in Baba I Village, North-West Cameroon. *Journal of Geoscience and Environment Protection*, 8, 87-104.
- Nigus KebedeWegahita, L. M., Jiankui Liu, Tingwei Huang, Qiankun Luo and Jiazhong Qian. (2020). Spatial Assessment of Groundwater Quality and Health Risk of Nitrogen Pollution for Shallow Groundwater Aquifer around Fuyang City, China. *Water*, 12. doi: 10.3390/w12123341

- Bhalme SP. and Nagarnaik PB. (2012). Analysis of drinking water of different places A review. *International Journal of Engineering Research*, 2.
- Purushothaman, P., Rao, M. S., Rawat, Y. S., Kumar, C.P., Krishan, G. & Parveen, T. (2014). Evaluation of hydrogeochemistry and water quality in Bist-Doabregion, Punjab, India. *Environmental and Earth Sciences*, 72(3), 693–706.
- Ramya Priya, R. a. E., L. (2018). Evaluation of geogenic and anthropogenic impacts on spatiotemporal variation in quality of surface water and groundwater along Cauvery River, India. *Environmental Earth Science*, 77(2).
- Şehnaz Şener, E. S. e. a. A. e. D. (2017). Assessment of groundwater quality and health risk in drinking water basin using GIS. *Journal of Water and Health*.
- Somvir Singh, N. C. M. a. V. S. S. (2017). Groundwater quality in and around Tuticorin town, Southeast coast of India. *Somvir Singh, N.C. M, 21*(1), 34-43.
- Tai T, W. J., Wang Y and Bai L. (2012). Groundwater pollution risk evaluation method research progress in our country. *Journal Beijing Norm Univ Natural Science*, 06, 648–653.
- Tamiru, A. (2004). Assessment of pollution status and groundwater vulnerability mapping of the Addis Ababa water supply aquifers, Ethiopia.
- Taye, A. (1988). Pollution of the hydrogeologic system of Dire Dawa groundwater basin.
- Tilahun K. Entonyos , D. K. D., and Vasudeva R. Pampana. (2022). Contemplated Investigation and Statistical Prediction of the Swelling Potential of Expansive Soils Using Index Properties of Holte Town, Southern Ethiopia. *Advances in Civil Engineering, Volume* 2022, 11. doi: https://doi.org/10.1155/2022/7056384
- Tirkey P, B. T., Chakraborty S, Baraik S. . (2017). Assessment of groundwater quality and associated health risks: a case study of Ranchi city, Jharkhand, India. *Groundwater Sustainable Development*, 5, 85–100.
- Tiwari T, M. M. (1985). A preliminary assignment of water quality index of major Indian rivers. Indian J Environ Prot *5*(4), 276–279.
- Tsega, N., Sahile, S., Kibret, M. and Abera, B. (2014). Bacteriological and Physicochemical Quality of Drinking Water Source in a Rural Community of Ethiopia. *African Health Sciences* 13, 1156-1161. doi: https://doi.org/10.4314/ahs.v13i4.42

- Varol, S. D., A. (2015). Evaluation of the groundwater quality with WQI (Water Quality Index) and multivariate analysis: a case study of the Tefenni plain (Burdur/Turkey). *Environmental and Earth Sciences*, 73, 1725–1744.
- Wagh, V. M., Mukate, S. V., Panaskar, D. B., Muley, A. A. and Sahu, U. L. (2019). Study of groundwater hydrochemistry and drinking suitability through Water Quality Index (WQI) modelling in Kadava river basin, India. *SN Applied Sciences*, 1(10). doi: https://doi.org/10.1007/s42452-019-1268-8
- Wagh, V. M., Panaskar, D. B., Jacobs, J. A., Mukate, S. V., Muley, A. A. and Kadam, A. K. (2019). Influence of hydro-geochemical processes on groundwater quality through geostatistical techniques in Kadava River basin, Western India. *Arabian Journal of Geosciences*, 12(1). doi: https://doi.org/10.1007/s12517-018-4136-8
- World Health Organization. (2011). Guidelines for drinking-water quality. WHO chronicle fivth edition. *38*(4), 104-108.
- Wongsasuluk P, C. S. W. a. R. M. (2014). Heavy metal contamination and human health risk assessment in drinking water from shallow groundwater wells in an agricultural area in Ubon Ratchathani province. Environ Geochem Health Thail. doi: 10.1007/s10653-013-9537-8
- Yahong Zhou, A. W., Junfeng Li, Liangdong Yan and Jing Li. (2016). Groundwater Quality Evaluation and Health Risk Assessment in the Yinchuan Region, Northwest China. *Expo Health*, 8, 443–456. doi: 10.1007/s12403-016-0219-5
- Yitbarek, A., Razack M., Ayenew, T. Zemedagegnehu, E. and Azagegn. T., . (2012). Hydrogeological and hydrochemical framework of Upper Awash River basin, Ethiopia: With special emphasis on inter-basins groundwater transfer between Blue Nile and Awash Rivers. *Journal of African Earth Sciences*(65), 46-60. doi: https://doi.org/10.1016/j.jafrearsci.2012.01.002
- Wu J. and Sun Z. (2015). Evaluation of shallow groundwater contamination and associated human health risk in an alluvial plain impacted by agricultural and industrial activities, mid-west China. Expo Health. 1–19. doi: 10.1007/s12403-015-0170-x

Comparative Performance Evaluation of HEC-HMS and SWAT Models in Stream Flow Simulation: the Case of Bilate and Gidabo Watersheds, Ethiopia

Bereket Dora Doliso¹, Samuel Dagalo Hatiye²

ABSTRACT

Many hydrological models have been developed to simulate watershed hydrology. However, identifying the most cost-effective and efficient hydrological models for a specific watershed with reasonable certainty becomes difficult. The purpose of this study was to compare the stream flow prediction efficiency of the HEC-HMS and SWAT models, as well as the associated uncertainty, in the Bilate and Gidabo watersheds. Model-sensitive parameters being identified, they were calibrated and validated. The parameter uncertainties were analyzed using Markov Chain Monte Carlo (MCMC) for HEC-HMS and Sequential Uncertainty Fitting version two (SUF-2) for SWAT. In the case of the HEC-HMS model, the results showed that constant loss rate (CR) was the most sensitive parameter, followed by lag time (LT) for both watersheds. SWAT detected ALPHA_BF in the Bilate Watershed and CN_2 in the Gidabo Watershed as the most sensitive parameters. Overall, both models could adequately simulate the hydrology of both watersheds. Despite their similar modeling capabilities, a comparison analysis revealed that the HEC-HMS model outperformed the SWAT model in simulating streamflow in both watersheds. The findings of this study can help potential model users make risk-informed decisions by selecting a representative model and quantifying associated uncertainty in the modeling field.

Keywords: Bilate and Gidabo watersheds, comparative evaluation, HEC-HMS, SWAT, flow simulation.

Received: 29 Sept 2022; accepted 15 Nov 2022.

¹ Arba Minch Water Technology Institute, Arba Minch University, Ethiopia; Faculty of Hydraulic and Water Resources Engineering.

¹ Arba Minch Water Technology Institute, Arba Minch University, Ethiopia; Faculty of Water Resources and Irrigation Engineering; Water Resources Research Center, Ethiopia.

^{*} corresponding Author; email: samueldagalo@gmail.com

1. INTRODUCTION

Many hydrological models had been developed and were accessible to water resources studies, such as water resources management, flood control, land planning, water quality, and climate change studies (Wu & Chen, 2015). The models were used to analyze the quantity of stream flow, reservoir system operation, surface and groundwater use management, flood forecasting, ecology, and a range of water management practices (Wurbs, 1998). According to a review of literature, the most commonly used hydrological models in Ethiopia were Hydrologiska Byran's Vattenbalansavdelning (HBV), Hydrologic Engineering Center's Hydrologic Modeling System (HEC-HMS), Soil and Water Assessment Tool (SWAT), Hydrological Simulation Program-Fortran (HSPF), and MIKE SHE. However, the ranges of applications of the models were different since the assumptions involved in each model varied, and catchments were heterogeneous. Additionally, many models required data unavailable in the watersheds, especially in developing countries (Sivapalan et al., 2003). As a result, potential model users increasingly found it challenging to determine the best, most cost-effective, and most efficient hydrological models to produce high-quality results.

The hydrological model selection was based on knowledge of modeling method, data quality and availability, model performance, and applicability. Earlier studies conducted around the world indicated that one model might represent the hydrological/physical process better than the other. The performance of each model varied from watershed to watershed (Abebe, 2017; Abyot, 2008; Aliye et al., 2020; Dhami & Pandey, 2013; Golmohammadi et al., 2014; Khoi, 2016). Therefore, earlier studies suggested that further studies needed to reach a sound conclusion about the superiority of one model over the other.

HEC-HMS and SWAT models had been extensively used in different parts of the world. However, hydrological models were highly subject to uncertainty owing to the assumptions of the model itself and the watershed system complexities, which concerned potential model users (Song et al., 2015; Zhanling et al., 2009). Uncertainty in model output arose from measurement errors associated with input data, model structure, and parameter uncertainty (Abbaspour et al., 2007). From these uncertainty sources, uncertainty from parameters was easy to control through appropriate model calibration (Wu & Chen, 2015). However, parameter values obtained through

the calibration process possessed a degree of quantifiable uncertainty because of incomplete knowledge of parameter value ranges, physical meaning, and temporal and spatial variability. Therefore, model predictions were unreliable when model parameter values were uncertain. In some cases, wastage of resources might occur due to overestimating uncertainty, and unexpected losses might occur due to underestimating uncertainty (Shen et al., 2012). Therefore, the uncertainty of hydrological models should be scrutinized (Abbaspour et al., 2007). In addition, Herrera et al. (2022) noted that when models are used to predict the future, it's crucial to limit the uncertainty of the outcomes. A variety of uncertainty analysis methods had been developed to characterize, control, and quantify the parameter and modeling uncertainties, such as sequential uncertainty fitting (SUFI-2), generalized likelihood uncertainty estimation (GLUE), Markov chain Monte Carlo (MCMC), and parameter solution (ParaSol). Among these methods, MCMC and SUFI-2 were widely used to quantify and control the uncertainty parameter in HEC-HMS and SWAT models. Abbaspour et al. (2007) stated that SUFI-2 was applied extensively to analyze the sensitivity of parameters and identify the critical source of uncertainty in watershed model outputs. MCMC was applied to quantify the uncertainty in modeling watersheds from model parameters. While HEC-HMS and SWAT models were widely used hydrological models, investigating the uncertainty assessment of the model was essential to improve the reliability of streamflow prediction.

The lack of data about the Ethiopian situation made hydrological modeling efforts challenging to manage water resources for sustainable development. Therefore, selecting models that require less data was economical and advantageous. Several hydrological modeling studies were conducted in Ethiopian watersheds. The HEC-HMS and SWAT models had been extensively used in different watersheds in Ethiopia (Abebe, 2017; Abyot, 2008; Aliye et al., 2020; Kassa & Forech, 2009). However, no exclusive studies were available on the suitability of these hydrological models in the Bilate and Gidabo watersheds. In light of this, the soil and water assessment tool (SWAT) and the hydrologic engineering centers-hydrologic modeling system (HEC-HMS) models are utilized in this work. Abyot (2008) suggested that the HEC-HMS model outperformed the RRL SMAR and RRL TANK models, capturing peak flow in both Bilate and Kulifo watersheds in the Abaya Chamo Basin. Kassa and Forech (2009) demonstrated that the models produced acceptable outputs in hydrological responses to land use and climate changes. They reported that the SWAT model

outperformed the HSPF model when monthly and seasonal stream flow analyses were conducted. Abebe (2017) found that both SWAT and HBV-light models successfully predicted the discharge in the Geba Catchment. Similarly, Aliye et al. (2020) conclude that the HEC-HMS model outperformed other models in simulating the rainfall-runoff process. However, there appears to be no previous studies conducted on the Bilate and Gidabo watersheds using comparative hydrologic models,. As a result, the purpose of this research was to compare the performance and applicability of the HEC-HMS and SWAT hydrological models to the Bilate and Gidabo watersheds. This study sheds light on which model to use and establishes parameters for future use in the two watersheds. Future researchers, hydrologists, agronomists, and water resource managers may find this study useful in their future endeavors.

2. MATERIALS AND METHODS

2.1. Description of the study area

Bilate and Gidabo watersheds are among the major watersheds of the Abaya-Chamo sub-basin, the Rift Valley Lakes basin in Ethiopia. The geographical location of the Bilate Watershed is approximately between 6°40′0″N to 8°5′00″ N latitude and 37°48′0″E to 38° 36′00″E longitudes. Similarly, the Gidabo Catchment is located between 6°15′0″and 6°55′0″N latitude and 38°15′0″ to 38°40′0″ E longitude.

Bilate River drains southwards into Lake Abaya in the main Ethiopian Rift Valley Basin (Figure 1). The study area of the Bilate Watershed covers an area of 5316km² at the entrance of Lake Abaya (outlet). The Bilate Watershed elevation ranges between 3329m a.m.s.l in the northern and 1193m a.m.s.l in the south with a mean elevation of 2261.5m a.m.s.l. The region drained by the Gidabo River is bordered by the southern part of the main Ethiopian Rift Valley Basin flowing eastwards into Lake Abaya (Figure1). The Gidabo Watershed lies in the Borena Zone of the Oromia Region, Gedeo Zone, and Sidama Region, Ethiopia. The estimated area of the Gidabo Watershed is 2310 km². The Gidabo Watershed area ranges between 1183 a.m.s.l near the outlet (at the Dam site) to 3173 a.m.s.l in the western part of the watershed with a mean elevation of 2261.5m a.m.s.l. The average mean maximum and minimum temperatures of Bilate are 32.6°C

and 13.3°C, respectively. Moreover, for the Gidabo Watershed, the mean monthly temperature at the Gidabo Dam is 15°C to 30°C. The rainfall trend in both watersheds is bimodal.

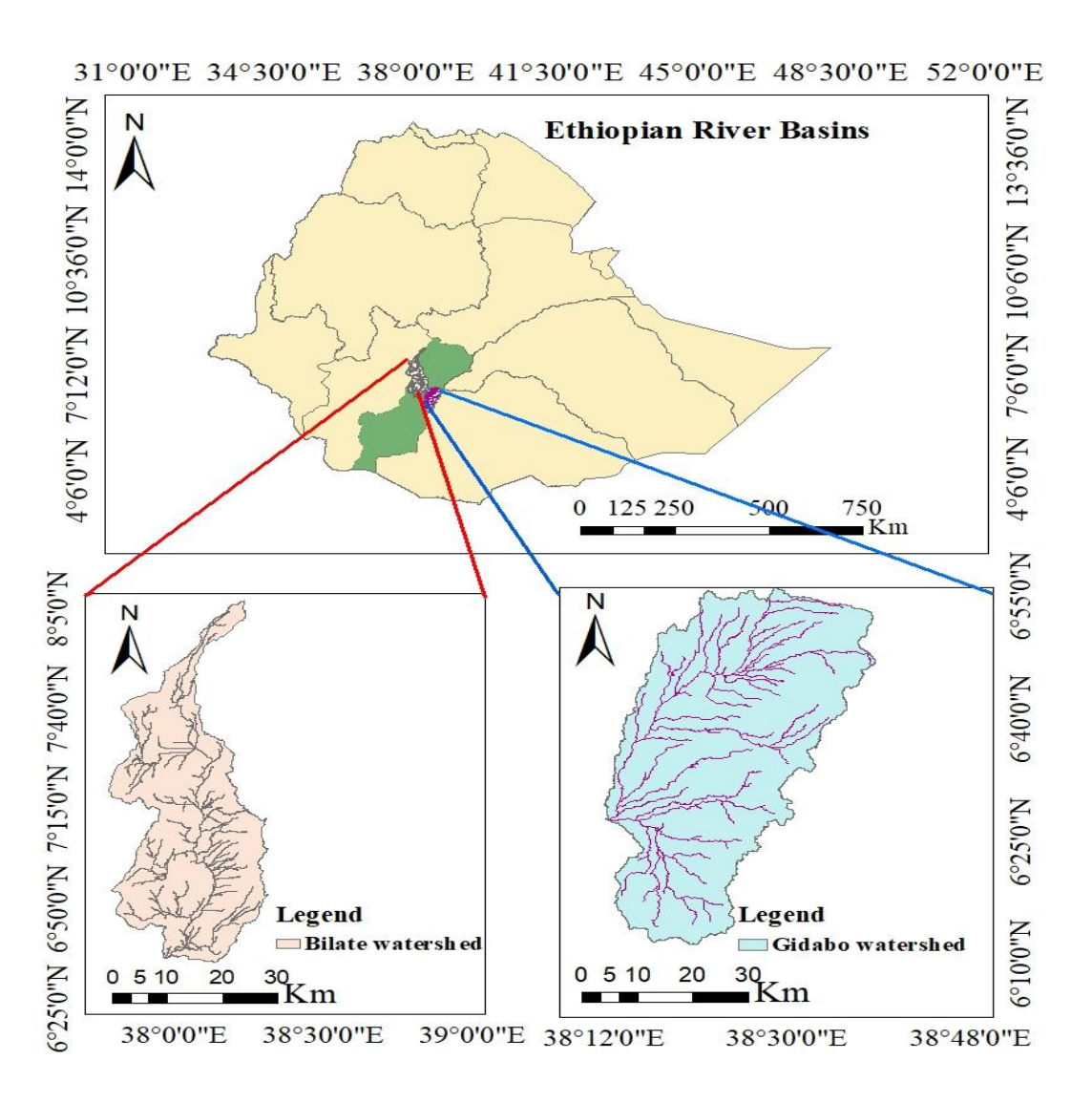


Figure 8. Location of study areas

2.2 Data Set

2.2.1. Meteorological data

The National Meteorological Agency (NMA) of Ethiopia provided meteorological data for both the Bilate and Gidabo watersheds, including daily stream flow, daily minimum and maximum temperature, daily sunshine hourly, daily wind speed, and daily relative humidity. In this study, eight and three meteorological stations are available within and near the study area for the Bilate and Gidabo watersheds, respectively. The data was checked for homogeneity and consistency; errors were fixed, and insufficient and missing data were filled in. The study collected daily meteorological data from 1987 to 2016.

The SWAT model requires daily climate data of rainfall, maximum and minimum temperatures, wind speed, relative humidity, and solar radiation. The meteorological stations chosen for this study had daily air temperature and precipitation data. However, because they have comprehensive weather data, data from the Hosana and Dilla gauging stations in the Bilate and Gidabo watersheds, respectively, were used in this study.

2.2.2. Stream flow

Observed stream flow was required for calibration and validation of both the HEC-HMS and SWAT models. Bilate Tena and Measso are terminal gauging stations on the Bilate and Gidabo river basins, and stream flow data were collected from the Ethiopian Ministry of Water, Irrigation, and Energy. The data were collected over a 17-year period (1999-2015) for Bilate and a 10-year period (1997-2006) for the Gidabo Watershed.

2.2.3. Digital Elevation Model

Using DEM data as input, HEC-HMS, and SWAT models, the accumulation of flow and stream networks were calculated, and the watershed were divided into a number of sub-basins based on elevation. A DEM data with a resolution of 30mx30m was used here. A digital elevation model of both watersheds is provided in Figure 2.

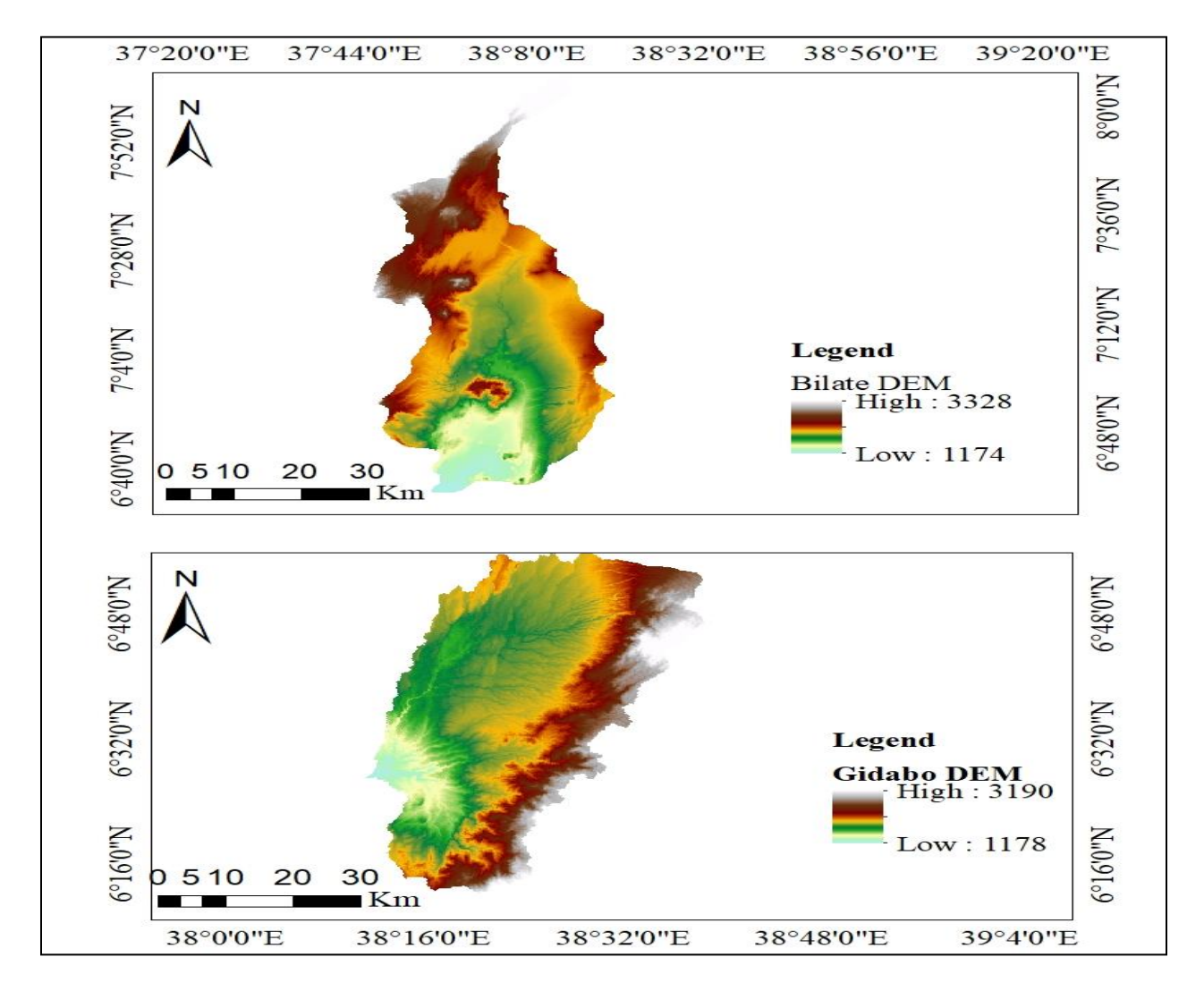


Figure 9: DEM of Bilate and Gidabo watersheds

The study areas' spatial and time series data were generated in the suitable model format and used in the model simulation. Using ArcGIS 10.3, a 30x30m DEM data resolution was used to delineate the watersheds at Bilate Tena and Measso gauging stations for Bilate and Gidabo watersheds, respectively. Accordingly, the entire Bilate and Gidabo watershed area were divided into 23 and 13 sub-basins, respectively. These sub-watersheds were further separated into Hydrologic response units (HRUs), a unique combination of soil, land use, land cover, and slope characteristic areas. The delineated watersheds are indicated in Figure 3.

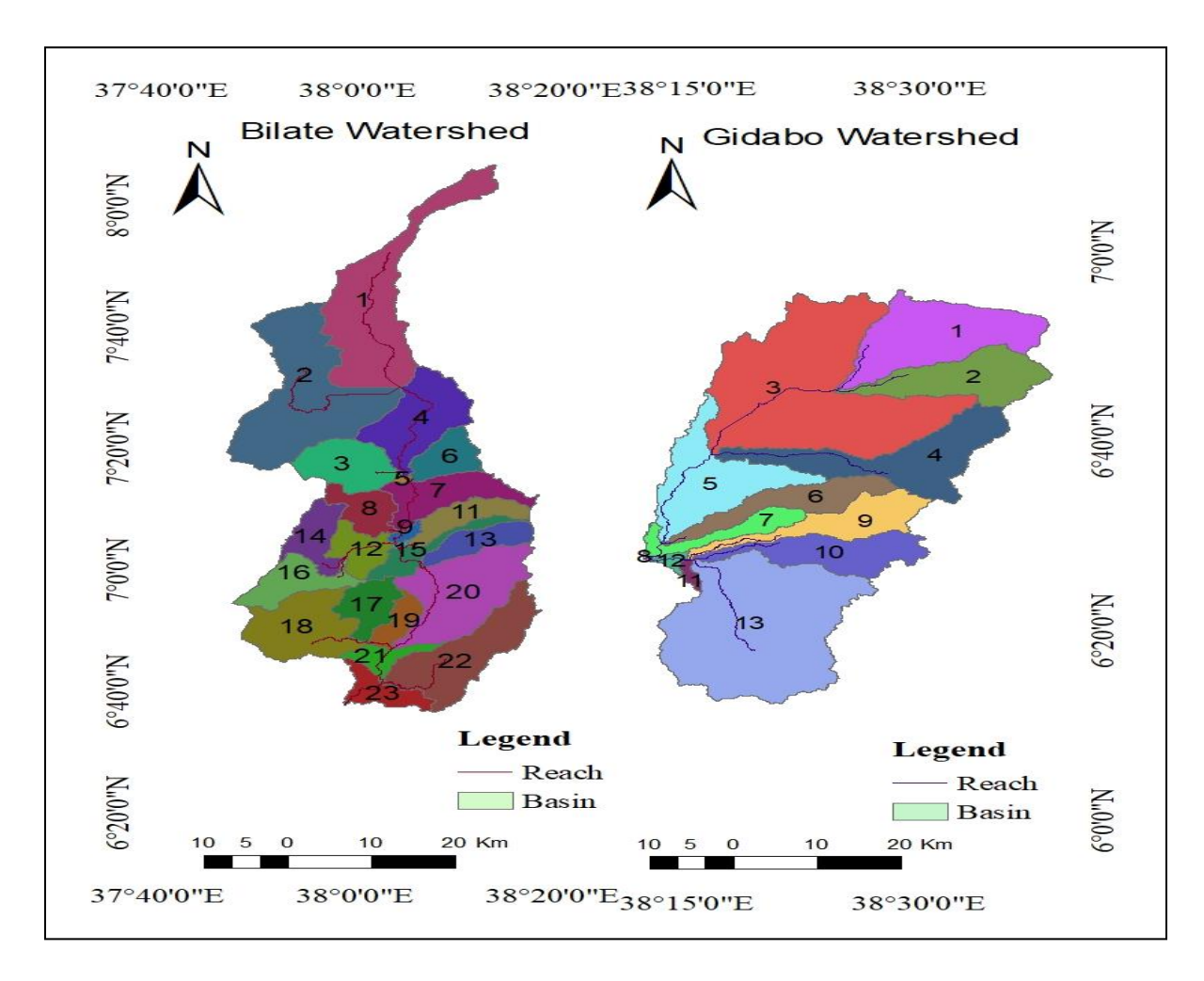


Figure 3: Bilate and Gidabo Watersheds

2.2.4. Land use and land cover

Land use and land cover impact a runoff watersheds, surface erosion, and evapotranspiration. The map depicts the various land use/cover classes as well as the physical extent of the study areas. The land use/land cover map of the Bilate and Gidabo watersheds was created using Arc GIS 10.3 software. The predominant land cover in both watersheds is intensively cultivated land.

2.2.5. Soil data

The Ethiopian Rift Valley Lake Basin Master Plan study was conducted in 2010, and soil samples were collected from all soil units of the basin. In this study, the soil data was collected from MoWIE. The Rift Valley Lake Basin Master Plan document was also used to get the soil

information (Halcrow, 2010). 203 soil samples from 12 different soil units in the Rift Valley Basin were collected, and their physical and chemical characteristics were examined.

2.3. Hydrological Models

The HEC-HMS and SWAT hydrological models were used here in this study. The background information and the necessary steps used in the modeling processes are described in the following sections.

2.3.1. HEC-HMS hydrological model

The Hydrologic Modeling System, HMS, was developed by the US Army Corps of Engineers Hydrologic Engineering Center (HEC) as a modeling tool for all hydrologic processes of dendritic watershed systems. It simplified complex tasks concerning hydrological studies, consisting of time series data, losses, runoff transform, open routing, rainfall-runoff simulation, and parameter estimation (Feldman, 2000; USACE, 2008). The HEC-HMS model is a physically based and conceptually semi-distributed model designed to simulate rainfall-runoff processes in many geographic areas, from large river basins to small urban and natural watershed runoffs. In addition, the HEC-HMS model uses a separate model that computes runoff, the base flow, and runoff volume. The model has four computation methods to address the responsiveness of watersheds, such as loss, transform, base flow, and routing.

The loss methods were designed either for event simulations or continuous simulations. The initial and constant loss methods were used to calculate the loss in the catchment, which was the maximum potential rate of precipitation loss constant throughout an event. These represented the physical properties of the watershed soil, land use, and antecedent condition (Razmkhah, 2016). HEC-HMS also had seven different transformation methods which simulated the process of the direct runoff from excess rainfall in a watershed. In this study, the Soil Conservation Service (SCS) Unit Hydrograph model was used to transform excess rainfall into runoff. The time of concentration (Tc) and lag time (T_{lag}) were employed in the transformation model to compute the runoff from excess rainfall.

The time of concentration was estimated based on the characteristics of the basin, including topography and the length of the reach, using Kirpich's method (Kirpich, 1940):

$$Tc = \frac{L^{0.77}}{S^{0.385}} \tag{1}$$

The lag time is computed as:

$$T_{lag} = 0.6 \times T_c \tag{2}$$

From different methods included in the model to compute base flow, the constant monthly base flow was selected in this study for its suitability to the study areas. The method used long-term simulations and required a separate monthly value for the overall simulation period. The average minimum flow value was taken before model calibration.

When runoff traveled through the channel reach, the flood became attenuated owing to channel storage effects. The Muskingum method of flood routing was selected in this study. It is often used for flood routing in natural channels (Sil et al., 2016). In this model, two parameters were calibrated: the coefficient K, which refers to the travel time of the flood wave through routing reach, and the dimensionless weighting factor (X), which corresponds to the attenuation of the flood wave as it moves through the reach. The Muskingum-Cunge routing equation is given by:

$$S_t = K[XI_t + (1 - X)Q_t] \tag{3}$$

where $S_t[L^3]$ is the storage; $I_t[L^3T^{-1}]$ is the inflow and $Q_t[L^3T^{-1}]$ is the outflow from a given reach.

Arc hydro and HEC-GeoHMS were used to characterize the watersheds. HEC-GeoHMS mainly creates a basin model and a meteorological model and controls specifications before running the HEC-HMS model. The prepared basin model and features were taken as background input map files and imported to HEC-HMS 4.3. Since we had no observation stations in each sub-basin, the precipitation values were estimated by the most widely used Thiessen Polygon method, and weights were worked out in HEC-GeoHMS software.

2.3.2. SWAT hydrological model

The soil and water assessment Tool (SWAT) is a semi-distributed physically based model developed to estimate the stream flow, sediment, and chemical yields in basins. Streamflow

generation is modeled along individual hydrologic response units (HRUs) using multiple watershed-scale characteristics such as hydraulic conductivity, available moisture content, pollutant loading, and management strategies. The HRU-scale results were then piled into subbasin-scale outputs using appropriate weighted average procedures. The hydrological entities at the sub-basin levels were then routed separately. SWAT simulates surface runoff volumes and peak runoff rates for each HRU using daily or sub-daily rainfall levels. The SCS curve number and the Green Ampt infiltration methods are two methods available in SWAT to estimate surface runoff volume. It was challenging to apply the latter method since the sub-daily time step data criterion was difficult to obtain for the study watersheds. Therefore, the SCS curve number method was adopted in this study. SWAT model performs the essential water balance computation to estimate the different flux components given by Equation 4 (Neitsch et al., 2011) as:

$$SW_t = SW_o + \sum_{i=1}^t (R_{day} - Q_{surf} - Ea - W_{seep} - Q_{aw})$$
 (4)

where SW_t is the final soil water content (mm), SW_0 is the initial soil water content (mm), t is time (days), R_{day} is the amount of precipitation on a day i (mm), Q_{surf} is the amount of surface runoff on a day i (mm), Ea is the amount of evapotranspiration on a day i (mm), W_{seep} is the amount of water entering the vadose level zone from the soil profile on day i (mm), and Q_{gw} , is the amount of return flow on day i (mm).

The model also calculates evaporation from the soil and plant canopy surface separately. The potential evapotranspiration (PET) and leaf area index (LAI), or the ratios of plant leaf area to the soil surface, are explicit functions of soil water evaporation. Depending on the input data available, the PET of the catchment could be computed using the Penman-Monteith, Priestley–Taylor or Hargreaves approaches. In the present study, the Penman-Monteith approach was used, which was given by (Allen et al., 1998):

$$ETo = \frac{0.408(Rnet - G) + \gamma \frac{900}{(T + 273)}U(es - ea)}{\Delta + \gamma (1 + 0.34U)}$$
 (5)

where, ET_o is daily reference crop evapotranspiration [mm day⁻¹], Rnet is net radiation flux [MJm⁻²day⁻¹], G is heat flux density in the soil [MJm⁻²day⁻¹], G is psychometric constant [KPA°C⁻¹], G is wind speed measured at 2 m height [ms⁻¹]; G is saturation vapor pressure G is relative humidity [%] and G is slope of the saturation vapor pressure curve [KPa°C⁻¹].

2.4 Model Sensitivity analysis

Sensitivity analysis determines how much a change in an input parameter affects the model response. Prior to assessing the major impact of input variability on certain model outputs of interest, the sensitive parameter was ranked. The output response changes when the most sensitive parameter is used. As a result, sensitivity analysis was used in this study to find sensitive model parameters and link them to catchment runoff generating features (Saltelli et al, 2000).

The sensitivity analysis was carried out manually in HEC-HMS to identify understand the most influential model parameter from selected key parameters. The SUFI-2, on the other hand, determines sensitivity for the SWAT model using global sensitivity analysis. The sensitivity ranks of parameters were assigned in the SUFI-2 method based on the p-value and t-stat values. Based on previous research on rainfall-runoff simulation using the SWAT model (Abebe, 2017; Aliye et al., 2020; Amaru Ayele & Gebremariam, 2020), key parameters were chosen to implement sensitivity and uncertainty analysis using the SUFI-2 model for both watersheds.

2.5. Model Evaluation and Statistical Analysis

Accuracy, consistency, and adaptability of hydrological models is essential for a better prediction of watershed responses. Therefore, the prediction efficiency criterion is required to assess the performance of the model. The performance of HEC-HMS and SWAT models was evaluated in terms of coefficient of determination (R²), Nash and Sutcliffe Simulation Efficiency (NSE), Relative Volume Error (RVE), Percentage Error Peak Flow (PEPF), and Mean Absolute Error (MAE). A common method of evaluating hydrological model performance and behavior is to compare computed and observed variables. The R² value represents the strength of the relationship between the observed and simulated values. The value of R² ranges from zero to one, with higher values indicating better agreement of simulated and observed values. The Nash-Sutcliffe Simulation Efficiency (ENS) displays the degree of fitness of the observed and simulated plots. The ENS also assesses how well the simulated results predict the measured data.

RVE indicates the variation between simulated and observed discharge on relative bases. The relative volume error can range between $-\infty$ and ∞ but it performs best when a value is zero showing there is no difference between simulated and observed discharge occurs.

The statistical indexes are given as:

$$R^{2} = \frac{\left[\sum_{i=1}^{n} (Ysim - \overline{Y}sim)(Yobs - \overline{Y}obs)\right]^{2}}{\sum_{i=1}^{n} (Ysim - \overline{Y}sim)^{2} (\left[Yobs - \overline{Y}obs)\right]^{2}}$$
(6)

where *Ysim* is simulated discharge, $\overline{Y}sim$ is the average of simulated discharge, *Yobs* is observed discharge, $\overline{Y}obs$ is the average of observed discharge (m³/s).

$$E_{NS} = 1 - \frac{\sum_{i=1}^{n} (Yobs - Ysim)^{2}}{\sum_{i=1}^{n} (Yobs - \bar{Y}obs)^{2}}$$
(7)

$$RVE = \frac{\sum_{i=1}^{n} Y_{sim} - \sum_{i=1}^{n} Y_{obs}}{\sum_{i=1}^{n} Y_{obs}}$$
(8)

Hence, the models were calibrated and validated using daily and monthly observed stream flow data obtained from MoWIE. For Bilate Watershed, the models were run from the simulation period (1999-2015). The first two years' data (1999-2000) were used for model initialization; the data for the next 10 years (2001-2010) was used for the model calibration and the remaining five years' (2011-2015) data was used for model validation. For the Gidabo Watershed, the data of one year (January1997-December 1997) stream flow was used for model warm-up; the data from 1998 to 2003 was used for model calibration and the remaining three years data (2004-2006) was used for the model validation. Both the HEC-HMS and SWAT models were automatically calibrated and validated at Bilate (Bilate Tena) and Gidabo (Measso) outlets. During calibration, sensitivity analysis was performed manually for the HEC-HMS model and automatically for the SWAT model using the SWAT CUP software's SUFI-2 program.

2.6 Model Uncertainty

2.6.1. Uncertainty analysis in the HEC-HMS model

Uncertainty refers to the state of being uncertain about something. So far, there are four major sources of uncertainty in hydrologic modeling: (i) input uncertainty, e.g., sampling and measurement errors in catchment rainfall estimates; (ii) output uncertainty, e.g., rating curve errors affecting runoff estimates; (iii) structural uncertainty (model uncertainty) arises from a lumped and simplified representation of hydrological processes in hydrologic models and (iv) parametric uncertainty, reflecting the uncertainty in hydrologic models (Renard et al. 2010).

There are several approaches available to estimate uncertainty in hydrological models. The "Markov Chain Monte Carlo" approach was chosen for this investigation and incorporated in the present study. Convergence is attained when statistical measurements of the watershed response do not change as more samples are computed. The convergence of MCMC to a stable posterior probability density function (PDF) was monitored using statistics (Gelman & Rubin, 1992). Convergence is declared when $R \le 1.2$ for all j = 1 d, where d represents the number of parameters. The calibration parameter constraints determine the simulated upper and lower bounds of the parameter (Scharffenberg, 2016). Finally, the upper, lower, and simulated hydrographs are plotted after determining the best upper and lower bounds for a hydrograph. The uncertainty is said to be low if most of the simulated hydrograph lies between the lower and upper bounds and high if the computed hydrograph lies outside the bound. As shown in equations 9, 10, and 11 below, the P-factor and R-factor are used to determine the strength of calibration/uncertainty of model parameters (Tegegne et al., 2019).

2.6.2. Uncertainty analysis in the SWAT model

SUFI2 was chosen for this investigation because it converged with fewer iterations and allowed for resuming unfinished iterations and breaking iterations into multiple runs. The SUFI-2 algorithm, in particular, was well suited to the calibration and validation of the SWAT model since it incorporated all sources of uncertainty (Abbaspour et al., 2007). The P-factor, the percentage of measured data bracketed by the 95 percent prediction uncertainty (95PPU)., quantified the extent to which all uncertainties were accounted. As a result, the percentage of data captured (bracketed) by prediction uncertainty indicated our uncertainty strength of analysis. The 95PPU was calculated at the 2.5 % and 97.5 % levels of the cumulative distribution of an output variable obtained through Latin hypercube sampling, with 5% of very bad simulations excluded.

The R-factor, the average thickness of the 95PPU band divided by the standard deviation of the measured data, was the other way to estimate the strength of a calibration and uncertainty analysis. As a result, SUFI-2 tried to bracket as much of the collected data as feasible with the smallest possible uncertainty band. The P-factor has a theoretical range of 0 to 100%, while the R-factor

has a theoretical range of zero to infinity. A simulation with a P-factor of 1 and an R-factor of zero corresponds to measured data.

$$P = \sum_{i=1}^{T} (Z_t/T) * 100 \tag{9}$$

$$Z_{t} = \begin{cases} 1, & \text{if } Q_{t}^{O} \in (Q_{t,2.5\%}^{S}, Q_{t,97.5\%}^{S}) \\ 0, & \text{Otherwise} \end{cases}$$
 (10)

where Z_t has a value of 1 when the observed discharge is within the 95PPU interval; t is the simulation time step; T is the number of time step in the observed data; Q_t^O the observed data at time step t; $Q_{t,2.5\%}^S$, and $Q_{t,97.5\%}^S$ represent the simulated lower (calculated at the 2.5% level of the cumulative distribution) and higher (97.5% level) boundaries at time t, with S indicating the simulated data, and O observed data.

$$R_{factor} = \frac{avr(Q_{t,97.5\%}^{S} - Q_{t,2.5\%}^{S})}{stdev\ of\ measured\ data}$$
(11)

3. RESULTS AND DISCUSSIONS

3.1 Sensitivity Analysis

The primary goal of sensitivity analysis is to describe how changes in model input values affect model outputs. Therefore, we performed sensitivity analysis manually to determine the most sensitive parameter in HEC-HMS. The sensitivity of the HEC-HMS model was evaluated using six key parameters from both watersheds. The results showed that constant rate (CR) and lag time (LT) were the most sensitive parameters. On the other hand, other parameters had no or only a minor impact on the model output (streamflow). Figure 4 shows the model-sensitive parameters.

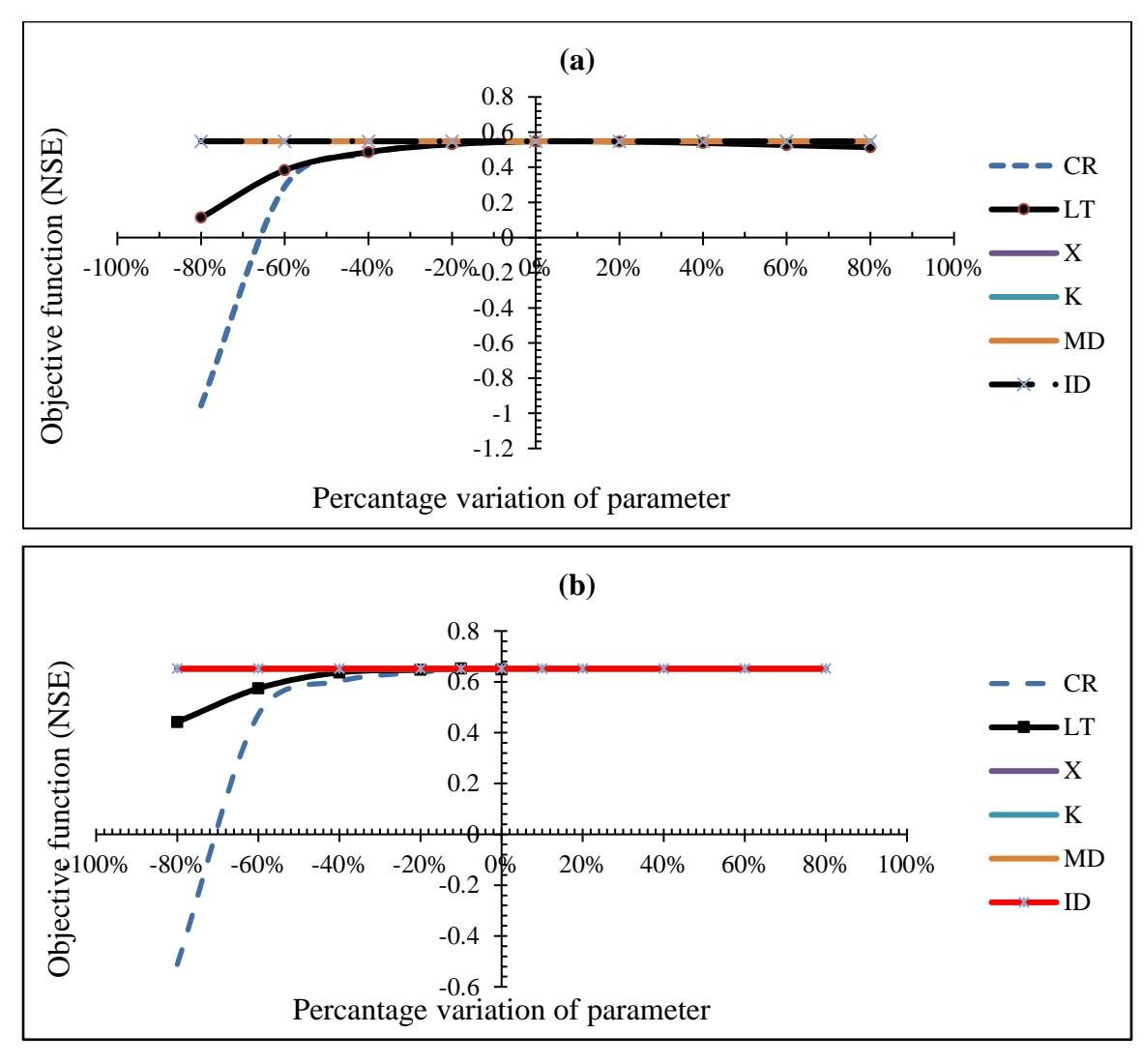


Figure 4. Model sensitivity using NSE in a) Bilate and b) Gidabo watersheds

In this study, we ran 1000 model runs in SUF-2 for sensitivity analysis. The sensitivity parameters were sorted based on the p-value and t-stat from the SUFI-2 sensitivity analysis. When the absolute value of the t-stat is significant, the parameter is more sensitive. At the same time, the p-value is closer to zero when the parameter is more significant. The results showed that the parameters governing subsurface water responses (ALPHA BF and GW REVAP) were found to be the most sensitive parameters in the Bilate Watershed, with a low p-value and a high absolute value of t-statistics. In the Gidabo Watershed, as represented in Figure 6, the relatively high sensitivity of CN-2 followed by SOL_AWC in the Gidabo Watershed indicated high runoff potential in the watershed. The lower soil layer had a greater capacity to hold water than the top soil layer. As a

result, percolation of water and aquifer return flow might be restricted (Saha et al., 2014). This could be due to the variable properties of the input catchment. The curve number parameter (CN_2) arising from land use and antecedent soil water conditions was found to be the most sensitive model parameter, followed by SOL_AWC. The other parameters were found to be less sensitive in the simulation of stream flow. Figure 5 and Figure 6 shows the model sensitivity analysis and parameters in the SWAT model.

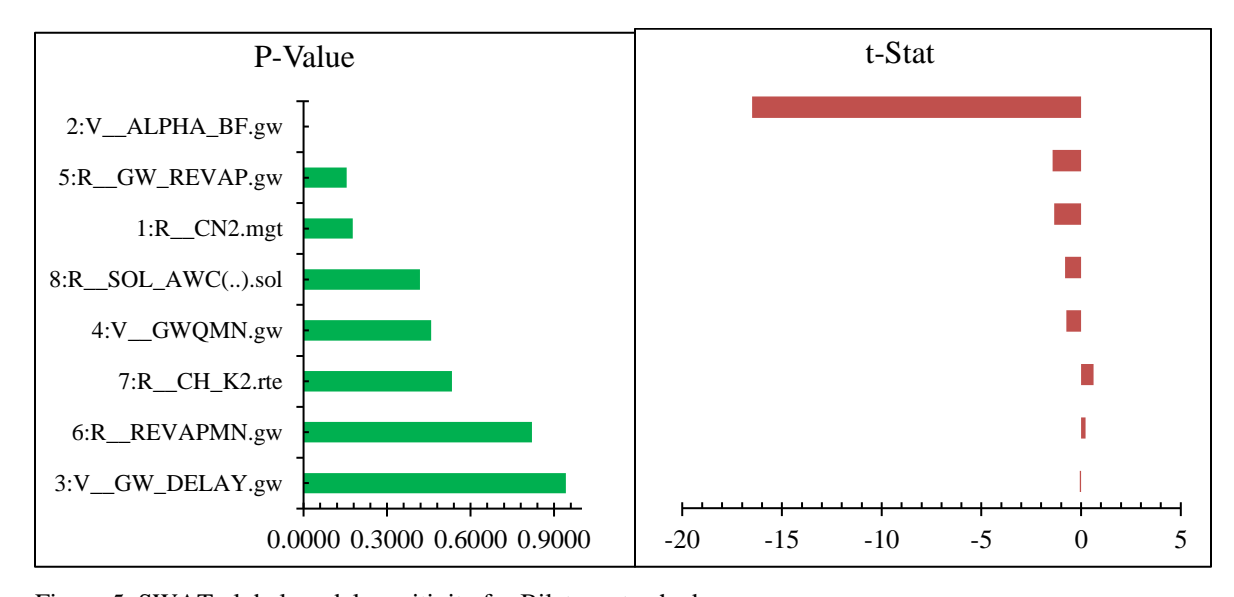


Figure 5. SWAT global model sensitivity for Bilate watershed

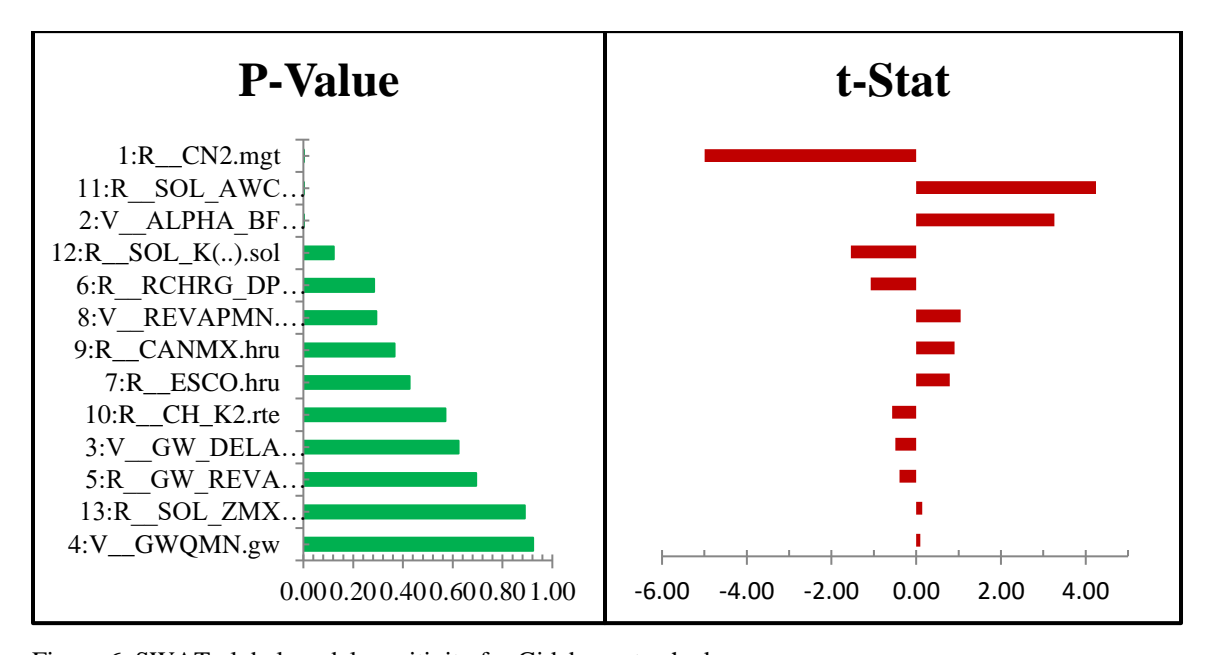


Figure 6. SWAT global model sensitivity for Gidabo watershed

3.2. Hydrological Model Calibration and Validation

Model calibrations were performed by fine-tuning the most sensitive model parameters within a given range in order to achieve agreement between simulated and observed stream flow in each watershed. The sections that follow describe the model calibration and validation efforts that were carried out using both hydrological models.

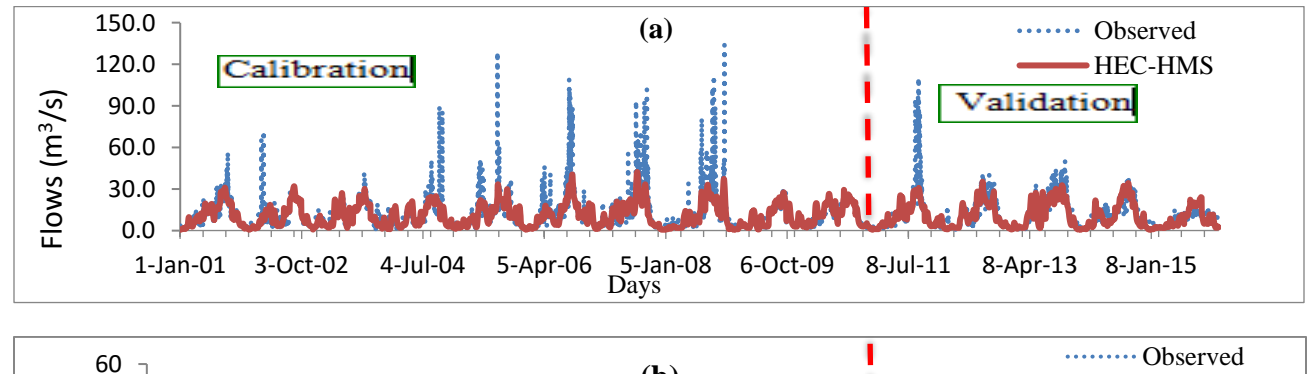
3.2.1. HEC-HMS model calibration and validation

The parameters_ constant loss rate and lag time _showed significant variability in the rainfallrunoff modeling (HEC-HMS) of both watersheds during the calibration period. In contrast, routing parameters (K and X) remained constant. According to the volume relative error result in HEC-HMS, RVE was low in both watersheds, with absolute values less than 10%. In the Bilate and Gidabo watersheds, the mean magnitude of computed daily stream flow values was within a very good range (RVE>10). In terms of reproducing the observed pattern of daily stream flow during calibration and validation (NSE = 0.55) and coefficient of determination (R2=0.55), satisfactory performance was observed in Bilate Watershed. The response of Gidabo Watershed to the HEC-HMS model was better than that of the Bilate Watershed in all evaluation criteria performed in daily and monthly stream flow simulations. HEC-HMS performed well during calibration (NSE=0.65) and was satisfactory in the validation period (NSE=0.63). Similarly, the regression coefficient indicated that the simulated discharge was (R² =0.65) during the calibration and validation period. This showed the capability of the HEC-HMS model in simulating the observed stream flow hydrograph and the good correlation with observed flow data in the Gidabo Watershed. These HEC-HMS model results were consistent with previous studies in the Rift Valley Basin: HEC-HMS (Aliye et al., 2020; Kebede, 2017; Legesse, 2020). Table 1 shows the model calibrated parameters and their ranges for both watersheds. The percentage error in peak flow (PEPF) of HEC-HMS model was 68% in the Bilate Watershed and 21% in the Gidabo Watershed. The value of these measures confirmed that HEC-HMS captured peak flow in both watersheds satisfactorily. Furthermore, the mean absolute error of the HEC-HMS model was 0.63 in the Bilate Watershed and 0.04 in the Gidabo Watershed, indicating that the HEC-HMS models simulated with a lower mean absolute error during the calibration and validation period in both watersheds.

Table 1: Parameter range an	d their calibrated	l values for Bilate and	Gidabo watersheds
Table 1. I didilicted fallige di	ia men camerated	i varues for Difate and	Oldabo Watersheus

No	parameters	Bilate	Gidabo		
		Range	Fitted value	Range	Fitted value
1	Constant rate (CR)	2.7-4.3	3.5	1.35-3.2	2.42
2	Initial deficit(ID)	0.1-2.3	1.89	0.001-2.1	2
3	Maximum deficit(MD)	2.8-5.8	5.7	2.11-2.99	2.5
4	Lag time (LT) in min	11000- 13000	12000	25100-27400	26000
5	Muskingum (K)	0.1-145	1	125-145	145
6	Muskingum (X)	0.1-0.44	0.1	0.01-0.45	0.1

The relationship between daily observed and simulated streamflow hydrographs (Figure 6) was better in the Gidabo Watershed than in the Bilate Watershed. Because of the inspection, the performance of the model in simulating the hydrograph's base flow and rising and falling limbs was better in the Gidabo Watershed than in the Bilate Watershed.



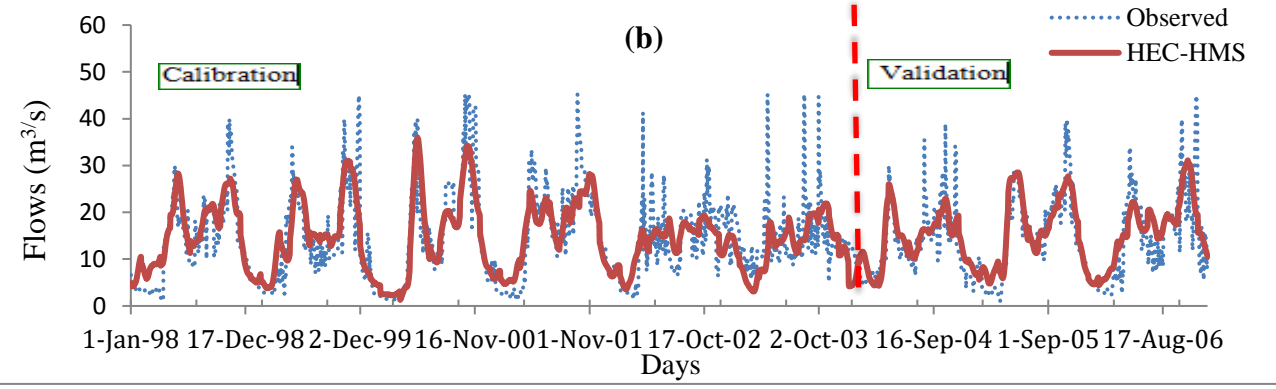


Figure 7. Daily observed and predicted stream flow hydrographs during the calibration and validation period for Bilate (a) and Gidabo (b) watersheds

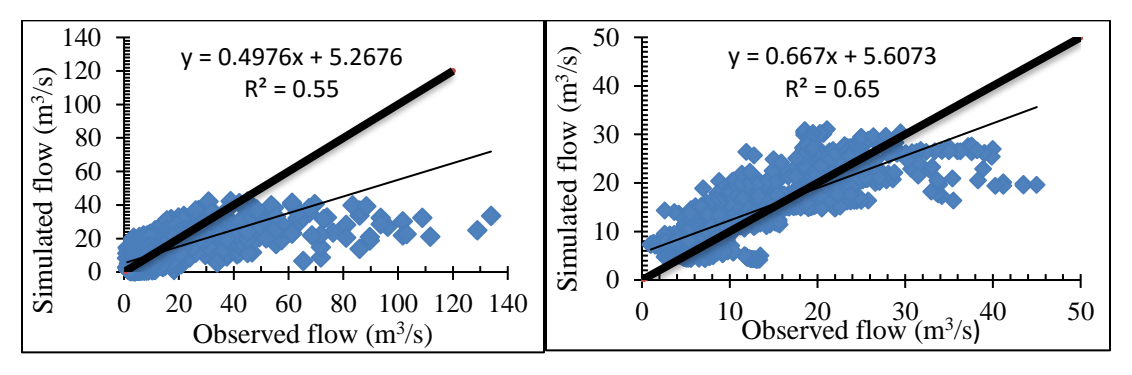
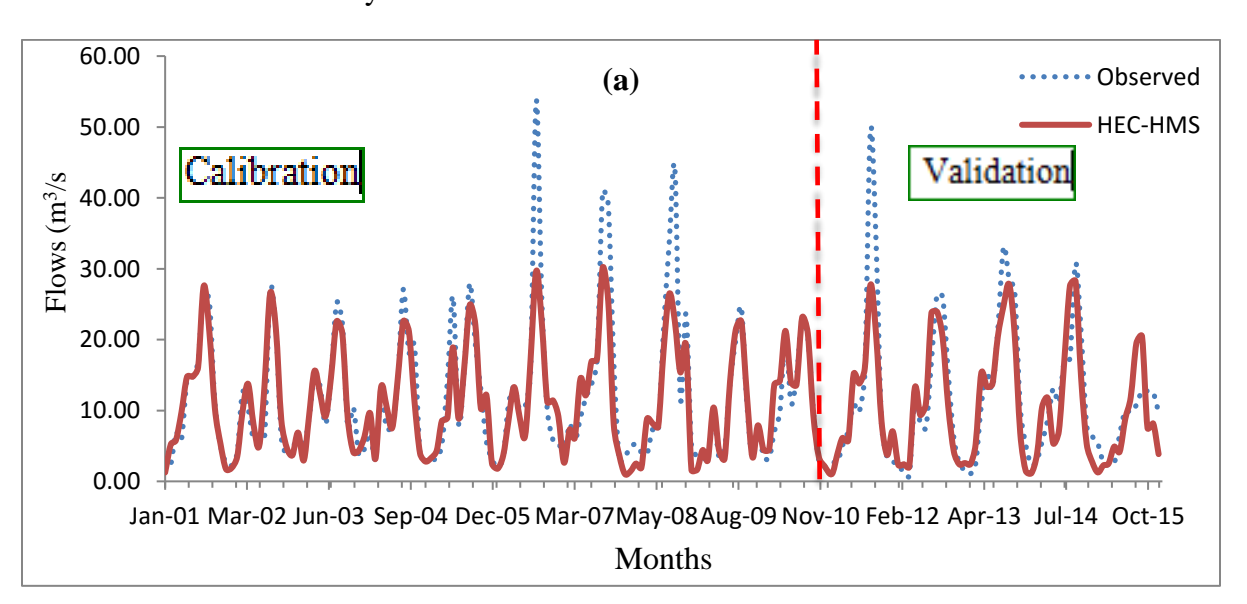


Figure 8. Scatter plot for the calibration Bilate (left) and Gidabo (right)

Figure 7 (left) illustrates a scatter plot of correlation analysis, demonstrating that more data are scattered below the 1:1 line in the Bilate Watershed, indicating that the model underestimated the predicted flow. On the other hand, the distribution values of Gidabo Watershed are over the 1:1 line as in Figure 7. It showed that the model slightly overestimated the stream flow. Hence, the model efficiency increased when the time step increased. As indicated in Figure 7, the observed and simulated hydrograph had a better mean monthly flow agreement than when the model was run for the daily time step. This is attributed to the hydrological models capturing less higher time resolution than lower time resolution. This is related to model uncertainty in model structure (Renard et al. 2010). Hence, the HEC-HMS model had limited capacity to capture the peakflow in both watersheds as indicated by PEPF.



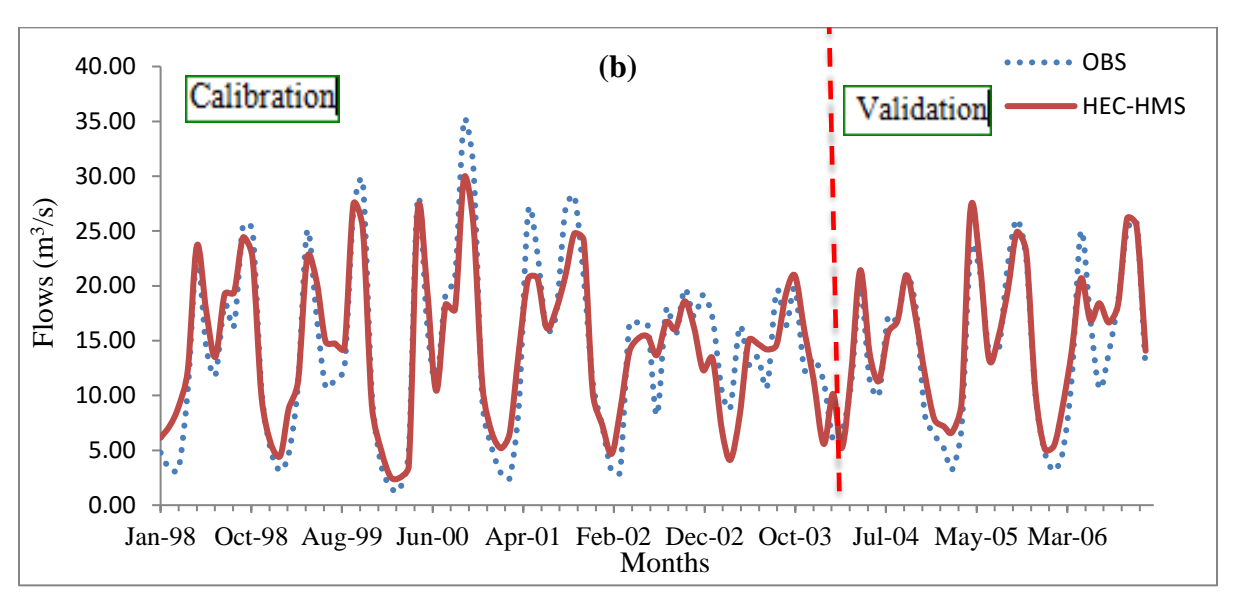


Figure 9. Monthly observed and predicted stream flow hydrographs during calibration and validation period for Bilate (a) and Gidabo (b) watersheds

3.2.2. SWAT model Calibration and Validation

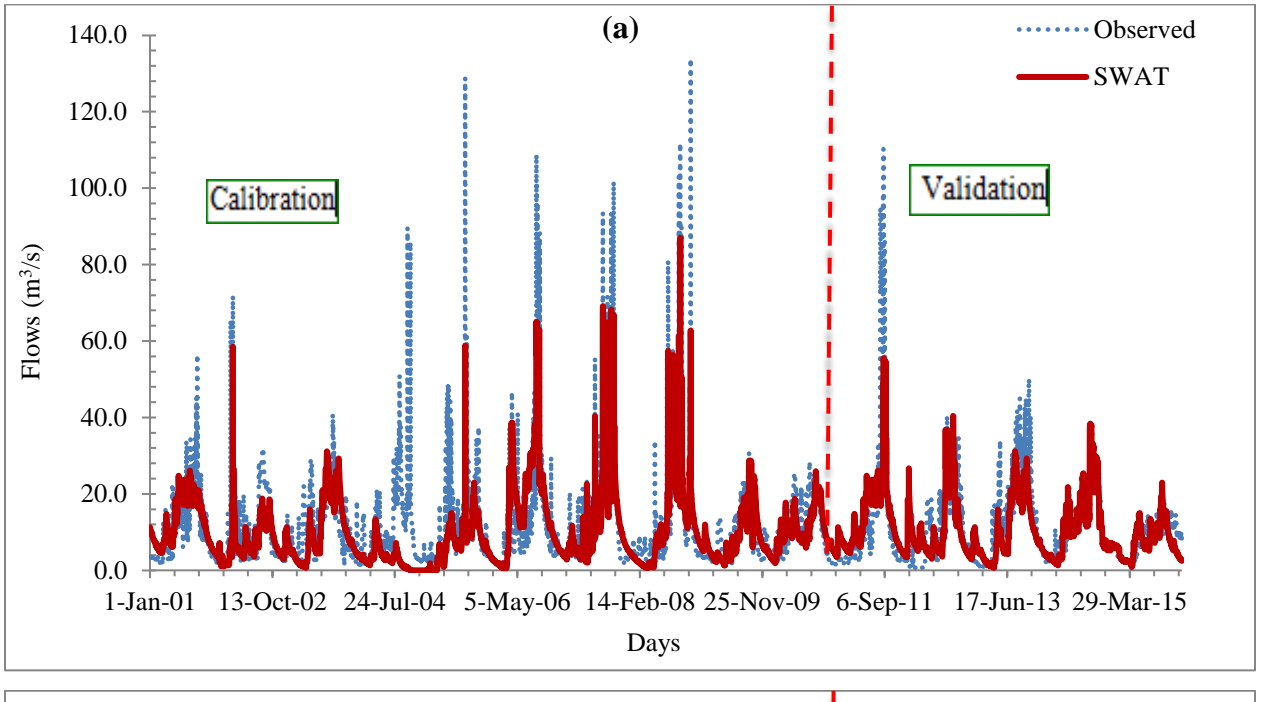
SWAT model enabled the observed daily stream flow to be reproduced during the model calibration and validation period (Figure 10). The observed and computed daily stream flow showed a 'satisfactory' agreement with NSE, RVE, and R² values varying in the range of 0.51 to 0.58, -14.5 to 1.3, and 0.52 to 0.61, respectively, for calibration and validation in both watersheds. Like HEC-HMS, the SWAT model performance can be rated as 'good' in both watersheds during the monthly calibration and validation (Figure 10) compared to daily streamflow simulation. Table 2 shows the calibrated-parameters and ranges for parameters. In addition, the percentage error in peak flow (PEPF) of the SWAT model is 35% in the Bilate Watershed and 18% in the Gidabo Watershed. These measures confirmed that SWAT captured the peak flow at both watersheds better than HEC-HMS. The error of the SWAT model was 1.7 in the Bilate Watershed and 0.19 in the Gidabo Watershed. This indicated that, the HEC-HMS models simulated with a lower mean absolute error than the SWAT model in both watersheds. Overall model performance on daily stream flow can be classified as "acceptable" during model calibration and validation periods based on evaluation criteria and (Moriasi et al., 2015; Rauf, 2018). In both watersheds during calibration and validation, the model performed with a greater agreement between observed and simulated monthly stream flow than daily stream flow simulation..

The statistical values were better on a monthly time scale in both models (HEC-HMS and SWAT) because monthly values were the mean of the physical phenomena, and models were good for average conditions compared to extreme events. Moreover, in monthly time steps, the differences that affected the hydrologic processes on a smaller temporal time step were smoothened.

Table 2. SWAT model calibrated parameters for Bilate and Gidabo watersheds

Parameters	Effect of parameter	Recomme	Fitted value	
	when its value increase	nded range	Bilate	Gidabo
ALPHA_BF	Increase the ground	0-1		
	water flow response to		0.01953	0.0001
CN2	changes in recharge Increase surface runoff	35-98	0.01933	1.7406
Groundwate	Decrease base flow	0-5000	0.23300	1.7400
	Decrease base now	0-3000	5.48984	840.50
r ESCO	Decrease evaporation	0-1	J.40904 *	0.0059
SOL_AWC	Increase groundwater	0-1	·	0.0039
SOL_AWC	recharge	0-1	0.95752	0.7972
CANMAX	Increase the canopy	0-10	0.93732	0.1912
CANWAA	water trapping and	0-10		
	storage		*	0.4716
REVAPMN	Decrease the actual	0-500	·	0.4710
KE V APIVIIN	amount of water	0-300		
	moving into the soil zone in response to			
	water deficiencies		165.589	0.1659
GWREVAP		0.02-	103.369	0.1039
GWKEVAP	Decrease base flow by			
	increasing water transfer from shallow	0.2		
			0.06791	0.2102
COL ZMA	aquifer to root zone	0.2500	0.06791	0.3193
SOL_ZMA	Maximum rooting	0-3500	*	0.5005
X	depth of soil profile	0.2000	4	0.5005
SOL_K	Saturated hydraulic	0-2000	*	02.201
CW DELA	conductivity	0.700	4	93.391
GW_DELA	Groundwater delay	0-500	2.24200	2.5000
Y	time	0.700	2.34398	2.5089
CH_K2	Effective hydraulic	0-500		
	conductive of main		110 740	0.72.62
DOUD C D	channel		113.742	0.7362
RCHRG_D	Deep aquifer	0.700		0.004.4
P	percolation fraction	0-500	*	0.0014

^{*}Indicate the parameters are insensitive and not significant in Bilate watershed



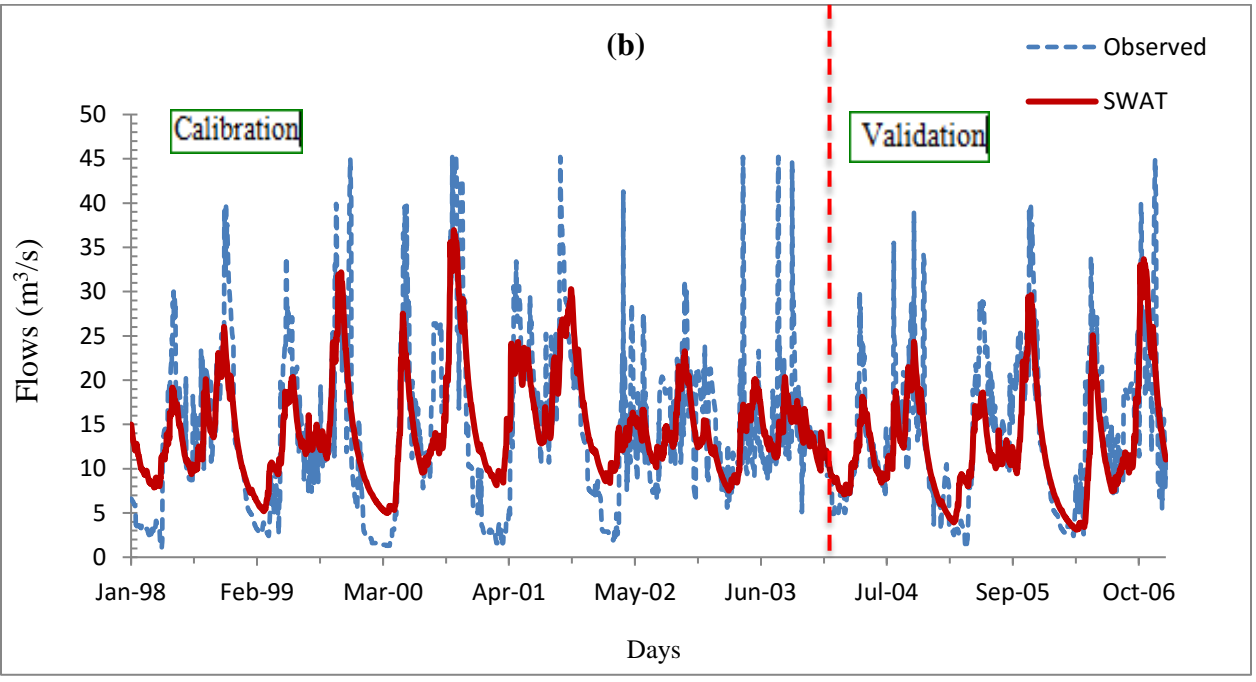


Figure 10. Daily observed and simulated stream flow hydrograph during calibration and validation periods for Bilate (a) and Gidabo(b) watersheds

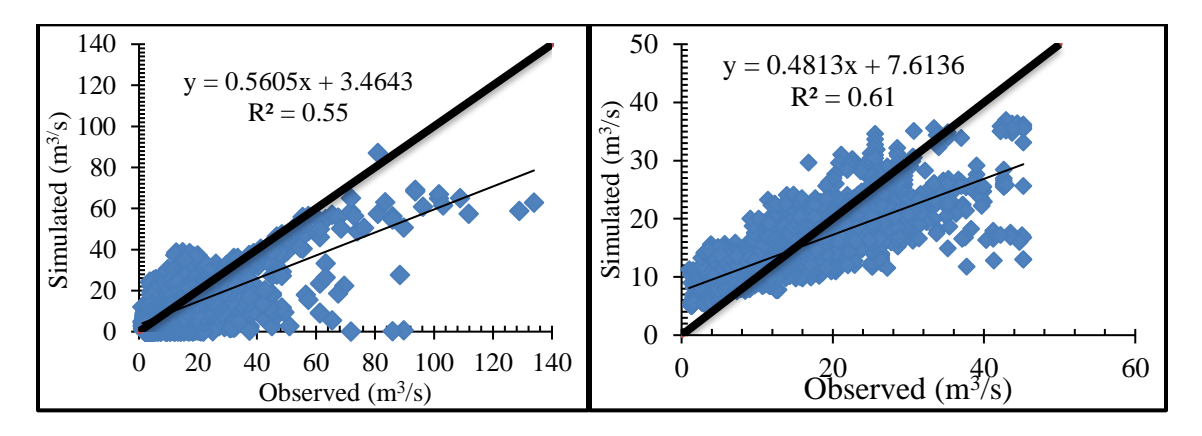


Figure 11. Scatter plot for the calibration Bilate (left) and Gidabo (right)

The observed versus simulated scatter plot in Figure 10 (left) showed more values distributed below the 1:1 line, indicating that the model underestimated simulated flows in the Bilate Watershed. In contrast, the distributed values simulated flows in the Gidabo Watershed (right) were above the 1:1 line, indicating that the model slightly overestimated simulated flow.

The statistical result of the SWAT model on daily stream flow for Nash Sutcliffe coefficients (NSE), coefficient of determination (R²), and relative volume error (RVE) in the Bilate Watershed were 0.53, 0.55, and -14.45%, respectively. The statistical values indicated that the model could satisfactorily simulate the daily stream flow to Bilate Watershed response. Figure 9 showed a close agreement between observed and simulated peak flow levels during calibration (R²=0.61) in Gidabo Watershed. The Nash criteria produced better outcomes between the simulated and observed streamflow (NSE=0.58), with a Relative Volume Error (RVE) of 1.31%. The relative volume error resulted in a very good outcome because the relative percent errors between the observed and simulated values were less than 5%. The simulated model performance findings for the SWAT model in this study were compatible with Tolera, 2012; Mohammed et al., 2020; Tewodros, 2012; and Golmar et al., 2014.

The percentage error in the peak flow (PEPF) of the SWAT model was 35% in the Bilate Watershed and 18% in the Gidabo Watershed. This confirms that SWAT captured peak flow at both watersheds better than HEC-HMS. The average error of the SWAT model was 1.7 in the Bilate Watershed and 0.19 in the Gidabo Watershed, which indicated that the HEC-HMS models simulated a lower mean absolute in both watersheds error than that of the SWAT model.

SWAT model was also used to build user confidence in the predictive capabilities of the model. As a result, the model was validated using daily data collected from both watersheds. During validation, the performance of the modelwas evaluated using R^2 , NSE, and RVE. The statistical values in the validation period were (R^2 =0.54), (NSE=0.52), and (RVE=-6) for the Bilate Watershed and (R^2 =0.6), (NSE=0.56), and (RVE=11) for Gidabo Watershed at the daily time step.

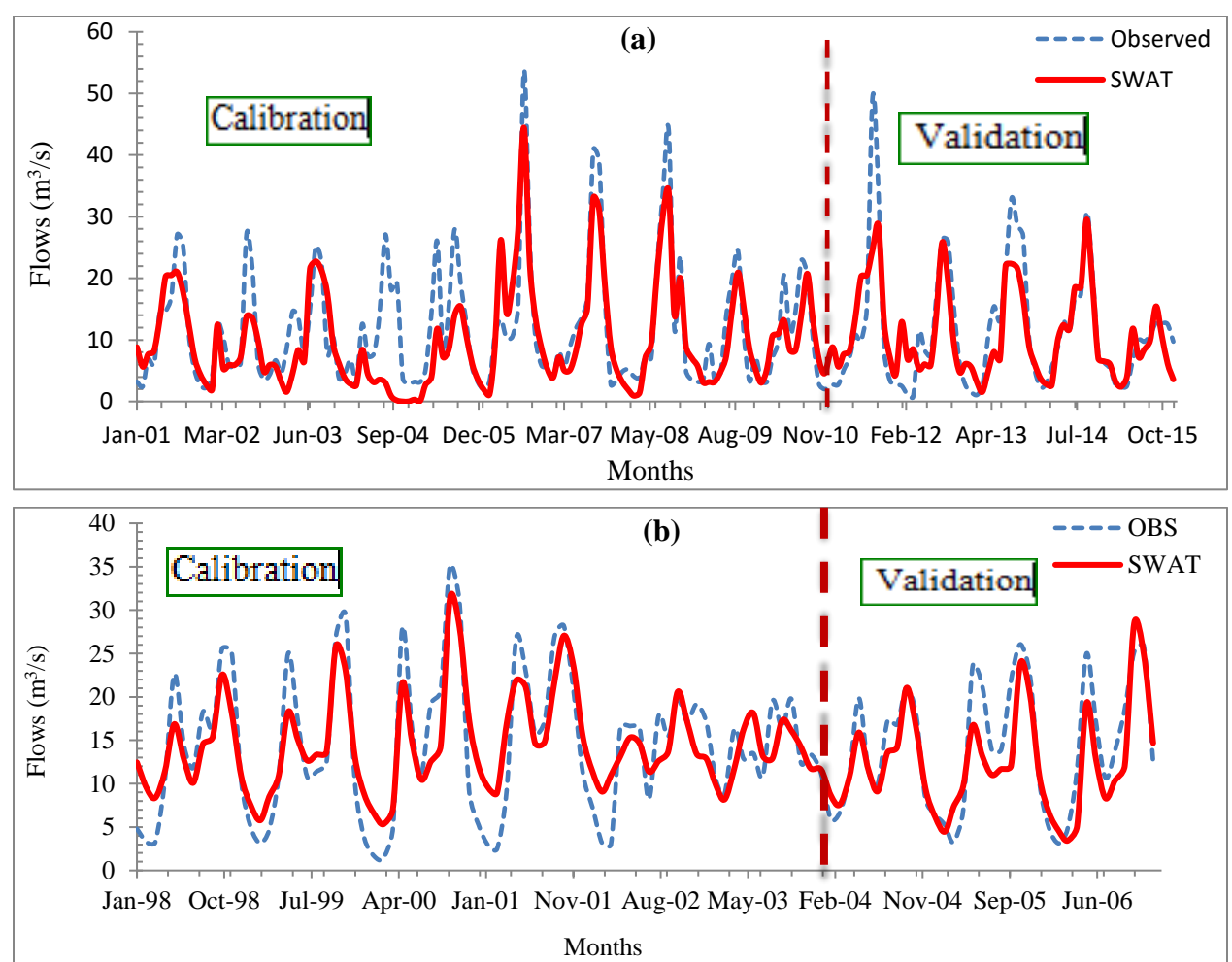


Figure 12. Monthly observed and simulated stream flow hydrograph during calibration and validation periods for Bilate (a) and Gidabo(b) watersheds

3.3. Comparison between HEC-HMS and SWAT Models in Simulating Stream Flow

Both models were compared for daily and monthly stream flow simulation. The two hydrological models differed in terms of runoff generation mechanisms, as well as model concepts and structures. When the models' overall performance was evaluated, both models were capable of

reproducing the stream flow adequately. Table 3 shows the statistical indices used to evaluate the model performances in both watersheds.

As per Moriasi et al. (2015), the two models were sufficient in terms of matching the observed pattern of stream flow hydrographs in both watersheds. Meanwhile, as evaluated by the coefficient of determination (R²), both models in the Bilate Watershed exhibited an acceptable correlation between observed and simulated flow peaks. HEC-HMS showed good performance in the Gidabo Watershed whereas SWAT model performed satisfactorily in the same watershed. Despite their similar modeling capabilities, a comparison analysis revealed that the HEC-HMS model was better in predicting the overall variation of stream flow for both watersheds. This may be attributed to the fact that SWAT needed more input variables and parameters than HEC-HMS. SWAT model simulations might have probably drawn many uncertainties and hence reduced the model performance during model calibration and validation times. It should be noted that the model uncertainties were also related to model inputs which a modeler could not easily identify. Input variables are acceptable and perfect despite having uncertainties as described by Renard et al. (2010). Similar observations were made by Aliye et al. (2020). Ismail et al. (2020) who simulated streamflow using the HEC-HMS model found that HEC-HMS was better than the SWAT model. Despite the performance of each model that differed from watershed to watershed, the selected models performed relatively better in the Gidabo Watershed than in the Bilate Watershed. This may be attributed to factors influencing runoff generation in both watersheds, including land use and land cover, climatic conditions (mainly rainfall characteristics), morphometric conditions, and soil. The Gidabo Watershed had a small area covered by forest whereas the Bilate Watershed had no forest land use.. On the other hand, the catchment area of Bilate was well above that of Gidabo, and its slope range was comparatively high. Therefore, a relatively average condition of hydrologic response was possible compared to hydrologic responses in the Bilate Watershed. This would favor hydrologic models to simulate responses better. However, future investigation of hydrologic responses and enforcement of variables concerning hydrologic models' capability should be done to capture these events. The HEC-HMS was a suitable and sufficient model for simulating daily and monthly stream flow compared to SWAT.

HEC-HMS consistently underpredicted peak flows. Ismail et al. (2020) also discovered that the HEC-HMS model was unable to model peak flows. (Meenu et al., 2010) agreed with this study

because HEC-HMS was unable to replicate peak flows. SWAT was found to be more effective than HEC-HMS in capturing targets in both watersheds over daily and monthly time intervals.

Table 3. Statistical indicators to evaluate the performance of models for daily and mean monthly time steps in Bilate and Gidabo watersheds

Watershed	Model	Process	Statistical	Daily	description	Monthly	Model
			Index				performance
		Calibration	NSE	0.54	satisfactory	0.79	Good
			R^2	0.55	satisfactory	0.81	very good
	HEC-		RVE	-5.39	good	-5.31	good
	HMS	Validation	NSE	0.55	satisfactory	0.72	Good
			R^2	0.55	satisfactory	0.73	Good
			RVE	-6.94	good	-6.49	good
Difate		Calibration	NSE	0.53	satisfactory	0.62	satisfactory
			R^2	0.55	satisfactory	0.65	good
	SWAT		RVE	-14.46	good	-14.45	satisfactory
		Validation	NSE	0.51	satisfactory	0.68	good
			R^2	0.52	satisfactory	0.65	good
			RVE	-6.01	good	-5.74	good
		Calibration	NSE	0.65	good	0.85	very good
	HEC-		R^2	0.65	good	0.86	very good
Gidabo			RVE	0.46	very good	0.5	very good
	HMS	Validation	NSE	0.63	good	0.86	very good
			R^2	0.65	good	0.88	very good
			RVE	6.02	good	6.59	good
		Calibration	NSE	0.58	satisfactory	0.73	good
	SWAT		R^2	0.61	good	0.77	good
			RVE	1.3	very good	0.49	very good
		Validation	NSE	0.56	satisfactory	0.73	good
			R^2	0.6	good	0.78	good
			RVE	-11.41	good	-11.44	good

3.4. Model Uncertainty

Uncertainty analysis helps understand the predictive power and limitations of a model, , and make informed decisions. According to Sánchez et al. (2015) uncertainty analysis is the formal process of defining a model and mapping it onto model output uncertainty, thereby measuring the range of possible outcomes.

The MCMC approach reduced the source of uncertainty resulting from parameters in HEC-HMS. The convergence of MCMC to stable posterior probability density function (PDF) was monitored by using statistics (Gelman and Rubin, 1992). The P-factor and R-factor were used to determine the strength of model calibration and uncertainty (Abbaspour, 2014). The P and R factors of Bilate Watershed were 0.34 and 0.1, respectively. In the Gidabo Watershed, they were 0.34 and 0.22, respectively. According to the uncertainty analysis results, the number of goodness-of-fit criteria (NSE, RVE, and R²)was within acceptable limits. As a result, the parameters used to simulate streamflow in the Bilate and Gidabo watersheds using HEC-HMS with input data were valuable and useful for future research (Figure 13).

SWAT CUP uses SUFI-2, an essential tool for continuous iteration, to help understand uncertainty in the SWAT model. In SUFI-2, all the uncertainty sources were not separately predicted but considered total model uncertainty to the parameters. The P and R factors were used from the 1000 model runs simulated in SUFI-2 to define how much of the simulated hydrograph brackets observed streamflow. A P-factor of 0.46 and an R-factor of 0.40 was obtained during calibration in the Bilate Watershed. In the Gidabo Watershed, the P-factor and R-factor were 0.80 and 0.88, respectively. Because the P and R factor values were in the optimum range, the goodness-of-fit of the model was reasonably acceptable (Figure 14).

Regarding model prediction uncertainty, MCMC in HEC-HMS predicted the smallest uncertainty band in both watersheds compared to SUFI-2 in SWAT. This was because MCMC in HEC-HMS would not account for input data and model structure uncertainty, resulting in an underestimation of prediction uncertainty (Zhang et al., 2015). Furthermore, the parameter uncertainty predicted by MCMC only accounted for a small portion of the total uncertainty, whereas SUFI-2 considered all sources of uncertainty, resulting in broader parameter ranges. Therefore, model prediction uncertainty analysis and parameter uncertainty value ranges were reasonably acceptable (Abbaspour, 2014)

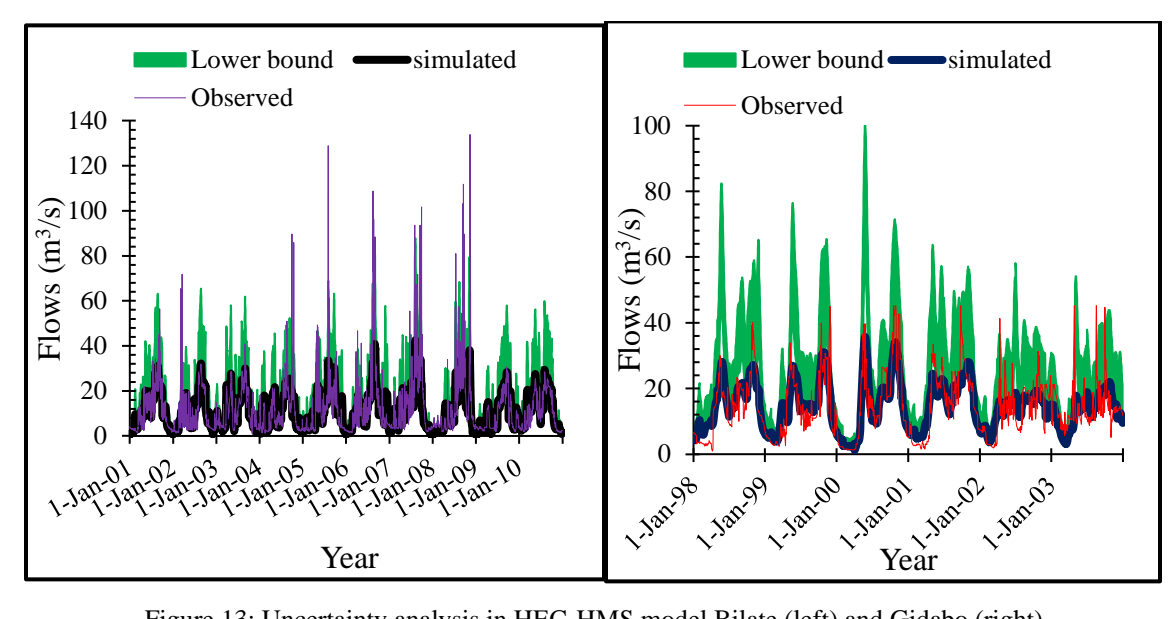


Figure 13: Uncertainty analysis in HEC-HMS model Bilate (left) and Gidabo (right)

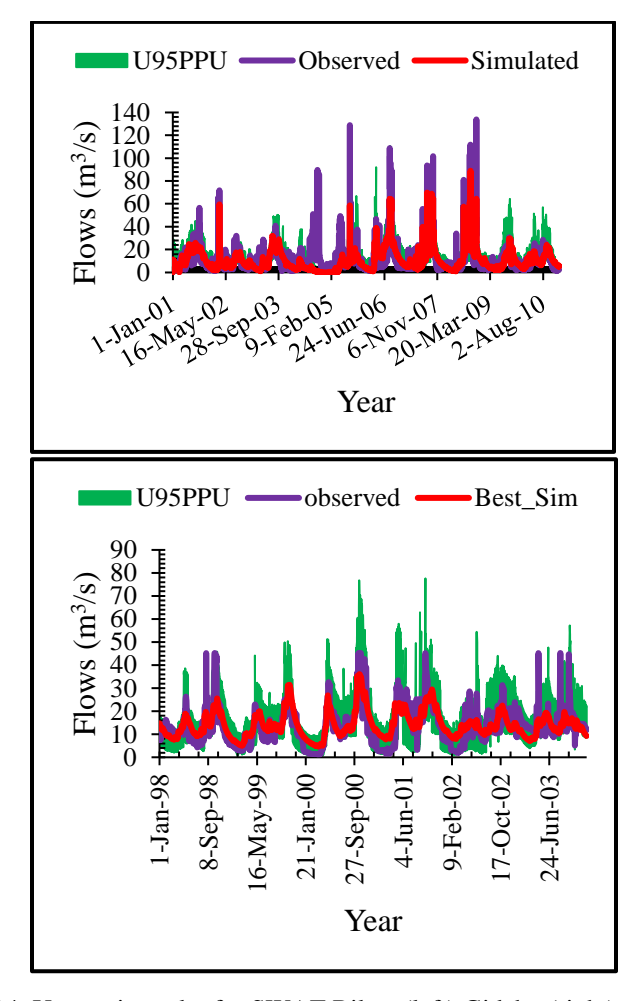


Figure 14: Uncertainty plot for SWAT Bilate (left) Gidabo (right) watershed

4. CONCLUSION

This study compared the performance of the HEC-HMS and SWAT models in stream flow simulation to determine the best model for the Bilate and Gidabo watersheds. Observed stream flow at the outlets of the Bilate and Gidabo watersheds were used for comparison. It was discovered that the performance of both models was superior in both watersheds. However, in both watersheds and for daily and monthly time steps, the HEC-HMS hydrological model outperformed the SWAT model. Furthermore, the HEC-HMS model was predicted to outperform the Bilate watershed in the Gidabo Watershed. As a result, the HEC-HMS hydrological model would be preferred to the SWAT hydrological model. In fact, due to the economics of hydrological modeling, the need for model input data in SWAT pushes it aside. Hydrologists are advised to look for the HEC-HMS model in general, and the Gidabo Watershed in particular, unless specific needs and high accuracies are not deemed necessary based on detailed input data. The uncertainty analyses also favored the HEC-HMS model, which predicts stream flow response with less uncertainty. This research will be beneficial to future hydrologists and practitioners.

Acknowledgements

The Ministry of Water and Energy, and the National Metrological Service Agency are acknowledged for providing the necessary data. The research was financially supported by Arba Minch University. The authors are also thankful to Arba Minch University.

Conflict of Interest

There is no conflict of interest related to this manuscript.

REFERENCES

Abbaspour, K. C. (2014). SWAT - CUP SWATCalibration and Uncertainty Programs.

Abbaspour, K. C., Yang, J., Maximov, I., Siber, R., Bogner, K., Mieleitner, J., & Zobrist, J. (2007). *Modelling hydrology and water quality in the pre-alpine / alpine Thur watershed using SWAT*. 413–430. https://doi.org/10.1016/j.jhydrol.2006.09.014

Abebe, T. (2017). Rainfall - Runoff Modeling a Comparative Analyses: Semi Distributed HBV Light and SWAT Models in Geba Catchment, Upper Tekeze Basin, Ethiopia.

Abyot, A. (2008). Hydrological Models Comparison for Estimation of Floods in the Abaya-

- Chamo Sub-Basin.M.s.c Theiss, Addis Ababa University. 1–110.
- Aliye, M. A., Aga, A. O., Tadesse, T., & Yohannes, P. (2020). Evaluating the Performance of HEC-HMS and SWAT Hydrological Models in Simulating the Rainfall-Runoff Process for Data Scarce Region of Ethiopian Rift Valley Lake Basin. *Open Journal of Modern Hydrology*, *10*(04), 105–122. https://doi.org/10.4236/ojmh.2020.104007
- Amaru Ayele, M., & Gebremariam, B. (2020). Evaluation of Spatial and Temporal Variability of Sediment Yield on Bilate Watershed, Rift Valley Lake Basin, Ethiopia. *Journal of Water Resources and Ocean Science*, *9*(1), 5. https://doi.org/10.11648/j.wros.20200901.12
- Dhami, B. S., & Pandey, A. (2013). Comparative review of recently developed hydrologic models. *Journal of Indian Water Resources Society*, *33*(3), 34–42.
- Gelman, A., & Rubin, D. B. (1992). Inference from iterative simulation. In *Statistical Science* (Vol. 7, Issue 4, pp. 457–511).
- Golmohammadi, G., Prasher, S., Madani, A., & Rudra, R. (2014). *Evaluating Three Hydrological Distributed Watershed Models: MIKE-SHE, APEX, SWAT.* 20–39. https://doi.org/10.3390/hydrology1010020
- Halcrow, G. (2010). Rift Valley Lakes Basin Integrated Resources Development Master Plan Study Project; The Federal Democratic Republic of Ethiopia-Ministry of Water Resources (MOWR): Addis Ababa, Ethiopia.
- Herrera, P. A., Marazuela, M. A., & Hofmann, T. (2022). Parameter estimation and uncertainty analysis in hydrological modeling. *Wiley Interdisciplinary Reviews: Water*, *9*(1), 1–23. https://doi.org/10.1002/wat2.1569
- Ismail, H., Kamal, M. R., Hin, L. S., & Abdullah, A. F. (2020). Performance of hec-hms and arcswat models for assessing climate change impacts on streamflow at bernam River basin in Malaysia. *Pertanika Journal of Science and Technology*, 28(3), 1027–1048.
- Kassa, T., & Forech, G. (2009). Watershed Hydrological Responses to Changes in Land Use and Land Cover, and Management Practices at Hare Watershed, Ethiopia. *Ph.D Thesis*, *University of Siegen, Germany*, 229.
- Kebede, B. Z. (2017). Evaluation of water availability under changing climate in the bilate catchment. *M.Sc. Thesis*.

- Khoi, D. N. (2016). Comparison of the HEC-HMS and SWAT hydrological models in simulating the stream flow. *Vietnam Journal of Science and Technology*, 53(5), 189–195.
- Legesse, M. (2020). Flood Inundation Mapping Under Climate Change In The Bilate Catchment, Ethiopia. 126.
- Meenu. R, S. Rehana, Mujumdar, P. P. (2010). Advanced Bash-Scripting Guide An in-depth exploration of the art of shell scripting Table of Contents. *Okt 2005 Abrufbar Uber Httpwww Tldp OrgLDPabsabsguide Pdf Zugriff 1112 2005*, 2274(November 2008), 2267–2274. https://doi.org/10.1002/hyp
- Moriasi, D. N., Gitau, M. W., Pai, N., & Daggupati, P. (2015). Hydrologic and water quality models: Performance measures and evaluation criteria. *Transactions of the ASABE*, *58*(6), 1763–1785. https://doi.org/10.13031/trans.58.10715
- Neitsch, S. ., Arnold, J. ., Kiniry, J. ., & Williams, J. . (2011). Soil & Water Assessment Tool Theoretical Documentation Version 2009. *Texas Water Resources Institute*, 1–647. https://doi.org/10.1016/j.scitotenv.2015.11.063
- Rauf, A. (2018). Impact Assessment of Rainfall-Runoff Simulations on the Flow Duration Curve of the Upper Indus River A Comparison of Data-Driven and Hydrologic Models. *Ateeq-Ur Rauf*. https://doi.org/10.3390/w10070876
- Saha, P. P., Zeleke, K., & Hafeez, M. (2014). Streamflow modeling in a fluctuant climate using SWAT: Yass River catchment in south eastern Australia. *Environmental Earth Sciences*, 71(12), 5241–5254. https://doi.org/10.1007/s12665-013-2926-6
- Sánchez, A., Skahill, B., Scharffenberg, W., & Smith, C. H. (2015). Computer-Based Model Calibration and Uncertainty Analysis: Terms and Concepts. *Us Army Corps of Engineers*, *July*.
- Scharffenberg, W. (2016). HEC-HMS User's Manual. *US Army Corps of Engineers Hydrologic Engineering Center*, *December*, 623. https://www.hec.usace.army.mil/confluence/hmsdocs/hmsum/4.7/release-notes/v-4-7-0-release-notes
- Shen, ZY., Chen, L, Chen, T. (2012). Analaysis parameter uncertainty in hydrological and sediment modelling using GLUE method: a case study of SWAT model applied three Gorges Reservoir region, China. *Hydrol. Earth Syst.Sci*, *16*(121–132).

- Sil, B. S., Borah, A., Deb, S., & Das, B. (2016). Development of river flood routing model using non-linear muskingum equation and excel tool "GANetXL." *Journal of Urban and Environmental Engineering*, 10(2), 214–220. https://doi.org/10.4090/juee.2016.v10n2.214220
- Sivapalan, M., Takeuchi, K., Franks, S. W., Gupta, V. K., Karambiri, H., Lakshmi, V., Liang, X., McDonnell, J. J., Mendiondo, E. M., O'Connell, P. E., Oki, T., Pomeroy, J. W., Schertzer, D., Uhlenbrook, S., & Zehe, E. (2003). IAHS Decade on Predictions in Ungauged Basins (PUB), 2003-2012: Shaping an exciting future for the hydrological sciences. *Hydrological Sciences Journal*, 48(6), 857–880. https://doi.org/10.1623/hysj.48.6.857.51421
- Song, X., Zhang, J., Zhan, C., Xuan, Y., Ye, M., & Xu, C. (2015). Global sensitivity analysis in hydrological modeling: Review of concepts, methods, theoretical framework, and applications. *Journal of Hydrology*, *523*(225), 739–757. https://doi.org/10.1016/j.jhydrol.2015.02.013
- Tegegne, G., Kim, Y. O., Seo, S. B., & Kim, Y. (2019). Hydrological modelling uncertainty analysis for different flow quantiles: a case study in two hydro-geographically different watersheds. *Hydrological Sciences Journal*, *64*(4), 473–489. https://doi.org/10.1080/02626667.2019.1587562
- Wu, H., & Chen, B. (2015). Evaluating uncertainty estimates in distributed hydrological modeling for the Wenjing River watershed in China by GLUE, SUFI-2, and ParaSol methods. *Ecological Engineering*, 76, 110–121. https://doi.org/10.1016/j.ecoleng.2014.05.014
- Wurbs, R. A. (1998). Dissemination of generalized water resources models in the united states. *Water International*. https://doi.org/10.1080/02508069808686767
- Zhang, J., Li, Q., Guo, B., & Gong, H. (2015). The comparative study of multi-site uncertainty evaluation method based on SWAT model. *Hydrological Processes*, 29(13), 2994–3009. https://doi.org/10.1002/hyp.10380
- Zhanling Li,; Zongxue Xu, ; Quanxi Shao, J. Y. (2009). Parameter estimation and uncertainty analysis of SWAT model in upper reaches of the Heihe river basin. *Hydrological Prosses*, 2274(November 2008), 2744–2753. https://doi.org/DOI: 10.1002/hyp.7371 Parameter

Guidelines to Authors

INTRODUCTION

Types of paper

(a) Research Papers: these papers are fully documented, interpreted accounts of significant findings of original research. The maximum acceptable length of a Research Paper is 8000 words (less 350 words for each normal-sized figure or table you include). Authors should aim for no more than eight figures per paper. Papers not conforming to these guidelines may be rejected, at the Editor's discretion.

(b) Review Papers: these are critical and comprehensive reviews that provide new insights or interpretation of a subject through thorough and systematic evaluation of available evidence. They should not normally exceed **8000** words. Manuscripts exceeding **10,000** words will not be accepted for review.

BEFORE YOU BEGIN

Ethics in publishing

You will be required to accept the Publishing Ethics Statement for Authors when you submit your paper to the journal. The statement covers authorship, originality and conflicts of interest.

Publishing Ethics Statement for Authors

Publishing and the Editors of the journal are committed to maintaining the highest standards of ethics in reviewing and publishing your submissions to this journal. Please review the following statement of these fundamental principles and indicate your acceptance before proceeding with your submission.

- Your paper is your original work and where you have included the work of others this has been fully and appropriately acknowledged.
- Authorship of the paper must include all those who have made significant contributions to the work, and they should be listed as co-authors. Persons who have not contributed significantly to the work must not be listed as co-authors.

- As corresponding author you must ensure that all co-authors have approved the final version of the paper and have agreed to its submission for publication.
- You have not already published in another journal a paper describing essentially the same material, nor is your paper currently being considered for publication in another journal.
- You should disclose in your paper any conflict of interest (financial or other) that might be construed to influence the content of this paper. All sources of financial support should be disclosed.

Acceptance: Before indicating your acceptance of these principles on behalf of coauthors, you confirm that you have informed all co-authors of these principles and are accepting them on their behalf.

Note that conference proceedings are a form of publication.

Changes to authorship

If you wish to add, delete or rearrange the authors of your accepted paper: Before online publication: The corresponding author should contact the Journals Manager, and provide (a) the reason for the change, and (b) the written consent of all co-authors, including the authors being added or removed. Please note that your paper will not be published until the changes have been agreed upon. After online publication: Any requests to add, delete, or rearrange author names in an article published in an online issue will follow the same policies as noted above

PREPARATION OF THE MANUSCRIPT

1. General

- a. Submission of papers must be accompanied by a covering letter confirming that the paper has not been published elsewhere nor simultaneously submitted to any other journal in any language.
- b. The papers should be written in a single column and submitted in Microsoft WORD format.
- c. The paper including all figures, tables, and references should be no longer than 16 pages written in Times New Roman, 1.5 line spacing, single column, and font size 12 printed on one front page throughout.
- d. No table in graphic format will be accepted
- e. Avoid color presentations

- f. Heading should be bold and in title cause and subheadings in sentence case and numbered throughout.
- g. Tables, figures, and equations should be numbered sequentially
- h. Authors must adhere to the Standards of International Units (SI)
- i. Indicate also the name and e-mail address of the corresponding author.

2. Structure of the manuscript

Title page

The essential contents of the title page are:

- Title. Provide the title of the research paper
- Author names and affiliations. Provide the names of the authors and their address (where the work was actually done. Indicate all affiliation with a lowercase superscript letter immediately after the author's name and in front of the appropriate address. Provide the full postal address of each affiliation, including the country name and, the e-mail address of each author.
- Corresponding author. Clearly indicate who will handle correspondence at all stages of refereeing and publication, also post-publication. Provide telephone (with country and area code) are provided in addition to the e-mail address. Contact details must be kept up to date by the corresponding author.

Subdivision

Divide your article into clearly defined and numbered sections. Subsections should be numbered 1.1, 1.2, etc. excluding the abstract, acknowledgment, and references. Any subsection may be given a brief heading.

Abstract

Provide a concise and factual abstract. The abstract should be stated briefly (**not more than 250 words**). It should inform the reader about the purpose of the research, the principal results, and major conclusions. An abstract is often presented separately from the article, so it must be able to

stand alone. For this reason, References and nonstandard or uncommon abbreviations should be avoided. Immediately after the abstract provide a maximum of 6 **keywords**.

Introduction

In this part, provide a brief background to the research title, statement of the research problems, and the main objectives of the investigation. Avoid a detailed literature survey or summary of the results.

Materials and Methods

In this section, briefly describe your research design, sampling methods, data collection, and methods of analysis as well as materials and procedures used to undertake the research. Methods already published should be indicated by a reference and only relevant modification (if any) should be described.

Results and Discussion

This section is the most important part of the paper in which the author describes the interpretation and the implication of the main findings. A clear presentation of experimental results obtained, highlighting any trends or points of interest. Avoid extensive citations and discussion of published literature.

Conclusions

This section can be standalone. In this part, briefly state the contribution of your research to the problem area and indicate specific exceptions (if any) and further research needs and recommendations (if any).

Acknowledgments

The purpose of this section is to give credit to people or organizations that have provided support to you while you are carrying out the research. This should be put at the end of the article and before the references.

Notations and abbreviations

All acronyms and notations should be provided when first used in the paper.

Figure captions

Provide a caption to each illustration used. Supply captions separately, not attached to the figure. A caption should comprise a brief title (**not** on the figure itself) and a description of the illustration.

Tables

Number your tables consecutively following their appearance in the text. Place footnotes to tables below the table body and indicate them with superscript lowercase letters. Avoid vertical rules. Be sparing in the use of tables and ensure that the data presented in tables do not duplicate results described elsewhere in the article.

References

Please make sure that every reference cited in the text is also present in the reference list (and vice versa). Unpublished results and personal communications are not recommended in the reference list but maybe mentioned in the text. If these references are included in the reference list they should include a substitution of the publication date with either 'Unpublished results' or 'Personal communication'. References recommended in a research paper are minimum 10 and a maximum of 25 is recommended.

Reference style

All citations in the text should follow the following style:

- For single author: the author's name and the year of publication;
- For two authors: both authors' names and the year of publication;
- For three or more authors: first author's name followed by 'et al.' and the year of publication.
- Reference listing should be arranged first alphabetically and then further sorted chronologically if necessary. More than one reference from the same author(s) in the same year must be identified by the letters 'a', 'b', 'c', etc., placed after the year of publication.

Examples:

Reference to a journal publication:

Ruijs A., Zimmermann A., van den Berg M., 2008. Demand and distributional effects of water pricing policies. Ecological Economics. 66, 506-516.

Reference to a book:

Gujer W., 2008. System Analysis for Water Technology. Springer-Verlag Berlin Heidelberg.

Reference to a chapter in an edited book:

Nathan R. and Evans R., 2011. Groundwater and surface water connectivity, in Grafton R.Q., Hussey K. (Eds.), Water Resources Planning and Management. Cambridge University Press, UK, pp. 46–67.

Contact us

Arba Minch University

P.O. Box 21

Tel: +251-46881-4986

Fax: +251-46881-0820/0279

Website: https://survey.amu.edu.et/ojs/index.php/EJWST/

Arba Minch, Ethiopia